The Functional Organisation and Role in Visually Guided Behaviour of the Top-Down Projection from Anterior Cingulate Cortex to Primary Visual Cortex

Eluned Broom

A thesis submitted for the degree of PhD in Neuroscience

Cardiff School of Biosciences

Cardiff University

June 2019

Summary

The interplay between bottom-up and top-down projections help the brain to build a perception of the visual world. Top-down projections, in particular, are believed to influence perception using previous experience and current context. One way in which they do this is in the direction of visual attention. Anterior cingulate cortex (ACC), a structure from which top-down projections are believed to emanate from, has been implicated in tasks requiring visual attention. Furthermore, studies in mice have shown an attentional-like effect in primary visual cortex (V1) neurons when a projection originating from ACC and terminating at V1 was artificially stimulated using optogenetics. The aim of the following studies was to determine whether ACC influenced the direction of visual attention under endogenous conditions.

To do this, two main approaches were taken. First, the functional organisation of ACC axons in V1 were compared to layer 2/3 V1 pyramidal neurons in order to investigate whether the two populations were retinotopically matched. Secondly, the activity of ACC axons during a visually guided discrimination task was examined to discern whether it was elevated when mice performed well. This was achieved using calcium sensitive genetic indicators including gCaMP6s and jrGECO1a to record neuronal activity while awake, behaving, head-restrained mice completed visual tasks. To investigate functional organisation, a retinotopic protocol was run where mice passively viewed gratings in 36 separate locations. The visual discrimination task consisted of a reward-based go/no-go structure.

It was found that significantly fewer ACC axons exhibited spatially specific responses than layer 2/3 V1 neurons. As well as this, instead of retinotopically matching layer 2/3 V1 neurons, ACC axons lying superficially to them relayed information about a wider

area of visual space in both azimuth and elevation. Although some ACC axons showed orientation selectivity, grouping them by the orientation preference did not result in any retinotopic matching. Together, these results demonstrated that ACC axons do not appear to be as visually responsive as or retinotopically matched to layer 2/3 V1 somas in the same location in V1 under passive conditions.

As well as this, it was found that ACC activity was not greater when mice performed trials correctly compared to incorrectly in visually guided tasks. This elevated activity appeared to occur during the response phase of the task and, in particular, in trials where mice carried out the motor response of licking. Taken together, these data suggested the neural projection from ACC to V1 was not involved directly in the perception of the visual stimulus, even when its onset could be predicted, and was instead associated with the motor response of the animal. On top of this, the activity of a fraction of these ACC axons appeared to be modulated by the addition of a reward.

Overall, the data presented here indicates that the ACC projection to V1 is involved in visually guided tasks but is associated more with the motor response of licking than the perception of the visual stimulus. The additional modulation by reward suggests that this association depends upon the outcome of trials and may therefore be important for behaviours such as reward timing.

Acknowledgements

The work presented in this thesis is my own but would not have been possible if not for all those who supported me throughout my PhD.

Firstly, I would like to thank my supervisors Prof. Frank Sengpiel and Dr Adam Ranson who guided me through each of the studies. They were both helpful and critical, allowing me to develop as a scientific researcher. Adam, especially, helped with teaching and giving advice on the techniques and analysis used throughout my thesis. I would also like to thank other members of the lab including Dr Richard Inman, who helped to develop the behavioural task, as well as Fangli Chen, who helped me carry out the detection task as well as providing mangoes.

I could not have asked for more supportive friends. I would like to especially thank Nicole Pacchiarini, Annelies de Haan, Richard Ludlow and Harley Worthy for always being up for coffee or a run whenever it was needed. Last, but by no means least, I would like to thank my family for their unwavering belief in me.

Contents

List of Figures

1 General Introduction

1.1 Introduction into bottom-up and top-down processing

The brain is a complex organ made up of an abundance of multifarious connections. The synergy of these allows it to interact with and interpret a vast number of stimuli from the outside world. To achieve this, two processing streams referred to as bottom-up and top-down, are used. Bottom-up processing involves detecting stimuli in the external world. It is, however, both impossible and undesirable to process information about the entire sensory environment at once and so top-down projections, which originate from within the brain itself, work to modulate sensory perception based on current context and previous experience. Each system must work dynamically to meet the demands of the current situation (Desimone and Duncan, 1995), and an imbalance between the two can lead to neuropsychiatric disorders such as schizophrenia (Friston, 1998).

Since the introduction of the concepts of bottom-up and top-down processing, their relative influence upon visual perception has been debated. The idea that visual perception is solely based on information carried by bottom-up processes, that are in turn driven directly by the sensory environment, was purported by Gibson's ecological theory of visual perception (Gibson, 1966; Gibson, 1979; Goldstein, 1981). This theory asserts that the dynamic optic array of light that reaches the eye is sufficient for the observer to interpret the environment without the aid of intervening top-down input. Integral to this theory is the accurate and efficient perception of invariants in the sensory environment such as gravity, the separation of two hemispheres of light at the horizon or the increasing density of optical texture. It cannot, however, explain natural visual illusions. On the other hand, Gregory (1970) argues for the contribution of top-down processing to visual perception. This involves the use of higher cognitive processing to apply past experience or stored knowledge to the interpretation of what is

perceived. It involves hypothesis testing, with errors leading to inaccuracies in perception, such as visual illusions. It is likely that both these systems are utilised. If faced with an unfamiliar situation, there would be no model on which to build visual perception and thus bottom-up processing would dominate the formation of visual perception. When situations gain familiarity, and perception can be based on learned constructs, this balance would shift to top-down processing.

To build a visual perception of the world from bottom-up and top-down processing, these streams must be organised so that information can be efficiently integrated and interpreted. In some instances, this is believed to be via a hierarchical organisation with bottom-up processing dominating ascending pathways and top-down dominating descending pathways (Theeuwes, 2010). In other cases, a more dynamic interpretation has been suggested where each type of processing can occupy ascending or descending pathways, and the demarcation is instead to do with flexibility in the information carried (Rauss and Pourtois, 2013). What is common to all approaches, however, is that bottom-up projections convey signals that faithfully represent the sensory environment and must thus illicit predictable activity in sensory cortices that remains robust and consistent regardless of context or learning. On the other hand, top-down projections need to be flexible so that their activity, and in turn influence, can change depending on experience and context.

Primary visual cortex (V1) is one site at which bottom-up and top-down projections converge and thus the influence on neural activity of both can be examined there.

1.2 Bottom-up projections in the visual system

The bottom up projection from the eye to V1, and subsequent receptive field properties observed there, are believed to faithfully relay information about the external environment to sensory cortices.

1.2.1 From the eye to primary visual cortex

Mice have two eyes positioned laterally resulting in hemi-panoramic vision (Priebe and McGee, 2014). The visual field of each eye covers both monocular and binocular locations with an overlap of approximately 40° of observable space (Figure 1.1).

Light hits the eye and travels through the cornea, pupil, lens and vitreous chamber before reaching rods and cones located at the retina. At this point, the light is converted into electrical impulses and this signal is carried to retinal ganglion cells (RGCs). As it is transmitted, it undergoes a filtering process by retinal interneurons including horizontal, bipolar and amacrine cells which shape the output carried by the RGCs. There are currently believed to be 33 different types of retinal ganglion cells (Baden *et al.*, 2016), which each respond to a particular aspect of the visual scene.

From here, the signals are transmitted to a diverse range of targets across the brain. Visualisation of these projections using cholera toxin B subunit has elucidated that no less than 46 brain regions are innervated directly by RGCs in the mouse (Morin and Studholme, 2014), providing visual information to circuits involved in multiple functions including image formation. One such target is the dorsal lateral geniculate nucleus (dLGN) which in turn relays information directly to the visual cortex. Other terminals include the superior colliculus and the pulvinar nuclei.

The projection from RGCs to visual cortex via the dLGN is crucial in image formation and subsequent visual perception. In this pathway, a proportion of RGCs cross hemispheres at the optic chiasm, the percentage of which is determined by the binocular visual range. Humans are highly binocular and so only approximately 50% of RGCs will cross at the optic chiasm. Mice, on the other hand, have a much smaller binocular range. This results in the majority of RGCs crossing, with only approximately 3-5% remaining on the ipsilateral side (Petros et al., 2008). From here, the RGCs project to the dLGN where the signals are filtered and modulated and then are transmitted to primary visual cortex (V1) via the optic radiation.

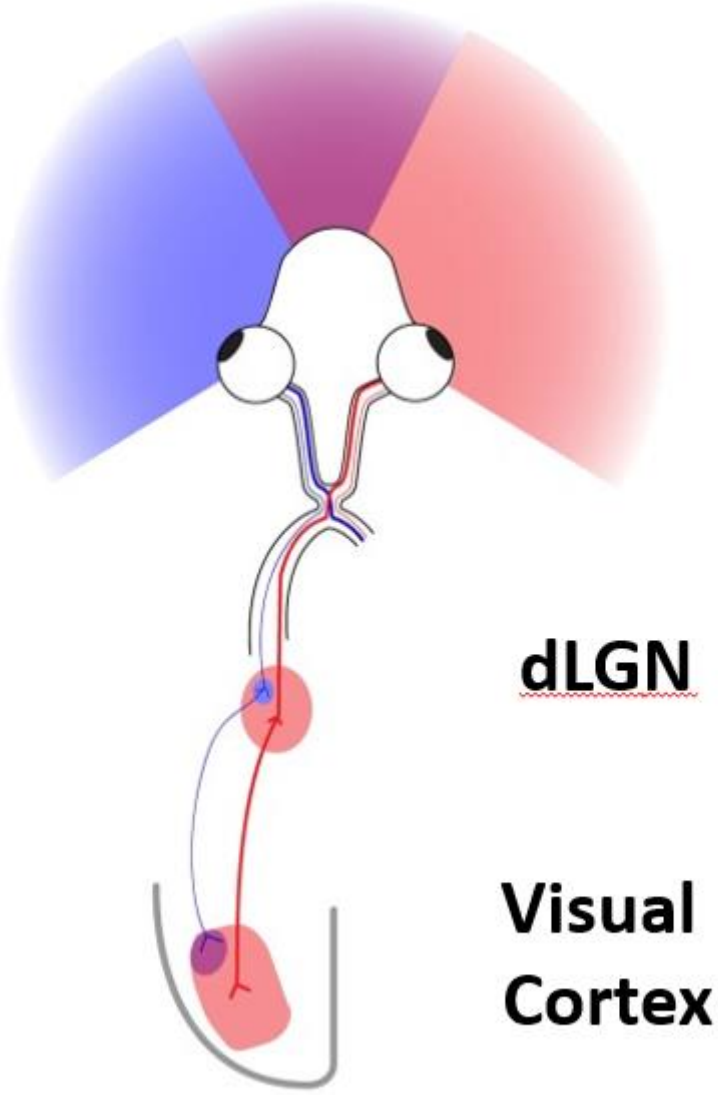

Figure 1.1: Schematic of the mouse visual system

The ipsilateral monocular (blue), contralateral monocular (red) and binocular (purple) visual fields are shown. Information about the visual scene is collected by the eyes and transmitted via the dLGN to visual cortex from both the ipsilateral (blue) and contralateral (red) eyes. Figure adapted from Priebe *et al.,* 2014.

1.2.2 The structure and classical visual properties of V1 neurons in mice

Visual cortex, and in particular primary visual cortex (V1), has been extensively studied across species. It consists of multiple anatomically and functionally distinct regions and features that together form a hierarchical structure to aid visual perception.

Anatomically, visual cortex resides in a posterior position of the neocortex of the mouse. Primary visual cortex (V1) lies within the centre of the visual cortex, is surrounded by higher visual areas (HVAs) identified via intrinsic signal imaging (Kalatsky and Stryker, 2003; Garrett *et al.*, 2014; Juavinett *et al.*, 2016) and responds to a broad range of visual stimuli (Andermann *et al.,* 2010). It covers approximately $3mm^2$ of the neocortex and consists of layers 1-6, with layer 1 being most superficial. Input from the thalamus is derived predominantly from core-type excitatory neurons that primarily project to layer 4, although there is also thalamic input to layer 1 (Rubio-Garrido *et al.*, 2009; Figure 1.2A). V1 additionally receives callosal projections from the contralateral hemisphere that terminate in layer 1-3 and 5 (Mizuno *et al.,* 2007).

Each layer of mouse cortex is populated with neurons that differ in morphology, function and projection patterns. One subset of these neurons are excitatory and can be divided into three main groups (Figure 1.2). Intratelecephalic pyramidal (IT) neurons are located in layers 2-6 and play the predominant role of receiving input from axons projecting from the dLGN in layer 4 of visual cortex. These neurons project only in the telencephalon and extensively connect left and right hemispheres via the corpus collosum and anterior commissure. Within this group of neurons there are numerous subtypes identified by their differing locations and projection patterns, something that may in turn be controlled by their genetic composition (Harris and Shepherd, 2015). Pyramidal tract (PT) neurons are located in L5B and project to subcerebral destinations such as the brainstem and spinal cord. Corticothalamic (CT) reside predominantly in layer 6 and project primarily to the ipsilateral thalamus (Harris and Shepherd, 2015).

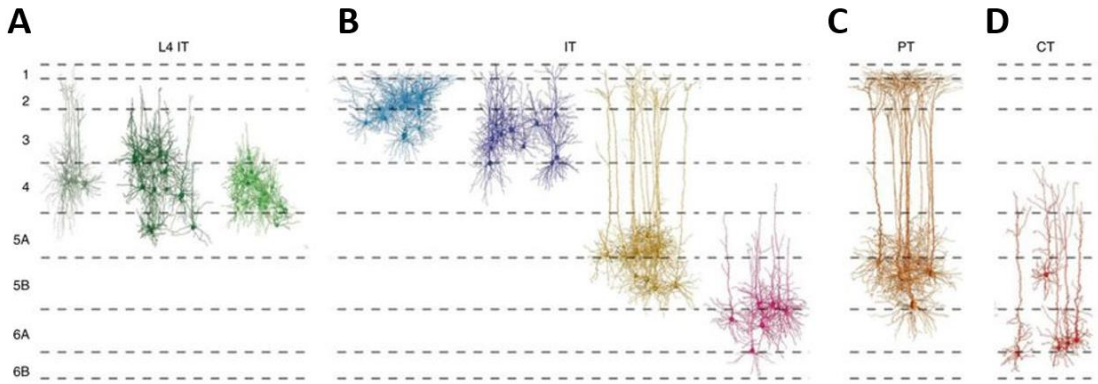

Figure 1.2: Excitatory neurons in V1

A: Intratelencephalic (IT) neurons that receive input from neurons projecting from the dLGN of the thalamus reside in layer 4 and project mainly to layer 2/3 of V1. **B:** IT neurons also constitute neuronal cell types in layers 2/3, 5 and 6 of V1. **C:** Pyramidal tract (PT) neurons are located in layer 5, project to superficial V1 and innervate subcerebral destinations. **D:** Corticothalamic (CT) neurons originate in layers 5 and 6 of V1. Figure adapted from Harris and Shepherd, 2015.

From visual cortex, pyramidal neurons project to other structures including ACC. Retrograde labelling has shown that, in this case, pyramidal neurons project from L2/3 and 5 of ACC to L1 of V1 (Zhang et al., 2014; Zhang et al., 2016; Figure 1.3A-C). Anterograde tracing using an AAV expressing mCherry injected into V1 has indicated that there is a reciprocal connection from V1 to ACC (Zhang et al., 2016; Figure 1.3D).

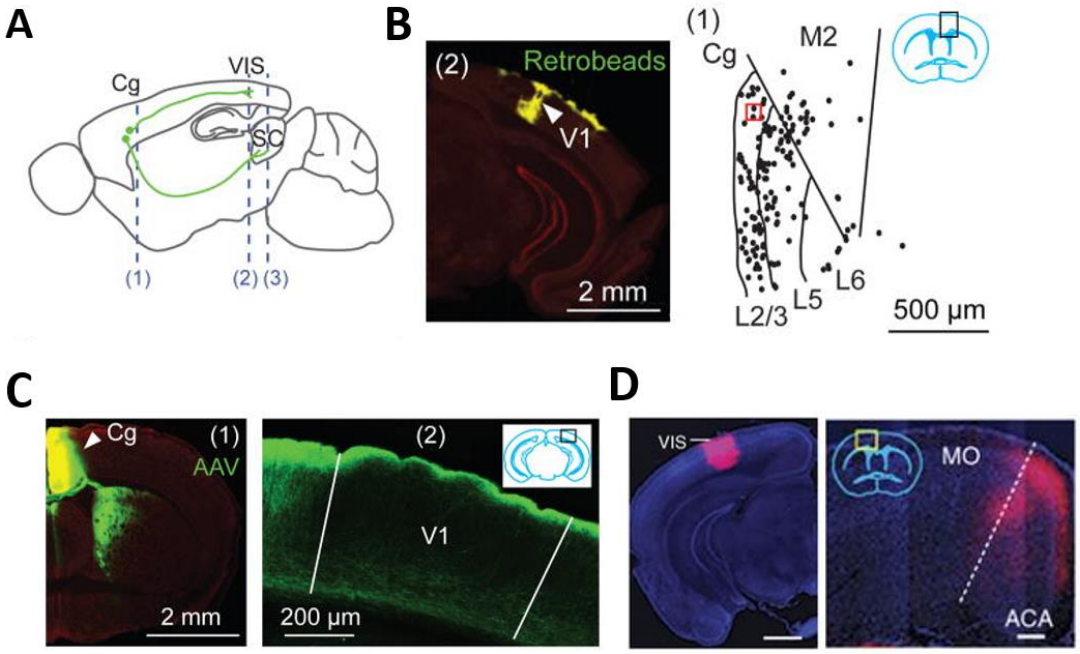

Figure 1.3: Reciprocal projection between ACC and V1

A: Sagittal diagram of a mouse brain indicating the locations of slices shown in B and C **B:** Left: The site from an injection of retrograde beads into V1. Right: All the locations of stained neurons in ACC as a result of the retrograde injection in V1. **C:** Left: An injection site at ACC for anterograde staining. Right: The stained neurons in V1 suggesting ACC axons project predominantly to L1 V1. **D:** Left: The injection site in V1 for anterograde labelling using mCherry. Right: ACC (also referred to as the anterior cingulate area (ACA)) neurons labelled from the injection of anterograde tracer in V1. Figure adapted from Zhang *et al.,* 2014 and Zhang *et al.,* 2016.

As well as excitatory pyramidal neurons, V1 contains an array of GABAergic interneurons arranged in a specific circuitry. Parvalbumin positive (PV+) cells strongly inhibit one another and pyramidal neurons, but provide little to other interneurons, Somatostatin positive (SST+) neurons are different in that they avoid inhibiting other SST+ cells and instead target all other populations. Vasoactive Peptide positive (VIP+) interneurons preferentially inhibit SST+ neurons (Pfeffer *et al.*, 2013; Figure 1.4B). This system allows for multi-tier modulation of pyramidal neurons, and connectivity across layers (Jiang *et al.*, 2015; Pakan *et al.*, 2016).

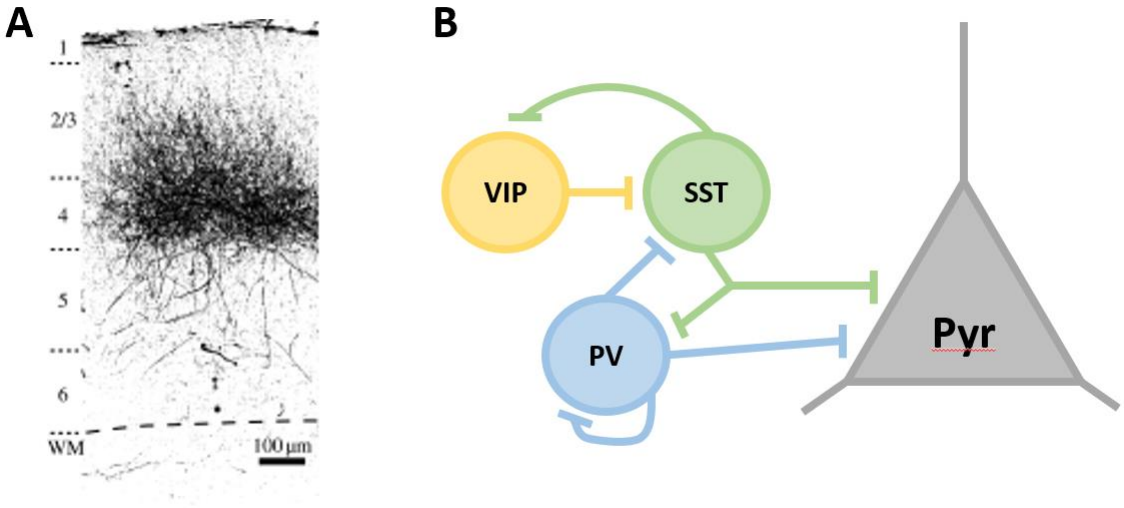

Figure 1.4: Structure within V1

A: Mouse V1 is made up of layers 1-6 and receives the majority of input from the thalamus via the optical radiation, which terminates mainly in layer 4 (adapted from Smith *et al*., 2008 and shown in more detail in Figure1.2). **B:** Interneuron networks in V1. VIP+ interneurons preferentially inhibit SST+ neurons. STT+ interneurons inhibit all other types, including excitatory pyramidal neurons. PV+ interneurons inhibit themselves as well as STT+ and pyramidal neurons. The majority of PV+ interneurons are basket cells and make multiple, large synapses on the proximal dendrites and cell bodies of pyramidal neurons. They are typically fast-spiking (Callaway, 2016). SST+ interneurons are a prominent source of input to the apical tufts of pyramidal neurons and possibly regulate feedback and lateral influences (Callaway, 2016).

A major primary functional organisation within V1 is the retinotopic map. Neurons positioned in medial V1 respond to more monocular areas of visual space, and more lateral V1 neurons represent binocular areas of central visual space. As well as this, anterior and posterior V1 respond to stimuli lower and higher in the visual field respectively (Kalatsky and Stryker, 2003). This results in a range of responses that systematically cover visual space.

Neurons within V1 also possess functional receptive field properties believed to be fundamental to visual processing. One such property is orientation selectivity, namely, where a neuron responds preferentially to edges presented at a specific orientation. It has been shown that this neuronal response is conserved across animals including cats (Hubel and Wiesel, 1962) and monkeys (Hubel and Wiesel, 1968; Wurtz, 1968). In these animals, they are arranged in secondary maps where multiple neurons with overlapping responses are organised in pinwheels (Maldonado *et al.*, 1997) and precise columns as little as one cell wide (Ohki *et al.*, 2005). Mouse V1 also contains neurons which show orientation preference and, despite some studies suggesting a comparatively disorganised 'salt and pepper' distribution (Dräger, 1975; Métin *et al.,* 1988), some clustering of similarly selective neurons may occur (Ringach *et al.*, 2016). Although initial reports suggested the minority of cells possessed orientation selectivity (Dräger, 1975), more recent investigation has indicated a much higher rate of up to 74% as well as a median tuning half width at half maximal response of 20° (Niell and Stryker, 2008). This was true for excitatory neurons in all layers, with the highest sharpness of orientation tuning being observed in layer 2/3, which was in contrast to inhibitory neurons which remained largely untuned (Sohya *et al.*, 2007; Niell and Stryker, 2008). Furthermore approximately 23% of neurons, mainly in layers 2/3 and 4 also showed direction selectivity at their preferred orientation (Niell and Stryker, 2008) and had a broad spectrum of preference for spatial and temporal frequencies (Andermann *et al.,* 2010).

Mice have also been observed to possess both simple and complex receptive fields. First reported in the cat (Hubel and Wiesel, 1962), responses of simple cells occur to a particularly oriented visual stimulus in a specific location in visual space. Whereas the response of simple cells is linear and can be predicted by the sum of responses at individual locations, complex cells demonstrate nonlinear spatial summation and respond to particularly oriented stimuli at a greater range of retinotopic locations. Both types have been identified in mouse visual cortex (Dräger, 1975; Niell and Stryker, 2008), although the majority of excitatory neurons in layers 2/3, 4 and 6 are classed as simple cells (Niell and Stryker, 2008). Thus, the mouse presents a useful model in which visual responses can be studied.

1.2.3 Higher visual areas in mice

The structural and functional properties of V1 make it ideal to process basic features of the visual scene before transmitting specific subsets of information to anatomically and functionally distinct higher visual areas (HVAs). Triple anterograde tracing has revealed feedforward projections from V1 that terminate in nine HVAs (Wang and Burkhalter, 2007; Figure 1.5A) surrounding V1. This, coupled with the advancement of intrinsic signal imaging techniques resulting in a dramatic increase in spatial resolution (Kalatsky and Stryker, 2003) has led to the identification of up to ten HVAs (Garrett *et al.*, 2014; Juavinett *et al.*, 2016; Figure 1.5B/C). Two-photon experiments in awake, behaving animals have shown that different HVAs respond preferentially to distinct ranges of stimulus parameters. Anterolateral (AL), lateromedial (LM), rostrolateral (RL) and anteromedial (AM) areas responded to stimuli with temporal frequencies three times greater than V1, but preferred stimuli with significantly lower spatial frequencies (Andermann *et al.,* 2010; Marshel *et al.*, 2011). AL, RL and AM also exhibited significantly more direction selectivity than V1, with all areas showing increased orientation selectivity (Marshel *et al.*, 2011). This suggests that HVAs may have

individual properties that allow each area to be independently specialised in processing specific elements of the visual environment involving motion- or pattern-related computations.

Furthermore, visual information is thought to pass from V1 to HVAs, and then enter circuits analogous to the dorsal and ventral streams documented in non-human primates. Lesion studies in non-human primates have revealed distinct functions for these two visual processing pathways (Mishkin *et al*., 1983). The ventral stream is crucial for object recognition, whereas the dorsal stream is important for the perception of motion and action, such as hand-eye coordination (Goodale and Milner, 1992). Visually driven activity in HVAs in mice can also be divided into two subnetworks where one, including areas PM, AM, A, RL and AL is believed to be analogous to the dorsal stream, and the other, including areas LM and LI, the ventral stream (Murakami *et al.,* 2017; Smith *et al.*, 2017).

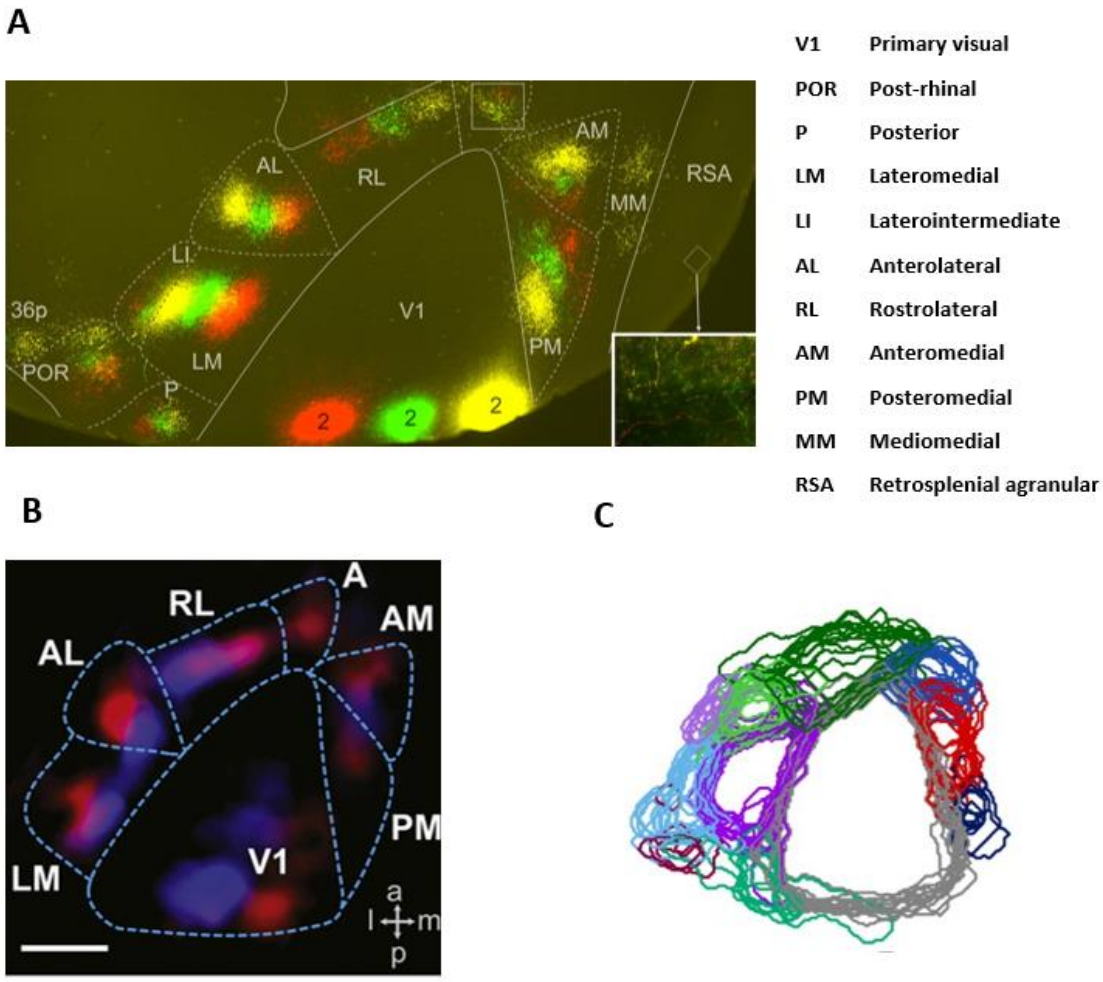

Figure 1.5: Arrangement of higher visual areas (HVAs) in visual cortex

A: Triple anterograde tracing revealed feedforward projections from V1 to surrounding HVAs. Sites of the injection are shown in red, green and yellow in V1, and sites where the neurons project to are shown in the corresponding colours in each extra-striate region (adapted from Wang and Burkhalter *et al*., 2006) **B:** Intrinsic signal imaging shows higher visual areas in visual cortex (adapted from Andermann *et al*., 2011). **C:** These higher visual areas have been grouped into at least 10 anatomically and structurally distinct regions (adapted from Garrett *et al*., 2014)

1.3 Top-down influences on the visual system

Sensory systems are continuously being bombarded by a plethora of stimuli from the external environment. These systems have limited processing capacity and so, in situations where these visual stimuli must be observed during motion or attended to by directing attention using previous experience, these bottom-up projections do not work in isolation. Instead, to improve processing efficiency, top-down projections, which originate from within the brain itself, are able to influence the receptive field properties of V1 neurons. It is thought that this occurs through the development of internal representations of the external environment to allow prediction. This phenomenon is most obvious in the way that visual illusions trick the brain (Weiss *et al.,* 2002). One example is the Kanizsa Triangle where a triangle can be perceived even though it is not physically there (Figure 1.6A). Another is the contrast-contrast illusion (Figure 1.6B) where people tend to report the centre image as being a lower contrast than it is (Dakin *et al.,* 2005).

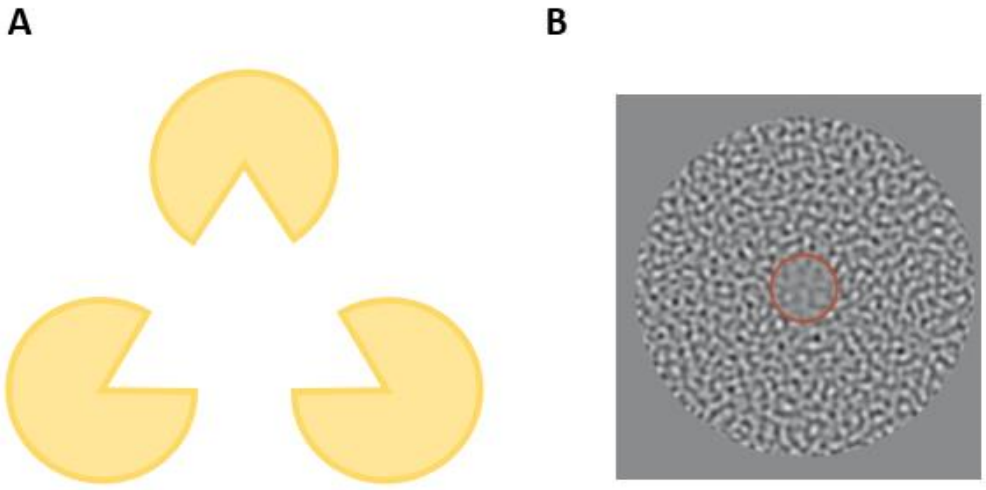

Figure 1.6: Optical illusions indicating the necessity of internal representations to interpret visual stimuli

A: The Kanizsa Triangle optical illusion tricks the brain into seeing a triangle which is not physically there. **B:** A contrast-contrast illusion where the contrast of the image in the centre is less than that of the outside. Participants frequently report the contrast of the centre image incorrectly (adapted from Dakin *et al*., 2005).

The ability to predict the visual environment based on previous experience would be beneficial in certain scenarios. For example, for a mouse, an efficient response would be advantageous when trying to evade predation.

1.3.1 Top-down modulation of V1 neurons during locomotion

Visual cortex neuronal responses are modulated by locomotion. Electrophysiological analysis and two-photon imaging of genetically encoded calcium indicators have shown that excitatory pyramidal neurons increase their firing rate during locomotion as opposed to when the mouse is stationary (Niell and Stryker, 2010; Keller, Bonhoeffer and Hübener, 2012; Bennett, Arroyo and Hestrin, 2013; Saleem *et al.*, 2013; Erisken *et al.*, 2014). This does not, however, affect stimulus selectivity (Niell and Stryker, 2010). Whole-cell electrophysiological recordings showed that, whilst a mouse runs, the membrane potential of layer 2/3 and layer 4 pyramidal neurons become more depolarised and less variable (Polack *et al.,* 2013) resulting in a higher likelihood of persistent firing to stimuli reported by bottom-up circuitry.

This activity is likely to be highly influenced locally by networks of interneurons. When mice run without any visual stimuli, pyramidal neurons and VIP+ interneurons are activated while SST+ interneurons show little activity (Pakan *et al.*, 2016; Dipoppa *et al.*, 2018) suggesting that modulation occurs through VIP+ interneurons activating SST+ interneurons which would lead to disinhibition of pyramidal neurons. When mice were presented with visual stimuli, however, the activity of SST+, VIP+ and PV+ cells all increased (Pakan *et al.*, 2016) indicating a complex network able to precisely control pyramidal activity depending on the state of the animal and context of the environment.

These networks are, in turn, likely to be modulated by longer-range direct top-down projections from brain regions converging into visual cortex as locomotion driven activity is not as easily observed in the dLGN, a major relay in the bottom-up pathway

(Erisken *et al.*, 2014) if any increase was seen at all (Niell and Stryker, 2010). Cholinergic input has been shown to be essential for maintaining membrane potential properties during immobility, whereas noradrenergic input is necessary for depolarisation associated with locomotion (Polack *et al.,* 2013). V1 receives cholinergic input from the basal forebrain, which is in turn innervated by the mesencephalic locomotor region (MLR), a structure implicated in the initiation of running (Lee *et al.*, 2014). Optogenetic stimulation of the MLR inputs to the basal forebrain has been associated with significant changes to spontaneous firing rates of V1 neurons (Lee *et al.*, 2014). On the other hand, studies have suggested the involvement of the glutamatergic ACC projection to V1 as it is thought to modulate mismatch signals observed in visual cortex while mice navigate a virtual reality tunnel (Fiser *et al.*, 2016). Furthermore, a projection from ACC and neighbouring M2 is thought to convey strong motor signals. Calcium imaging has shown that axons of this projection terminating in V1 show increased activity that begin before animals start to run, and if this activity is inactivated then their locomotion triggered V1 responses are decreased (Leinweber *et al.*, 2017).

1.3.2 Top-down modulation of V1 during visual attention

Top-down modulation of attention is believed to influence the already established receptive field properties of visual cortex neurons. Pyramidal cells are retinotopic and show orientation selectivity. These responses can be amplified or suppressed depending on the demands of the current situation.

In attentional tasks, it has been observed that neurons tuned to properties of the behaviourally relevant stimulus show increased responses, whereas neurons tuned to ignored stimuli have a reduction in response. Studies in which non-human primates have been trained to attend to a stimulus in one location have shown increases in neural responses in areas V1, V2 and V4 whose receptive fields are at the attended

location (Moran and Desimone, 1985; Spitzer, Desimone and Moran, 1988; Motter, 1994; Reynolds, Pasternak and Desimone, 2000).

Training non-human primates to pick out contours from complex visual scenes leads to an increase or suppression of responses from neurons in the corresponding retinotopic region of the contour and background components respectively (Li *et al*., 2008; Yan *et al.*, 2014). In tasks that involve discriminating between orientations, attention enhances responses to the preferred one, but does not change the width of the orientation tuning curve (McAdams and Maunsell, 1999; Schoups *et al.*, 2001). This is also true for direction selective neurons where increases in gain area observed for the attended stimulus without narrowing the direction curve (Treue and Maunsell, 1996). This increase in gain is not observed to be linear, but instead dependent on properties of the attended stimulus such as contrast (Reynolds *et al*., 2000; Williford and Maunsell, 2006). Neuronal responses have also been observed to dramatically reduce for unattended stimuli (Moran and Desimone, 1985).

Surround suppression, a phenomenon where the response of a neuron decreases as the stimulus it is responding to is enlarged (Blakemore and Tobin, 1972; Sengpiel *et al.,* 1997), is important in visual processing, and also appears to be important in the direction of visual attention. This is especially true when the attended and ignored stimuli are in close spatial proximity as irrelevant stimuli that appear within the receptive field of V1 neurons responding to the location of an attended stimulus could elicit a response that could degrade that to the attended stimulus. A number of studies have shown that spatial attention can prevent this by modulating surround suppression, thereby eliminating the suppressive responses to the unattended stimulus (Kastner *et al.*, 1998; Kastner and Ungerleider, 2000; Chen *et al.*, 2008; Sundberg *et al.,* 2009). Furthermore, this suggests that attentional influences need to be spatially organised in V1. This appears to be the case as other experiments have shown that, during

functional magnetic resonance imaging (fMRI) imaging of humans requiring shifts of visual attention from one location to another, cortical topography of the attention driven activity was matched by that evoked by cued targets (Tootell *et al.*, 1998; Brefczynski and DeYoe, 1999). Studies suggest that both the prefrontal and parietal cortices are crucial in modulating visual attention. Changes in activity detected using fMRI have shown elevated levels in both cortical areas when performing tasks involving visual attention (Beauchamp *et al.*, 2001; Corbetta and Shulman, 2002) while lesions to frontal or parietal cortex have shown deficits in visual attention in non-human primates (Gregoriou *et al.*, 2014) and rodents (Broersen and Uylings, 1999).

In tasks in which mice were required to complete visually guided tasks, a similar trend to that observed in non-human primates has been demonstrated in which neurons that show preference for the relevant stimulus have increased responses, while responses of others are suppressed. In one such study, mice learned to discriminate two visual patterns that differed in orientation while navigating through a virtual reality corridor. Two-photon imaging of a calcium activity indicator in layer 2/3 of V1 showed that improvements in the ability of the mouse to gain a reward in response to the relevant stimulus and thus improved performance was closely associated with distinguishable differing responses over time. Neurons that preferred the rewarded stimulus exhibited an increased amplitude of response over days, whereas neurons that responded to the unrewarded stimulus exhibited a decrease (Poort *et al.*, 2015). Furthermore, neurons that preferred the orientation of relevant stimuli in other orientation discrimination tasks displayed sharper orientation tuning when stimuli of their preferred orientation gained relevance (Goltstein *et al.*, 2013; Jurjut *et al.*, 2017). Furthermore, neurons that preferentially responded to similar orientations increased their tuning bandwidth (Goltstein *et al.*, 2013), thus leading to additional neuronal responses to the relevant stimulus. This has also been demonstrated in visuospatial processing. In this case, two stimuli of the same orientation were presented in different locations in visual space.

Two photon imaging indicated enhanced population coding for retinotopic location of the neurons that preferentially responded to the location of the rewarded stimulus (Goltstein *et al.,* 2018).

Taken together, this evidence suggests that activation properties of V1 neurons appear to undergo modulation in mice when the stimuli they response to gain relevance during visually guided behaviour. This occurs by increasing or decreasing their likelihood of firing depending on whether the stimuli match the location or features of the attended object.

1.3.3 Predictive coding as an explanation for visual perception

In visually guided tasks, the brain must combine information conveyed by bottom-up projections that faithfully represent the external environment with top-down inputs. It has been shown that, over the course of learning, the relative impact of each of these types of projection is flexible with the influence of top-down inputs strengthening after task dynamics become familiar (Makino and Komiyama, 2015). The influence of top-down inputs is thought to depend first upon the ability of the brain to encode which stimuli in the environment are associated with favourable outcomes and secondly to adaptively update these predictions based on changing experience. One model able to describe this is predictive coding. This model posits that top-down and bottom-up inputs are arranged in a hierarchical network where top-down predictions generated by an internal model are compared with actual sensory stimuli to detect errors so that the behavioural response with the most favourable outcome can be made (Rao and Ballard, 1999; Friston, 2005; Clark, 2013; Figure 1.7). This has been used to successfully simulate visual neuronal properties such as endstopping (Rao and Ballard, 1999). For this to work successfully, the system must be able to encode the visual stimulus, and whether a behavioural response to it will result in a favourable outcome, as well as detect errors. Each of these levels of processing may be done at different

levels in the hierarchy and thus there must be reciprocal connections so that signals driven by bottom-up and top-down projections can converge in order to detect any discrepancies between the top-down prediction and bottom-up information. Top-down influences would then flexibly adapt depending on errors in the prediction.

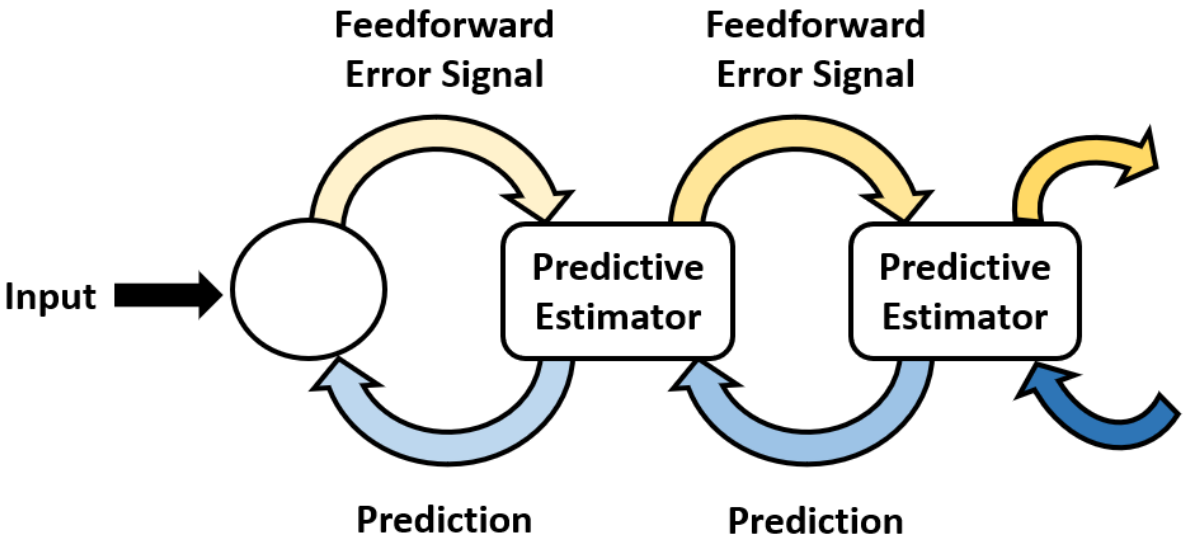

Figure 1.7: Schematic of predictive coding model

The hierarchy proposed to be present in the generation and updating of internal representation of the external world. Feedback (top-down) pathways carry predictions based on context and previous experience, and these predictions are compared to feedforward (bottom-up) signals at multiple levels of cortical processing. Errors that are generated are used to update the representation (adapted from Rao and Ballard, 1999).

1.3.4 An imbalance in top-down and bottom-up processing can result in neuropsychiatric conditions such as schizophrenia

Imbalances in bottom-up/top-down influence have been associated with the neuropsychiatric disorder schizophrenia. Schizophrenia is characterised by positive, including delusions and hallucinations, and negative, including diminished emotional expression or avolition, symptoms. People with schizophrenia exhibit altered cognition and show significant deficits in performance in tasks involving selective and sustained visual attention in comparison to healthy controls (Neuchterlein *et al.*, 1991; Fioravanti *et al.*, 2005; Carter *et al.*, 2010). One possible explanation for it is the disconnection hypothesis which stipulates that these cognitive deficits arise as a result of a failure of proper functional integration of systems in the brain responsible for adaptive sensorimotor integration and cognition (Friston, 1998, 2005). This would involve aberrant communication between bottom-up and top-down circuits, likely as a result of impaired *N*-methyl-D-aspartate (NMDA) receptor functioning (Coyle, 2012). This could result in an impaired capacity to store and flexibly update an internal representation of the external environment and manifest as schizophrenic symptoms such as visual hallucinations. Although it must be noted that schizophrenia is a complex disorder that is not well understood and is characterised by more than just NMDA receptor hypofunction. Another explanation is the dopamine hypothesis which postulates that schizophrenia is as a result of hyperactivity of dopamine D2 receptors in subcortical and limbic brain regions (reviewed in Baumeister and Francis, 2002).

Aberrant activity in top-down and bottom-up circuits can be examined in a number of ways. Studies using a masking paradigm, where an image is used to conceal a relevant visual stimulus, can distinguish between bottom-up and top-down mechanisms by appearing either before or after the relevant visual stimulus respectively have indicated that schizophrenic participants show deficits in top-down, but not bottom up

processing (Green *et al.*, 1999; Dehaene *et al.*, 2003). Moreover, inaccurate reports of stimulus properties from healthy people when faced with visual illusions, something that inherently rests upon prior experience to induce a false percept, are often not observed in people with schizophrenia (Butler *et al.,* 2008; Barch *et al.*, 2012; Brown *et al.*, 2013). Taken together, these data suggest that there are deficits in top-down processing, something that is supported further by known hypoactivation of regions in the brain thought to influence this processing, such as ACC and PFC (Dehaene *et al.*, 2003). People with schizophrenia, however, also report hallucinations which have been associated with a shift that favours prior knowledge over incoming stimuli (Teufel *et al.*, 2015; Powers *et al.,* 2017). In the schizophrenic mouse models with global NMDAR hypofunction, aberrant top-down frontal cortex activity in ACC axons projecting to primary visual cortex has been observed in. Under these conditions, ACC axonal activity is significantly increased which subsequently leads to an ACC dependent net suppression of activity in V1. The different balance between the relative influence of top-down and bottom-up influences in this model compared to untreated controls is likely to lead to perceptual disturbances (Ranson *et al.*, 2019). Overall this suggests there is an imbalance of top-down and bottom-up processing, which is also likely to explain visual attention deficits observed.

Those with schizophrenia have profound problems in focusing attention on salient cues and ignoring distracting influences (Braff, 1993; Carter *et al.*, 2010; Hoonakker, Doignon-Camus and Bonnefond, 2017), especially in tasks requiring precise attentional control (Coleman *et al.*, 2009). To extend understanding of how schizophrenia, and other disorders related to the imbalance of top-down and bottom-up impact, it is important to study how top-down projections function to modulate sensory cortices such as V1.

1.4 The top-down influence of ACC upon V1

1.4.1 The structure and function of ACC lends itself to maintaining and updating representations

ACC has been implicated in modulating the activity of V1 neurons via top-down projections, and its erroneous activity has been linked to schizophrenia (Dehaene *et al.*, 2003). To be involved in top-down modulation ACC must be able to build and update internal representations of the world. With regards to the direction of visual attention, this would involve association of visual stimuli with a favourable outcome, and possibly the ability to influence behavioural responses. Each would require reciprocal connections to V1, reward processing structures and motor cortices.

In humans, the ACC is located in Brodmann's area 24, 25 and 32 and is classically considered as part of the limbic system. It has also, however, been implicated in playing a role in visually-guided tasks that require selective attention, especially under conditions of increased response competition (Carter *et al.*, 1998). Functional magnetic resonance imaging of humans performing the Stroop test, where a particular colour is written in an ink of a different colour and the participant is required to report the colour of the ink, activity in the ACC is elevated (Pardo *et al.*, 1990). In particular, this activity was noted during the response (MacDonald *et al.*, 2005). ACC has also been implicated to play a role in visual attention in non-human primates (Isomura *et al.*, 2003) and rodents (Zhang *et al.*, 2014; Wu *et al.*, 2017).

Interestingly, ACC has been implicated in the perception of and response to rewarding stimuli across species. A reward acts as a positive reinforcer that will increase the probability of a behaviour being repeated. These types of stimuli activate dopaminergic neurons in the ventral tegmental area of the midbrain which then project to the nucleus

accumbens, the ventromedial portion of the caudate nucleus, the basal forebrain and the frontal cortex, of which the ACC is a part (Geisler *et al.*, 2007). Activation of the ACC has been observed in mice after administration of substances known to activate reward systems in the brain such as cocaine (Liu *et al.*, 2016) and nicotine (Dehkordi *et al.*, 2015). Human fMRI studies suggest that there is significant activation of the ACC in response to liquid consumption (Kringelbach *et al.*, 2003) and that this is positively correlated with ratings of pleasantness (de Araujo *et al.*, 2003) while being independent of satiety (Kringelbach *et al.*, 2003; Rolls and McCabe, 2007). Reward responses have also been observed in the ACC in non-human primates. Single cell recordings of neurons in the macaque suggested the presence of different types of cellular activity in the ACC in response to reward. Certain neurons were particularly active immediately after the reward, while the activity of others progressively increased in advance of the next (Shima, 1998). In addition to this, neurons in the ACC were observed to increase in activity as monkeys progressed through a visually cued multi-trial reward schedule in which a reward was gained only if they responded correctly to four visual colour discrimination trials in a row (Shidara and Richmond, 2002). Taken together, these data suggest that the ACC both responds to and predicts the likelihood of obtaining rewards across species and that these rewards can be visually cued and thus must reflect specific attentiveness to incoming sensory stimuli. This suggests that a connection to the visual system is essential.

ACC contains populations of motor neurons and is well connected to regions of the brain and nervous system involved in motion. In non-human primates, it has reciprocal connections with both the primary motor cortex and supplementary areas, as well as corticospinal outputs that terminate in the intermediate zone of the spinal cord (Dum and Strick, 1991; Morecraft and van Hoesen, 1992). Projections to M1 were also observed in the rat and are thought to be involved in the regulation of motor activity that

involves orofacial and forelimb parts of the body (Wang *et al.*, 2008). Human fMRI studies have shown that, while participants carried out a normal and a task-switching version of the Stroop test, ACC is specifically active during the response phase of the task (MacDonald *et al.*, 2005). Furthermore, studies in non-human primates performing a delayed conditional go/no-go discrimination task found responses in cingulate motor areas that exhibited attention-like activity in response to visual cues (Isomura *et al.*, 2003). Taken together, this evidence suggests a role for ACC in instigating the motor output during tasks that involve decision making.

Overall, this suggests a role for ACC in performing visually guided behaviour requiring selective attention, and that its modulation is most likely to be involved in instigating the motor output during tasks that involve decision making. ACC is reciprocally connected to V1 in mice (Zhang et al., 2016) and thus has the circuitry to be a candidate for this top-down modulation.

1.4.2 Projection profile of ACC neurons in mice

ACC sends projections to multiple structures within the brain, each with differing density. Filinger *et al.,* (2018) iontophoretically injected the anterograde tracers *Phaseolus vulgaris* leucoagglutinin and biotin dextran amine along the rostrocaudal extent of both ACC, denoted as areas 24a and 24b, and medial cingulate cortex (MCC), denoted as areas 24a' and 24b' and visualised where axons emanating from these areas projected to. Figure 1.8 shows an overview of the projection density to all identified terminals of labelled ACC axons. ACC provides a dense input to visual cortex, especially higher visual areas located medially. Light labelling from 24a and moderate to dense labelling from 24b to V1 suggests a topographical arrangement of projections from ACC. It is also noteworthy that areas 24a and 24b have dense

projections within their own regions, and that there is a moderate to dense projection to the medial and ventral oribital areas. Filinger *et al.,* (2018) also show a plethora of other projections from ACC. Of note are the dense projections to the ipsilateral caudate-putamen (CPu) in the non-cortical forebrain, the claustrum (Cl), also shown by Qadir *et al.,* (2018), the anteromedial and reticular nucleus of the thalamus and various targets in the brainstem including the periaqueductal grey and the superior colliculus.

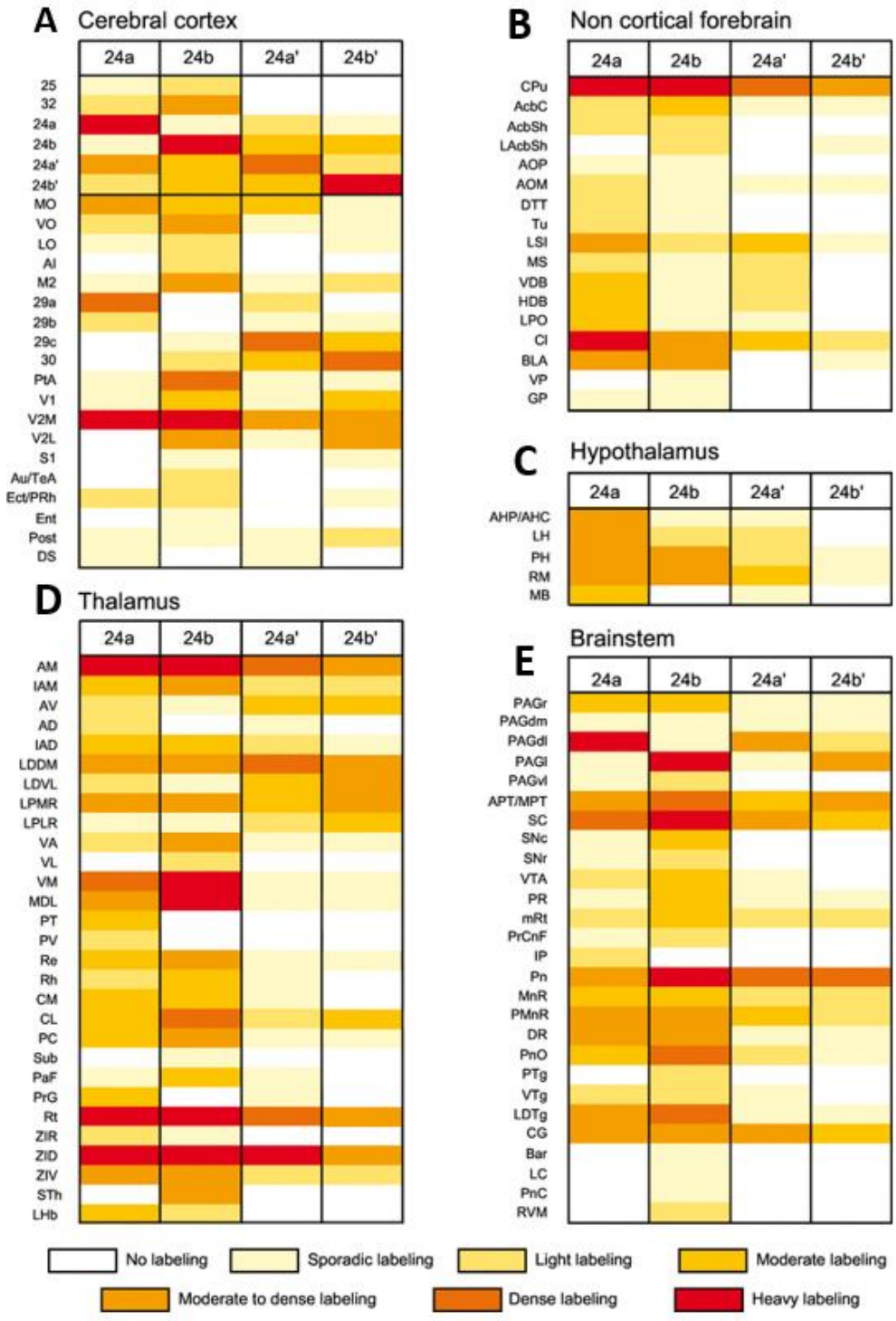

Figure 1.8: The density profile of ACC projections

ACC projects to various structures neural structures with differing densities, shown here where red indicates dense and pale yellow sparse. The areas which ACC project to have been divided into the brain regions in which they preside including the cerebral cortex (A), non-cortical forebrain (B), Hypothalamus (C), Thalamus (D), and brainstem (E). Abbreviations are shown in Table 1.1. Figure adapted from Filinger *et al.,* (2018).

AcbC Accumbens N, core region;

AcbSh Accumbens N, shell region;

AD Anterodorsal thalamic N;

AHC Anterior hypothalamic area, central part;

AHP Anterior hypothalamic area, posterior part;

AI Agranular insular cortex;

AM Anteromedial thalamic N;

AOM Anterior olfactory N, medial part;

AOP Anterior olfactory N, posterior part;

APT Anterior pretectal N;

Au Primary auditory cortex;

AV Anteroventral thalamic N;

Bar Barrington's N;

BLA Basolateral amygdaloid N, anterior part;

CG Central gray;

Cl Claustrum;

CL Centrolateral thalamic N;

CM Central medial thalamic N;

CPu Caudate putamen;

DR Dorsal raphe nucleus;

DS Dorsal subiculum;

DTT Dorsal tenia tecta;

Ect Ectorhinal cortex;

Ent Enthorinal cortex;

GP Globus pallidus;

HDB Diagonal band of Broca, horizontal limb;

IAD Interanterodorsal thalamic N;

IAM Interanteromedial thalamic N;

IP Interpedoncular N;

LAcbSh Lateral accumbens, shell region;

LC Locus coeruleus;

LD Laterodorsal thalamic N;

LDDM LD, dorsomedial part;

LDTg Laterodorsal tegmental N;

LDVL LD, ventrolateral part;

LH Lateral hypothalamic area;

LHb Lateral habenula;

LO Lateral orbital cortex;

LPLR Lateral posterior thalamic N, laterorostral part;

LPMR Lateral posterior thalamic N, mediorostral part;

LPO Lateral preoptic area;

LSI Lateral septal N, intermediate part;

M2 Secondary motor cortex;

MB Mammillary bodies;

MDL Mediodorsal thalamic N, lateral part;

MnR Median raphe N;

MO Medial orbital cortex;

MPT Medial pretectal N;

mRt Mesencephalic reticular formation;

MS Medial septal N;

PaF Parafascicular thalamic N;

PAG Periaqueductal gray;

PAGdl Periaqueductal gray, dorsolateral part;

PAGdm Periaqueductal gray, dorsomedial part;

PAGl Periaqueductal gray, lateral part;

PAGvl Periaqueductal gray, ventrolateral part;

PAGr Periaqueductal gray, rostral part;

PC Paracentral thalamic N;

PH Posterior hypothalamic N;

PMnR Paramedian raphe N;

Pn Pontine N;

PnC Pontine reticular N, caudal part;

PnO Pontine reticular N, oral part;

Post Postsubiculum;

PrCnF Precuneiform area;

PrG Pregeniculate N of the prethalamus;

PR Prerubral field;

PRh Perirhinal cortex;

PT Paratenial thalamic N;

PtA Parietal associative cortex;

PTg Pedunculotegmental N;

PV Paraventricular thalamic N;

Re Reuniens thalamic N;

Rh Rhomboid thalamic N;

RM Retromamillary N;

Rt Reticular N;

RVM Ventromedial medulla region;

S1 Primary somatosensory cortex;

SC Superior colliculus;

SNc Substantia nigra, *pars compacta;*

SNr Substantia nigra, *pars reticulata;*

STh Subthalamic N;

Sub Submedius N;

TeA Temporal association cortex;

Tu Olfactory tubercle;

V1 Primary visual cortex;

V2L Secondary visual cortex, lateral area;

V2M Secondary visual cortex, medial area;

VA Ventral anterior thalamic N;

VDB Diagonal band of Broca, vertical limb;

VL Ventrolateral thalamic N;

VM Ventromedial thalamic N;

VO Ventral orbital cortex;

VP Ventral pallidum;

VTA Ventral tegmental area;

VTg Ventral tegmental N;

ZI Zona incerta;

ZID ZI, dorsal part;

ZIR ZI, rostral part;

ZIV ZI, ventral part;

Table 1.1: Abbreviations linked to Figure 1.8

Abbreviations of each structure identified as a projection target of ACC in Figure 1.8. Arranged in alphabetical order.

1.4.3 Impact of top-down projections on V1 in mice

The projection from ACC to V1 in mice has been implicated in top-down modulation, but its precise function has been debated. Some studies propose its involvement in forming an internal representation of visual space based on spatial location and locomotion (Fiser *et al.*, 2016; Leinweber *et al.*, 2017), whereas another contends for it controlling selective visual attention (Zhang *et al.*, 2014).

Fiser *et al.* (2016) proposed the former. In this study, mice were allowed to repeatedly explore a virtual tunnel. The movement of the visual environment presented to the mouse was coupled with its own movement. Mice were encouraged to run to the end of the tunnel where they would receive a liquid reward. Visual stimuli were, for the most part, presented in a predictable manner. When the mice had gained experience of the process, a subset of neurons in layer 2/3 of mouse V1 exhibited responses that were predictive of the upcoming visual stimulus in a spatially dependent manner. This indicated that an internal representation had formed that was able to predict visual stimuli. Omitting any of these stimuli would result in an error between the prediction and sensory information from the external environment and was observed to drive strong responses in V1 neurons. This indicated that V1 neurons were able to predict spatially relevant stimuli, as well as detect those that did not fit the internal representation. These responses were also observed in ACC axons projecting to V1, suggesting these ACC axons as a source of this prediction (Fiser *et al.*, 2016). Furthermore, the activity of axons projecting from ACC and neighbouring M2 have been shown to be strongly correlated with locomotion while mice navigated a virtual environment. Two-photon imaging has shown that these axons increase in activity before the mouse begins to run, and that inactivating the projection leads to reduced mismatch and locomotor activity in V1, while activating it induces activity in running-related V1 neurons (Leinweber *et al.*, 2017).

The projection from ACC to V1 has also been implicated in selective visual attention. Zhang *et al* (2014) carried out a study where ACC was artificially stimulated in mice via optogenetics and subsequent attentional modulation in V1 neurons examined. Artificial stimulation of this projection led to an increase in V1 neuron firing rate to a stimulus of the neurons preferred orientation, but not the non-preferred orientation, reminiscent of the increase in visual cortical neuronal firing previously reported in attentional tasks (McAdams and Maunsell, 1999; Reynolds, Chelazzi and Desimone, 1999; Schoups *et al.*, 2001; Williford and Maunsell, 2006; Figure 1.9A). Furthermore, ACC activation significantly improved the ability of the mice to perform a visual discrimination task (Figure 1.9B).

Zhang *et al.* (2014) subsequently optogenetically stimulated ACC axons in V1 demonstrated that this sharpening of the tuning curve persisted, suggesting it was, at least in part, modulated by a direct connection between ACC and V1. Systematically moving this stimulation outwards from a central site resulted in a reduction in the tuning curve amplitude 200 μm from the recorded V1 neurons. This indicated ACC activity may contribute to a spatial response modulation involving surround suppression, something already observed in visual cortical responses during attentional tasks (Kastner *et al.*, 1998; Kastner and Ungerleider, 2000; Chen *et al.*, 2008; Sundberg, Mitchell and Reynolds, 2009; Figure 6C/D). Further examination by Zhang *et al* (2014) indicated that this was as a result of local inhibitory interneuron circuits, most likely VIP+ neurons causing spatially localised disinhibition by preferentially innervating SST+ interneurons.

Zhang et al., (2014) strongly suggest a role for the ACC in visual attention. Stimulation of ACC in passive environments leads to responses in V1 neurons that resemble those

seen when carrying out tasks requiring visual attention. On top of this, it also improves performance in behavioural tasks that require the mice to discriminate visual stimuli, something that requires the association of the stimulus to a reward and subsequent timed response to obtain the reward. Lastly, stimulation of this ACC to V1 projection axons shows spatial preference indicating a possible retinotopic organisation as well as properties resembling surround suppression.

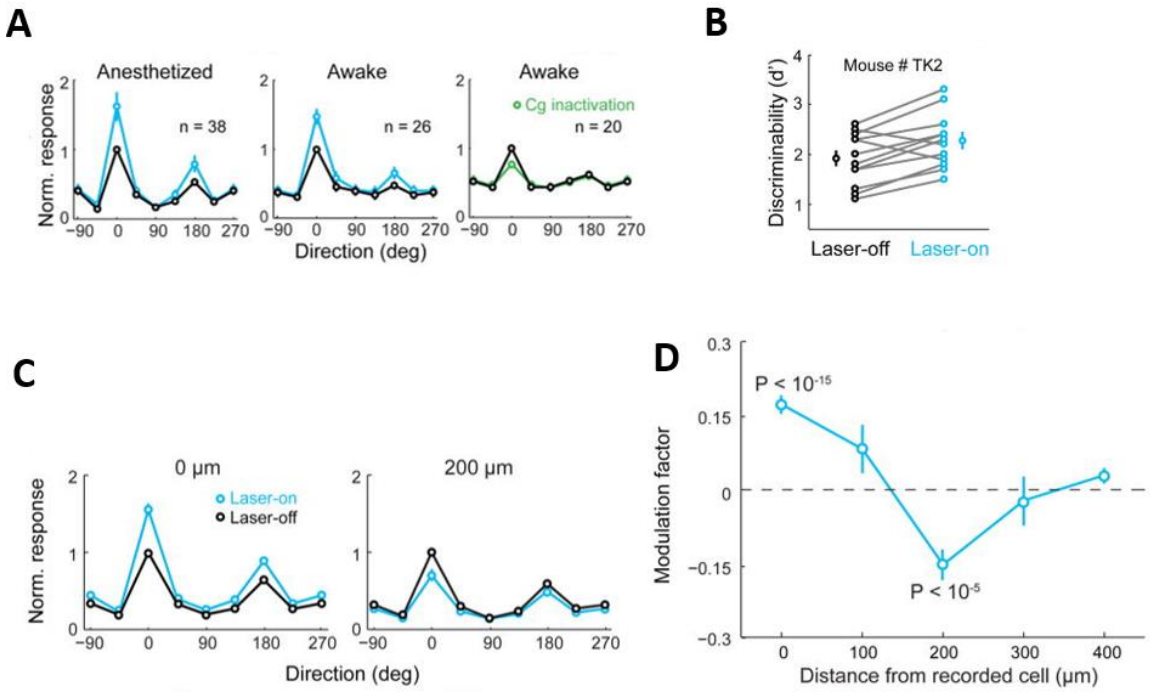

Figure 1.9: Artificial stimulation of ACC neurons via optogenetics projecting to V1 leads to attentional effects (adapted from Zhang et al., 2014)

A: Response of a V1 neuron to preferred and non-preferred orientations under normal conditions (black), when ACC is stimulated (blue) and when ACC is inactivated (green). **B:** Ability of the mice to discriminate between two visual stimuli in a Go/No-go task increases when ACC is stimulated. **C:** Increased response to preferred stimuli is dependent on spatial location of the stimulation of ACC axons in layer 1 V1. Responses are decreased if stimulation is 200µm away **D:** This inhibitory input was strongest at 200µm away.

1.5 Use of two-photon imaging of calcium sensitive indicators

To be able to record activity from ACC axons and V1 somas while mice are presented with visual stimuli or required to complete visually guided tasks, two-photon imaging of calcium sensitive activity indicators were used. These calcium sensitive indicators were injected into the brain structure of interest and entered the soma of pyramidal neurons via viral transfection before being transported to other regions of the neuron including both dendrites and axons. The system must be sensitive enough so that fluorescent signals can be detected at the resolution of a single neuronal soma, dendrite or axon.

Calcium sensitive activity indicators can be used as a proxy of neuronal activity, as calcium rapidly enters neurons or is released from intracellular stores when neurons fire action potentials. The genetically encoded indicator GCaMP6s consists of a circularly permuted green fluorescent protein, the calcium binding protein calmodulin and M13 peptide. When calcium binds to calmodulin, a conformation change arises which leads to increased brightness of the green fluorophore. Expression of GCaMP6s in individual layer 2/3 visual cortical neurons of mice results in reliable detection of activity in response to differently oriented visual stimuli (Chen *et al.*, 2013). A version of GCaMP6s has also been developed that specifically targets axons. It shows an increased signal-to noise ratio and robust photostability, allowing for improved imaging of axons in terms of both signal strength and later motion correction (Broussard *et al.*, 2018). This is important in studies involving locomotion and behaviour. Furthermore jRGECO1a, a genetically encoded protein construct similar to GCaMP6s, but which fluoresces red due to a fluorophore based on mApple, has been developed (Dana *et al.,* 2016). This can also be used to record fluorescent transients in response to visual stimuli. Although not as bright or sensitive as GCaMP6s, the red-shifted excitation and emission of jRGECO1a leads to reduced scattering and absorption by the tissue which consequently results in reduced phototoxicity (Dana *et al.*, 2016).

Viruses are used to infect cells with these calcium indicators. They are coupled to promoters which determine which cell type they will be expressed in. In the following studies, the expression of both gCaMP6s and jrGECO1a was driven by the synapsin promoter. It has been shown that this promoter coupled with an AAV infects both excitatory and inhibitory neuronal populations in cortex (Nathanson *et al.*, 2009). Long range cortico-cortical projections are usually glutamatergic (Zhang *et al.*, 2014) and thus, with regards to the ACC, the axons examined here are likely excitatory. In the case of jrGECO1a expression in somas, it is likely that both excitatory pyramidal and inhibitory neurons are infected.

To detect the fluorescent signals emitted by these fluorophores, two-photon microscopy is used. Here, two low energy photons collide to cause a higher energy transition in a fluorescent molecule. As the intensity is highest at the point of focus and drops off quadratically with distance, fluorescence excitation can occur at a resolution as high as $0.1\mu m^2$. Furthermore, the relatively long wavelengths needed for two-photon imaging are better able to penetrate tissue as scatter absorption by the tissue is reduced when compared to single-photon microscopy. This allows imaging at deeper tissue depths (Svoboda and Yasuda, 2006).

Combining genetically encoded calcium imaging and two-photon imaging in mice enables imaging large-scale networks of neurons at the resolution of a single soma, spine or bouton (Goard *et al.*, 2016; Li *et al.*, 2018). It is thus a powerful technique to investigate processing in sensory cortices while animals are exposed to visual stimuli or learn visually guided behaviour in real time.

1.6 Aims of the study

The ACC has been strongly implicated in the control of visual attention. In mice projections between the ACC and V1 have been proposed as a substrate of selective visual attention. However, the evidence in support of this notion derives primarily from experiments in which V1→ACC axon terminals were optogenetically activated during visual discrimination behaviour (Zhang *et al.,* 2014). It therefore remains unclear the extent to which this circuitry is 'naturally' recruited in behaving animals. The aim of the following work was two-fold. First, it was important to establish the functional organisation of ACC axons in layer 1 of V1 under passive viewing conditions. Second, the activity of ACC axons in layer 1 of V1 was examined while mice carried out a visual discrimination task under natural conditions without artificial stimulation.

2 Materials and Methods

2.1 Animals

All procedures performed on animals were carried out in accordance with institutional animal welfare guidelines and the UK Animals Act 1986. They were licensed by the UK Home Office. Mice were kept in standard laboratory conditions which involved cycles of 14 hours of light and 10 hours of darkness at 24°C. They were provided with a standard diet and water ad libitum. The two exceptions to this occurred when mice were dark reared and when water restriction was implemented during specific behavioural tasks. These occasions are identified and described in the method statements of the relevant chapters. Experiments involved both wildtype (WT) animals and mice in which parvalbumin (PV+) interneurons were labelled, achieved by crossing B6.Cg-Gt(ROSA)26Sortm14(CAG-tdTomato)Hom/J and B6;129-Pvalbtm1(cre)Arbr/J (Jackson Laboratory, JAX Stock 007914 and 008069, respectively). Wildtype mice were ordered from Charles River and PV-CRE mice were bred in-house. All mice were housed with same sex littermates with running wheels.

2.2 Viral Injection and Cranial Window Implant

Surgery was conducted to inject the calcium sensitive activity indicators gCaMP6s or jrGECO1a (Penn Vector Core) into the appropriate brain region depending on the experiment being conducted, as well as to implant a cranial window so that visual cortex could be imaged using two-photon microscopy. These injections were made to either anterior cingulate cortex (ACC), primary visual cortex (V1) or lateral medial cortex (LM) of the visual cortex depending on the experiment. Each injection is described in detail in the relevant chapter. The general surgery set-up and cranial window implant remained the same throughout and was carried out as follows.

Mice were placed under anaesthesia using isoflurane (5%) and oxygen (0.2 L/min). When there was no response to a tail pinch, injections of anti-inflammatory drugs dexamethasone (0.15mg/kg; MSD Animal Health) and Rimadyl (5mg/kg; Zoetis), as well as the antibiotic Baytril (5mg/kg; Bayer) were made. Mice were then placed onto a heating pad to maintain their body temperature at 37˚C, and head fixed using ear bars into a stereotaxic frame. The isoflurane was subsequently reduced to 1-2% for maintenance of anaesthesia throughout the rest of the surgery.

Once animals were breathing at a steady rate of approximately one breath per second, a protective ophthalmic cream (Chloramphenicol 1.0% w/w; Martindale Pharma) was applied to the eyes and hair was removed from the scalp. The scalp was then cleaned with ethanol (70%) and iodine before two injections of lidocaine (2% w/v; Braun) were made subcutaneously between the ears. The scalp was then removed from posterior of lambda to anterior of bregma and laterally enough to expose all of the coronal suture. Cortex buffer (125 mM NaCl, 5 mM KCl, 10 mM Glucose, 10 mM HEPES, 2 mM $CaCl_2$, 2 mM $MgSO_4$, adjusted to pH 7.4) was applied to the skull to aid with the removal of the periosteum and, once this had been done, the edges of the incision were attached to the skull using a tissue adhesive (3M™ VetBond™ Tissue Adhesive).

A custom-made steel head-plate was placed above primary visual cortex and attached to the skull using dental acrylic (C&B-Metabond®) which covered the exposed parts of the skull but left enough room to make a 3mm diameter craniotomy above V1. A cranial window consisting of two pieces of glass 3mm in diameter glued together using a UV curable adhesive (Norland Optical Adhesive 61) before being attached to a 5mm diameter piece of glass (Harvard Apparatus) in the same way was used to replace the part of the skull removed from above V1. The two smaller glass pieces mimicked the depth of the skull and the larger piece of glass anchored the entire insert to the skull of the mouse. This was then secured using Vetbond and dental acrylic. The mouse was

then placed in a heated recovery chamber until observed to be mobile and eating after which it was returned to the home cage. Mice were observed five days post- surgery and given drinking water supplemented with Rimadyl and Baytril.

2.3 Intrinsic Signal Imaging

Mice previously implanted with a cranial window and custom-made head-plate were placed under anaesthesia using isoflurane (5%) and oxygen (0.2L/min). When there was no response to a tail pinch, they were transferred to a heating pad to maintain their body temperature at 37˚C, and the head-plate attached securely to a custom-made head-plate holder. The isoflurane was subsequently reduced to 1% for maintenance throughout the rest of the imaging session.

The cortex was illuminated using a lightsource with interchangeble bandpass filters. Initially green light (546nm) was used so that an image of the cortical surface vasculature exposed by the craniotomy could be acquired and stored for later reference (Figure 2.1A/B). As haemoglobin is highly absorbent of light at this wavelength, the contrast of blood vessels was maximised and thus ideal to act as a reference. The filter was then changed to red light (700nm) for intrinsic signal imaging (ISI) using a CCD camera (Figure 2.1C). A bandpass filter was used to further filter incident light reflected by the cortex and from the stimulus monitor used to display visual stimuli. The focal point of the camera was adjusted to 150-200μm below the surface of the cortex. A screen was positioned 30cm away from the nose of the mouse at a 45° angle to the sagittal plane so that stimuli could be presented to the left eye of the mouse which was contralateral to the imaged hemisphere in both the monocular and binocular receptive field.

To identify V1 and higher visual areas, an episodic protocol was used. The mice were presented with nine stimuli in total including four of varying orientations in the monocular receptive field as well as the binocular receptive field and one blank. The orientations presented were 0˚, 45˚, 90˚, 135˚ and each stimulus was 100% contrast with a spatial frequency of 0.03 cycles/degree. The presentation of each individual stimulus consisted of 1.8s of being stationary before drifting in directions 0˚, 45˚, 90˚, 135˚ and then 180˚, 225˚, 270˚, 315˚ for each respective stimulus for 1.8s. Visual stimuli drove activity in visual cortex which resulted in the direction of blood flow to the specific areas of visual cortex required to process it. This blood flow was in turn detected by the CCD camera. Images were acquired using the Imager 3001 (Optical Imaging inc, Mountainside, NJ), running on VDAQ software. Video frames were captured at a rate of 25 Hz.

ISI was carried out to identify the location of monocular and binocular V1, as well as LM. This information was used to guide the subsequent location of imaging using two-photon microscopy. In surgeries with a viral injection to LM, ISI was carried out to functionally identify the injection site during surgery. In this case, the same method was repeated as outlined above, except that a cranial window had not yet been implanted so imaging was done through the skull. To make this possible, saline was applied to the skull after the head-plate implant until the skull was translucent.

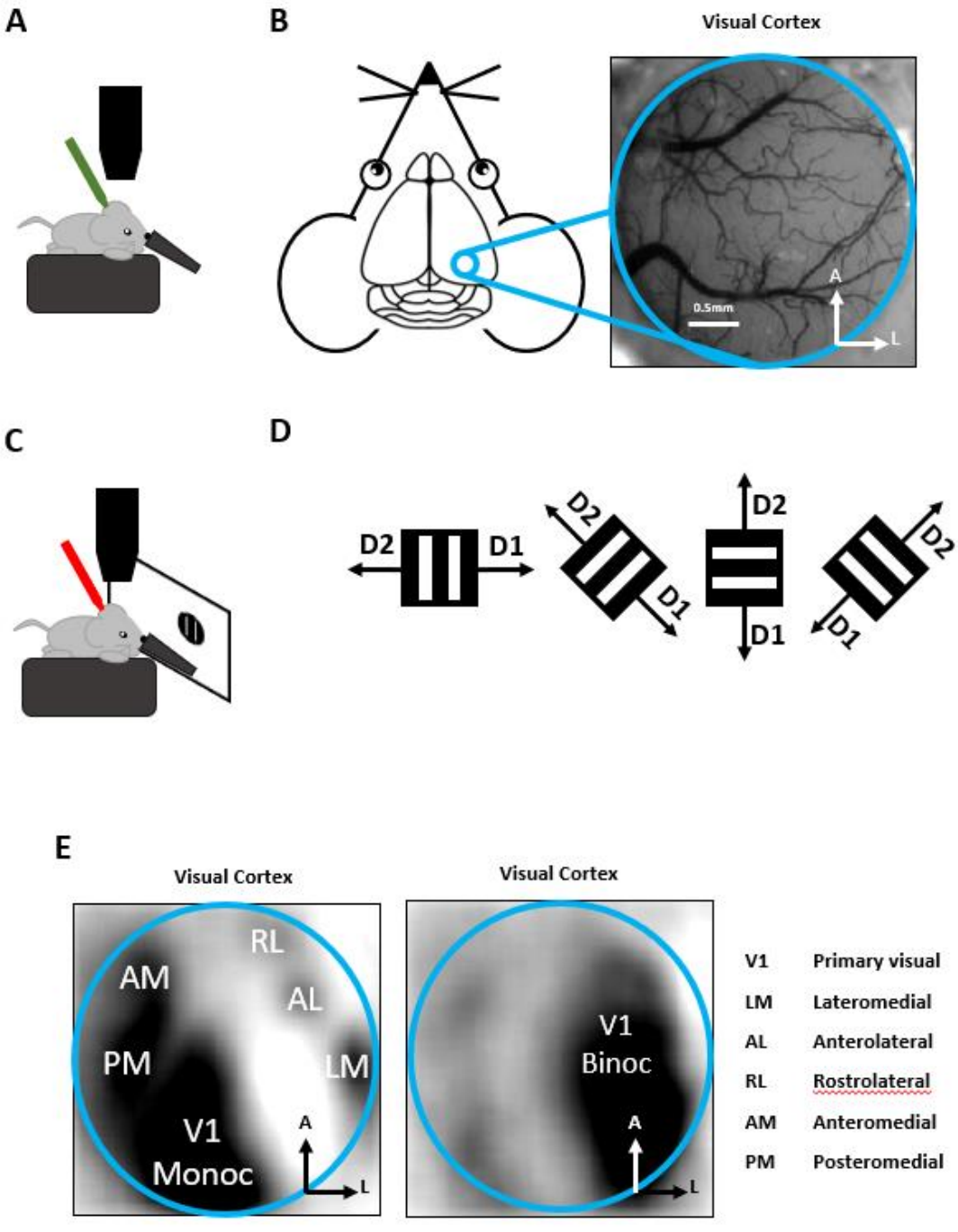

Figure 2.1: Intrinsic signal imaging to identify areas of visual cortex

A: Schematic of the set-up for taking an image of the cortical surface **B:** An example of an image taken of the cortical surface **C:** Schematic of the set-up for detected visual cortex areas. Light of wavelength 700nm was applied to the cortex and visual stimuli shown on a monitor **D:** Schematic of visual stimuli shown. Each stimulus was presented independently in both monocular and binocular regions of visual space, would remain stationary initially and then would drift in the directions indicated **E:** Examples of the identification of monocular (left) and binocular (right) areas of visual cortex.

2.4 Two-Photon Imaging

All in-vivo calcium imaging was performed on a resonant scanning two-photon microscope (Thor Labs), equipped with a Ti:sapphire laser (Coherent; Chameleon) and a 16 x 0.8 NA objective 3 mm working distance (Nikon) with a maximum laser power of 50 mW. Fluorescence data was acquired at a 60 Hz frame rate and subsequently averaged to 10 Hz. Animals were head-fixed and placed on a custom-designed fixed axis cylindrical treadmill coupled to a rotary encoder (Kübler, 0.5.2400.1122.0100). This allowed both experiments where the animals were able to run freely and movement was recorded, as well as those where the wheel was locked to prevent locomotion. Imaging, behavioural and visual stimulation timing data were acquired using Scanimage 4.1 and custom-written DAQ code (MATLAB) and a DAQ card (NI PCIe-6232; National Instruments).

2.5 Visual Stimuli

Visual stimuli were generated in MATLAB using the psychophysics toolbox and displayed on calibrated LCD screens (Iiyama, BT481). The types of stimuli shown depended on each individual task and are discussed in the relevant chapters.

2.6 Calcium Imaging Data Analysis

Images were initially processed using Suite2p (Pachitariu *et al.*, 2017). This included registering them to correct for brain motion, identifying active neuronal soma and axon regions of interest (ROIs) using a combination of automated detection (Figure 2.2/2.3) and manual selection and extracting calcium time courses from them. The version of Suite2p used here was able to detect a large number of axons and somas for a number of reasons. Firstly, the registration method implemented a phase correlation which applies spatial whitening to images before computing the cross-correlation maps to identify groups of pixels with similar fluorescence fluctuations that are likely to make up

the same axon or soma. Interpolation of the phase correlation map by the Suite2p system allowed the detection of sub-pixel shifts. This method was found to be superior than those used previously relying on finding the cross-correlation peak between a frame and a target image. On top of this, the system does not assume that a cell's activity should be independent of the surrounding neuropil. Furthermore, it is not based on a non-negative matrix factorisation thus resulting in greater sensitivity (Pachitariu *et al.,* 2017).

Manual selection was carried out for all somas and axons. Somas appeared as circular with a dark spot in the centre were the nucleus was located. Presence of this central dark spot indicated that the neuron was likely healthy. Axons appeared as long, thin strands with bulbous protuberances known as boutons located along them. These differed in morphology from dendrites as they instead have terminals located on spines which extend further out from the main strand. Suite2p grouped together pixels with highly correlating activity. This was done within pre-defined areas of the imaged region. It is therefore possible that an axon that spread across the entirety of the imaged region would have multiple areas identified and could bias the sample towards its specific activity. To counter this, it would be possible to use additional correlational analysis via custom-written MATLAB scripts and set the threshold correlational level to that of axons. There is, however, difficulty in doing this because the threshold level of correlation would be arbitrary. One way to set the threshold would be to compare the detected and group pixels to a video or registration image to see if axons identified by the correlational activity could be verified using morphology. It would be difficult to do this here, however, because the image plane was incredibly thin and axons could therefore move in and out of the plane, thus resulting in not being able to observe the entire morphology of the axon. Future studies could implement multi-plane imaging of these axons where the planes are arranged such that a three-dimensional image of the

imaging plane could be built. As this was not possible here, and with all the discussed drawbacks of trying to group together pixels across an entire imaging window, the grouping strategy implemented by Suite2p was used. The raw fluorescence values for each ROI were then converted to ΔF/F and, in cases which are stated, these traces were broken up on a trial-by-trial basis.

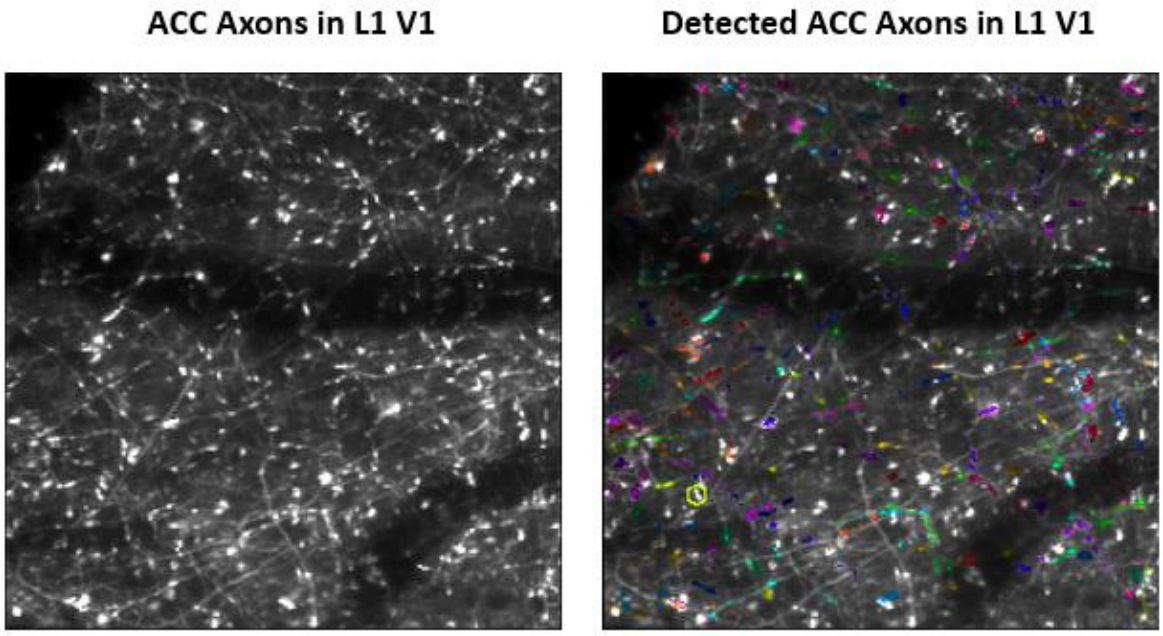

Figure 2.2: Example of axonal labelling and detection

A: Example of axonal labelling using the activity indicator GCaMP6s **B:** Detection of axonal regions of interest using Suite2p. Each region was accepted using a combination of automatic and manual detection. Each coloured region in the image to the right indicates the location of an individual axon.

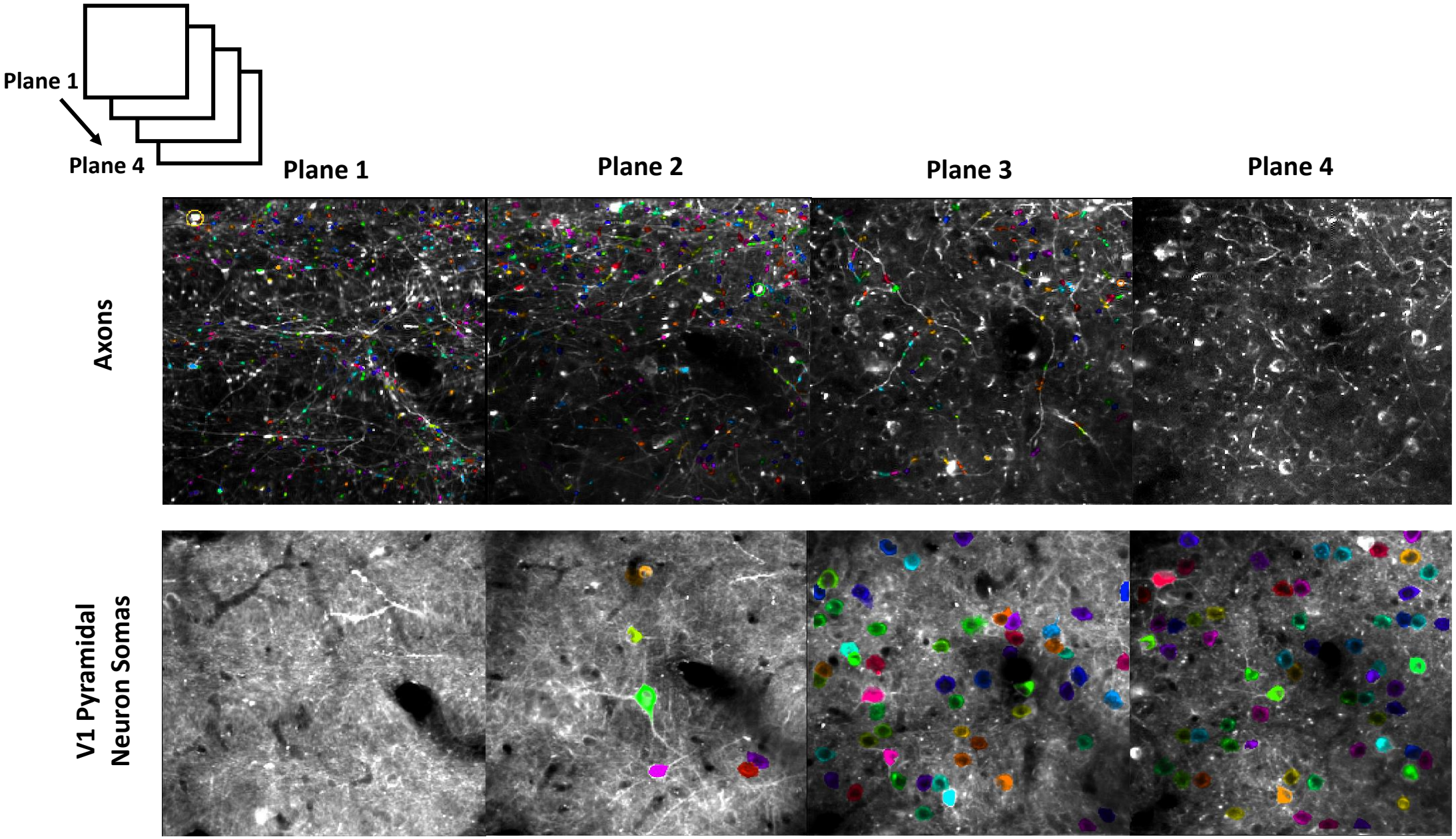

Figure 2.3: Example of axonal and soma labelling over multiple planes

Axons were labelled with gCaMP6s and V1 pyramidal somas were labelled with jrGECO1a. Multiplane two-photon imaging was then carried out across layer 1 and superficial layer 2/3. Axons were most detected at the two most superficial planes and V1 somas at the two deepest planes. Each coloured region in the image to the right indicates the location of an individual axon.

3 Functional Organisation of Anterior Cingulate Cortex and Lateral Medial Cortex Axons Terminating in Primary Visual Cortex

3.1 Introduction

The sensory cortex processes information through an integration of bottom-up and top-down information streams. It is currently not well understood how information is integrated between these streams, and specifically whether they are functionally organised with one another. Primary visual cortex (V1) is an ideal site to explore this for several reasons. It is a site at which signals from these streams converge, is highly organised and specific modulation of V1 neurons during contexts believed to involve top-down processing has been characterised. Furthermore, it receives top-down projections from multiple sources including both within and outside visual cortex that are each likely to modulate V1 neuronal responses for specific and separate purposes, and therefore exhibit different organisational properties.

3.1.1 Properties of V1 neurons and modulation during contexts requiring top-down processing

Mouse V1 processes basic features of the visual scene. It has spatially well-defined receptive fields (Niell and Stryker, 2008) with neurons that show selectivity to a broad spectrum of orientations, directions and spatial and temporal frequencies (Andermann *et al.,* 2010). Furthermore, these properties are modulated during contexts and environments believed to require top-down input. During locomotion, for example, the firing rate of V1 pyramidal neurons increases across visual cortex (Niell and Stryker, 2010; Keller *et al.,* 2012; Bennett *et al.,* 2013; Saleem *et al.*, 2013; Erisken *et al.*, 2014). In states involving the direction of attention, altered V1 activity profiles have also been observed. Tasks that require

spatially specific visual attention have shown an increase in response in neurons located in the corresponding retinotopic location of V1 to relevant stimuli, as well as a decrease in response in equivalent areas when irrelevant stimuli are presented (Li, Piëch and Gilbert, 2008; Yan *et al.*, 2014; Poort *et al.*, 2015). When tasks require the discrimination of stimuli with differing orientations, the responses of V1 pyramidal neurons that prefer the relevant orientation show sharper orientation tuning (McAdams and Maunsell, 1999; Schoups *et al.*, 2001; Goltstein *et al.*, 2013; Jurjut *et al.*, 2017).

V1 neuronal activity is driven both by bottom-up and top-down activity. Bottom-up signals are driven by elements of the visual scene which are faithfully reported to V1. Regions that send top-down projections to V1 are driven both by these and by the relevance of stimuli. These top down projections are then able to modulate V1 neuronal responses themselves. To amplify and suppress responses to spatially relevant stimuli, axons of top-down projections would need to be retinotopically matched with V1 neurons. This would involve a functional organisation resulting in the ability to influence the activity of specific subsets of V1 neurons. Iacaruso *et al*., (2017) used two-photon imaging of the dendritic spines of layer 2/3 V1 somas, onto which these top-down signals converge, to show a functionally specific arrangement. Dendrites located closer to one another on the same dendritic branch were more likely to represent similar features from the same location in visual space as one another than those located further away. On top of this, dendrites with the same orientation preference but a receptive field offset from that of the V1 soma itself followed an organisational pattern. The receptive fields of these dendrites were offset along the axis of their preferred orientation (Iacaruso *et al.,* 2017). This suggests that signals converging into layer 1 V1 follow a gross functional organisation.

3.1.2 Input from ACC

V1 receives top-down input from regions outside of visual cortex. One such projection originates at ACC and terminates in layer 1 of V1 (Zhang *et al.*, 2014). Studies have indicated an involvement of this projection in exerting spatially specific top-down modulation on sensory processing in V1, something that is a hallmark of selective attention (Zhang *et al.*, 2014). It has also been shown that, if a mouse is allowed to explore a virtual environment where visual stimuli appear predictably, then V1 responses become increasingly informative of spatial location, something that is reflected in ACC axonal responses (Fiser *et al.*, 2016). Taken together, this has shown that activation of this projection is able to enhance V1 soma responses to their preferred stimuli and that this is retinotopic. One way of achieving this modulation would be for ACC axons to be arranged to retinotopically match V1 neurons.

3.1.3 Input from lateral medial cortex of visual cortex

V1 also receives top-down input from structurally and functionally distinct areas within visual cortex itself. The mouse visual cortex is comprised of V1 as well as a group of higher visual areas (HVAs), each of which surround and reciprocally connect with V1. Triple anterograde tracing has revealed feedforward projections from V1 that terminate in nine HVAs (Wang and Burkhalter, 2007), defined by intrinsic signal imaging (Valery A. Kalatsky and Stryker, 2003; Garrett *et al.*, 2014; Juavinett *et al.*, 2016), one of which is the lateral medial area (LM). Two photon imaging has shown that axons from V1 projections that terminate in LM had stronger responses to lower spatial frequencies and that these preferences were distinct from other HVAs as well as being mirrored by somas present in LM itself (Andermann *et al.,* 2010; Glickfeld *et al.*, 2013). This demarcation of functional properties between HVAs suggests that each process specific information about the visual scene.

Signals are also transmitted back to V1 from LM. Marques *et al*., (2017) have shown that inputs to V1 from LM are largely retinotopically matched, but many of them relay distal information. Orientation selective LM axons that are also spatially selective respond to areas of visual space perpendicular to their preferred orientation and direction selective axons were biased towards stimuli that moved in their anti-preferred direction. Together this suggested an involvement in the processing of moving visual stimuli. An overrepresentation of LM inputs to V1 preferring temporal-nasal motion also suggested a specialisation in modulating responses during locomotion.

3.1.4 Aims of this study

To extend understanding of how bottom-up and top-down projections integrate information, this study investigated and compared their functional organisation. To do this, data were collected using two-photon microscopy scanning at multiple depths to acquire neural activity from layer 2/3 V1 pyramidal cell somas and either ACC or LM axons terminating in layer 1 of V1 simultaneously in response to the same visual stimulus. V1 somas were likely receiving input from these axons. Using this method, it was possible to ask whether top-down projections originating in areas both inside and outside visual cortex were driven by visual stimuli, and, if this were the case, whether the functional organisation of their receptive fields matched those of L2/3 pyramidal V1 somas located in the same area of visual cortex. I predicted that ACC axons terminating in L1 V1 would be retinotopically matched to L2/3 V1 somas as they are believed to be involved in modulating the visual attention response (Zhang *et al.,* 2014) which has spatial pressures and previous evidence has suggested organisation within this feedback projection (Leinweber *et al.*, 2017). If this ACC projection appears not to be organised retinotopically, this could mean that it may not be directly involved in modulating

attention, in particular spatial visual attention. On the other hand, it may also mean that it requires learning a visual attention task to develop retinotopic properties.

3.2 Materials and Methods

3.2.1 Mice

All procedures performed on animals were carried out in accordance with the UK Animals (Scientific Procedures) Act 1986, and the European Commission directive 2010/63/EU. Light reared animals were housed in standard laboratory conditions with 14 hours of light and 10 hours of dark; and dark reared animals were housed in the dark from P1 until imaging commenced. All mice were provided with a standard laboratory diet and water ad libitum. All mice were wildtype and obtained from Charles River.

3.2.2 Viral Injection and Cranial Window Implant

Mice were placed under anaesthesia using isoflurane (5%) and oxygen (0.2 L/min). When there was no response to a tail pinch, injections of the anti-inflammatory drugs Dexamethasone (0.15 mg/kg, intramuscular) and Rimadyl (5 mg/kg, subcutaneous), and the antibiotic Baytril (5 mg/kg, subcutaneous) were made. Mice were then placed onto a heating pad to maintain their body temperature at 37°C, and head fixed using ear bars into a stereotaxic frame. The isoflurane was subsequently reduced to 1-2% for maintenance of anaesthesia throughout the rest of the surgery.

Once animals were breathing at a steady rate of approximately one breath per second, they were prepared for the viral injection and cranial window implant as described in the general methods.

For the ACC surgery, a small craniotomy was made 0.3 mm lateral and 0.1 mm anterior of bregma above the right hemisphere of the brain by a dental drill. An oil-filled micropipette (Alpha Labs) was used to inject a virus driving GCaMP6s

(rAAV2/1-hSynapsin1-axon-GCaMP6s; titre after dilution 1.5x1014 GC/ml, 50 nL) expression at a depth of 0.9 mm and 0.6 mm with a microsyringe driver (WPI, 357 UltraMicroPump). The pipette was left in the cortex for five minutes post injection before slowly being removed. To allow the animal to subsequently be head-fixed, a custom-made head plate was attached to the cranium above V1 in the right hemisphere using dental cement (Super Bond C&B). A 3 mm craniotomy centred above V1 was made before injecting jrGECO1a (pAAV.Syn.NESjRGECO1a.WPRE.SV40 (AAV1), titre after dilution 5x1012 GC/ml, 100 nL) into monocular and binocular V1 and closed with a glass insert. Injection site locations were later confirmed as being in monocular and binocular V1 using episodic ISI as previously described.

For the LM surgery, the custom-made steel headplate was placed above V1 and attached to the skull as described for the ACC surgery directly after removal of the scalp. The dental acrylic was left to dry before carrying out episodic ISI as previously described to identify the location of the lateral medial area and primary visual cortex. The mouse was removed from the stereotaxic frame and attached to a custom made headplate holder while maintaining anaesthesia at 1%. Cortex buffer was used to submerge the part of the skull above visual cortex that was enclosed by the headplate until translucent and vessels on the surface of the brain were visible. To store an image of the vessels for future reference, green light (546 nm) emanating from a lightsource with interchangeable bandpass filters was used to illuminate them. The filter was then changed to emit red light (700 nm). Nine different grating stimuli were presented to the mouse on a screen positioned 30 cm away from the nose of the mouse at a 45° angle, specifically, four in the binocular region and four in the monocular region at 0°, 45°, 90° and 135° orientation with one blank. Images were acquired using the Imager 3001 (Optical Imaging inc, Mountainside, NJ) running on VDAQ software (Figure 3.1). Using this method, it

was possible to functionally identify the location of LM and V1. These locations were then cross referenced with the image of the cortex to act as a guide for the injections site.

Once LM and monocular and binocular locations in V1 had been located, the mouse was returned to the stereotaxic frame. A 3mm diameter craniotomy was made above the three identified sites and the bone flap was removed. The calcium indicator jrGECO1a was injected into monocular V1 and binocular V1 (pAAV.Syn.NES-jRGECO1a.WPRE.SV40 (AAV1), titre after dilution 5x1012 GC/ml, 100 nL) while the calcium indicator GCaMP6s axon variant was injected into LM at a depth of 250 µm and 550 µm (rAAV2/1-hSynapsin1-axon-GCaMP6s; titre after dilution $1.5x10^{14}$ GC/ml, 50 nL). A cranial window was inserted above visual cortex as described in the general methods. The mouse was then placed in a heated recovery chamber until mobile and eating, before being returned to the home cage. Drinking water was supplemented with Baytril and Rimadyl and animals were observed for five days post surgery. Examples of the gCaMP6s injection into LM and ACC are shown in Figure 3.1.

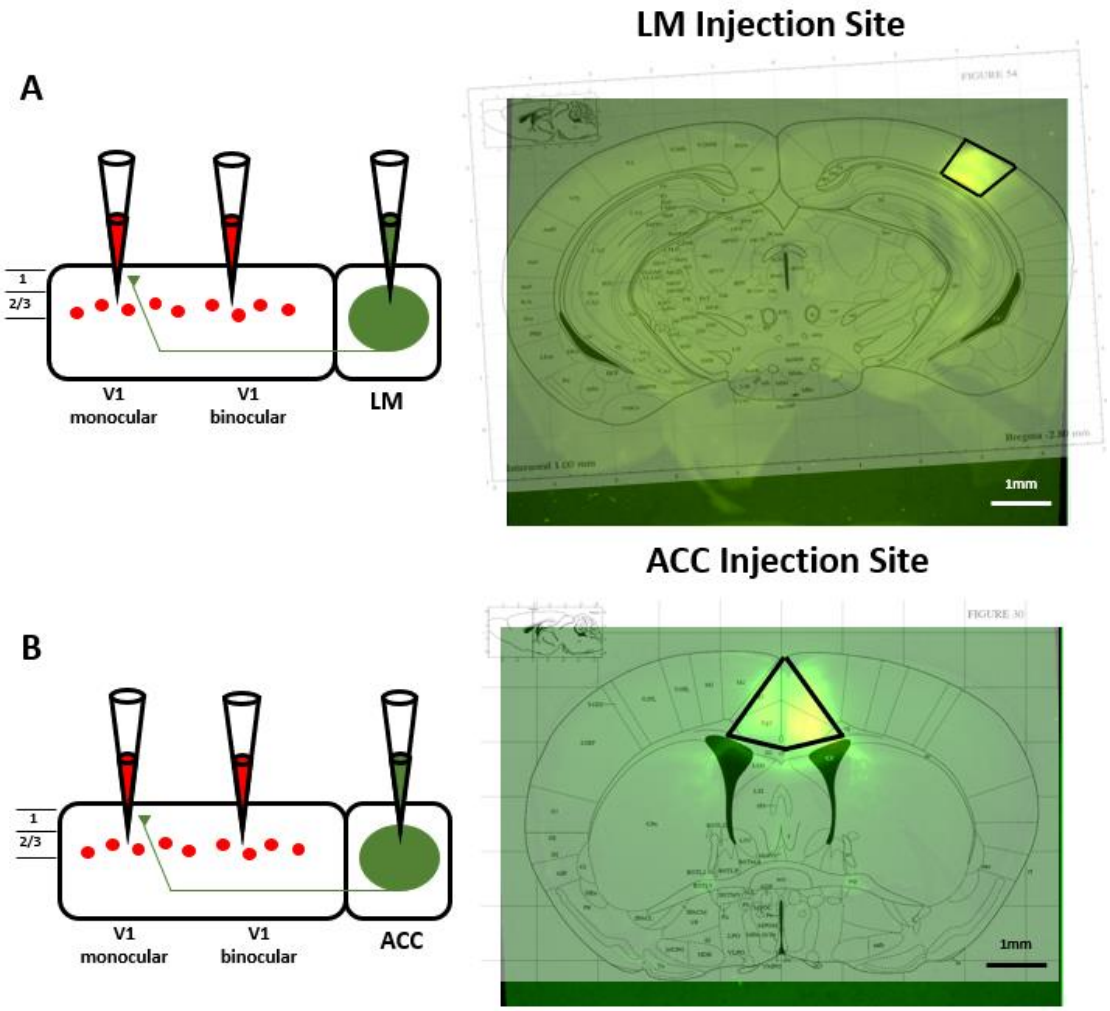

Figure 3.1: Injection sites of gCaMP6s

A: Left: an injection schematic showing an injection of gCaMP6s into LM of visual cortex and jrGECO1a into V1. Right: A brain slice showing the injection site of LM with a mouse brain map superimposed. LM in the right hemisphere is outlined in black. **B:** As in A but for ACC.

3.2.3 Two-Photon Imaging

All in vivo calcium imaging was performed using a two-photon resonant scanning microscope (Thorlabs, B-Scope), equipped with a Ti:sapphire laser (Coherent, Chameleon) using a 16x 0.8 NA objective (Nikon). Awake mice were headfixed to a custom made headplate holder and allowed to run on a spherical treadmill with movement being measured by a rotary encoder. All imaging was carried out using ScanImage4. Data were collected from five separate planes ranging from layer 1 to shallow layer 2/3 of V1 in the right hemisphere, using a wavelength of 980 nm to detect changes in fluorescence in both the jrGECO1a and gCaMP6s indicators, while visual stimuli were presented to the contralateral eye of mouse.

3.2.4 Visual Stimulus Protocol

Visual stimuli were gratings 15° by 15° in size and appeared in 36 locations consisting of 4 rows and 9 columns (Figure 3.2). Four orientations and eight directs were shown consisting of 0˚, 45˚, 90˚, 135˚, 180˚, 225˚, 270˚ and 315˚. A blank was also shown in each location. They drifted at a temporal frequency of 2 Hz and had a spatial frequency of 0.05 cycles/deg. Each stimulus was presented for one second and the onset of the next stimulus occurred immediately after the termination of the previous one. Each stimulus condition was repeated 15 times. Stimuli were presented on IIyama LED monitors positioned around the mouse with one to the front of the mouse 10cm away and the remaining two on either side, positioned 15cm from the mouse. Stimuli were presented from the centre of the binocular field of view directed in front of the mouse, denoted as 0°, to 80° in the direction of the eye contralateral to the imaged hemisphere.

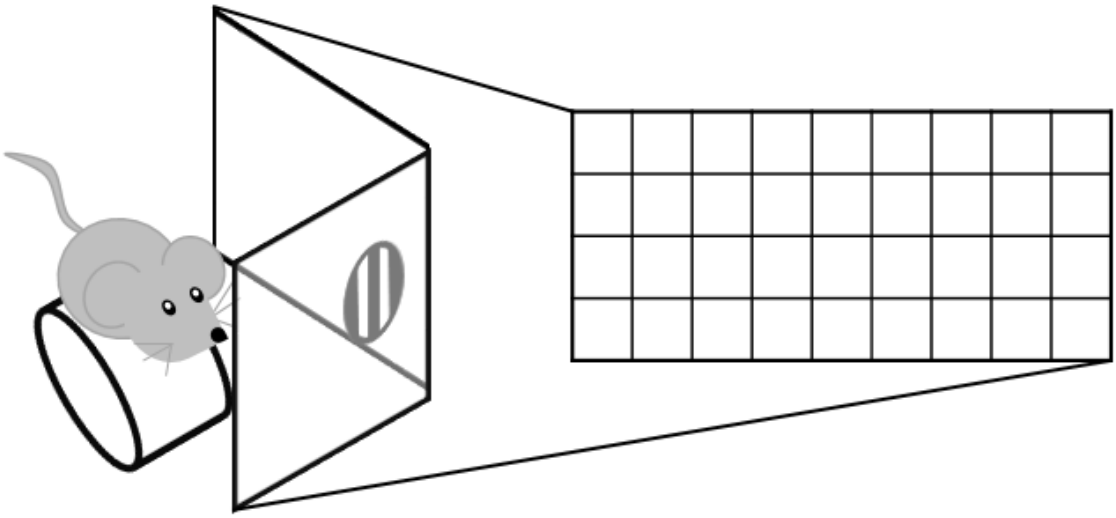

Figure 3.2: Schematic of the retinotopy protocol

Mice were presented with visual stimuli in 36 positions consisting of four rows and nine columns. Presentation in azimuth ranged from 0˚ (in front of the mouse), and through binocular and monocular regions of visual space of the eye ipsilateral to imaging by 80˚.

3.2.5 Analysis

Images were initially processed using Suite2p (Pachitariu *et al.*, 2017). This included registering them to correct for brain motion, identifying active neuronal somas and axons using a combination of automated detection and manual selection and extracting calcium time courses from them described previously in the general methods. Examples of fluorescence recorded from ACC axons and V1 somas are shown in Figures 3.3 and 3.4 respectively.

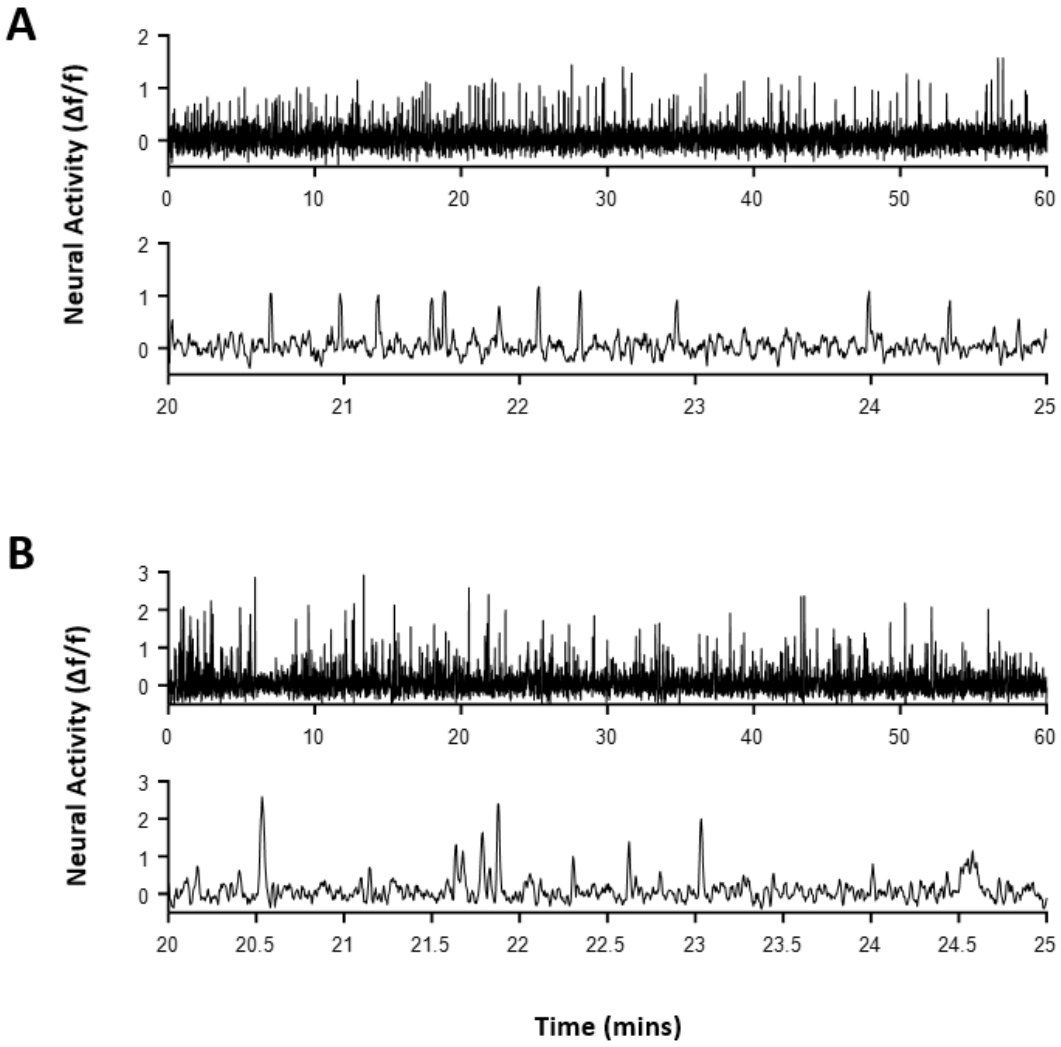

Figure 3.3: Example fluorescence traces extracted from ACC axons

A: Example of the fluorescence fluctuation of an ACC axon over the course of an entire trial (top) and for a selected five minute period (bottom). **B:** As in A, but for a different axon.

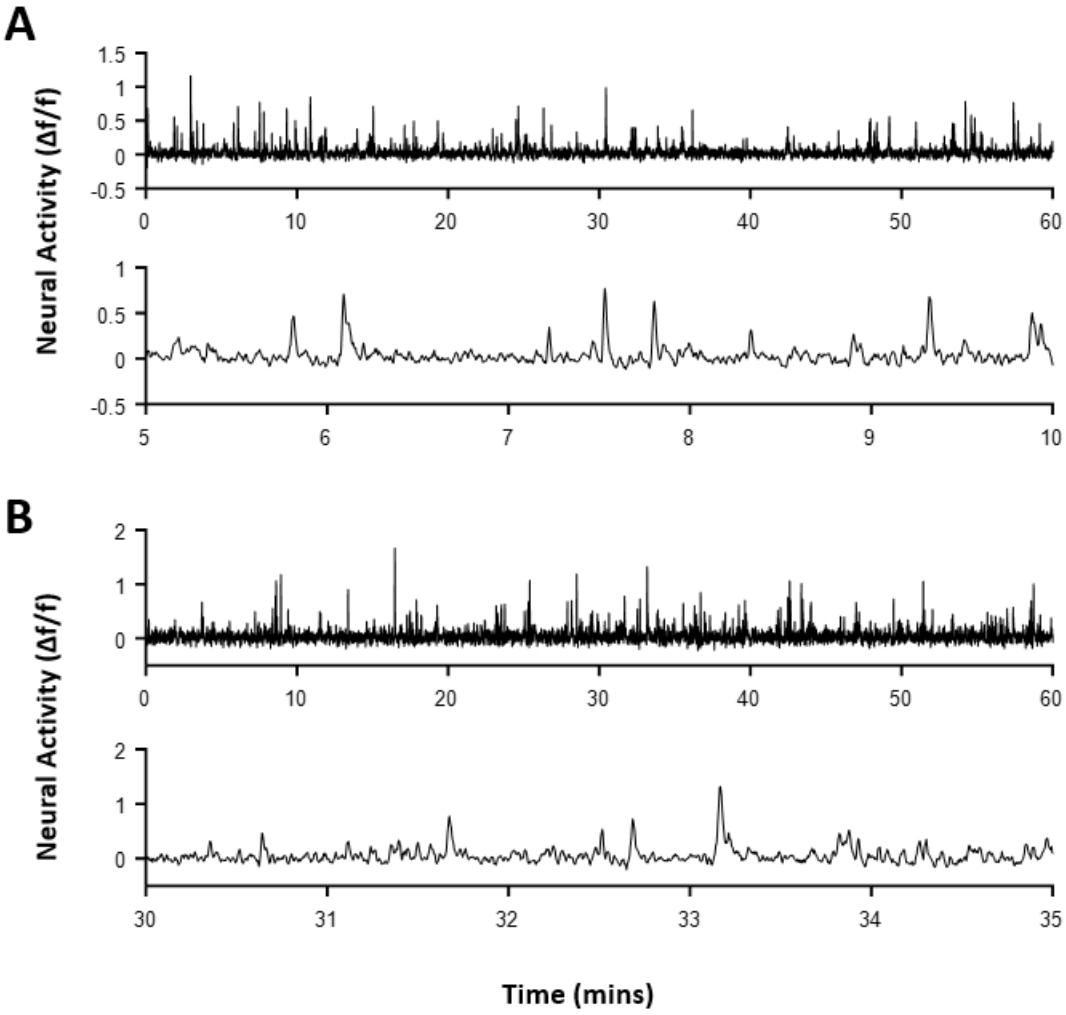

Figure 3.4: Example fluorescence traces extracted from V1 somas

A: Example of the fluorescence fluctuation of a V1 soma over the course of an entire trial (top) and for a selected five minute period (bottom). **B:** As in A, but for a different soma.

Time courses within individual experiments were then broken up on a trial-by-trial basis. All analysis subsequent to this was carried out using custom written code in MATLAB. For each identified soma or axon (regions of interest, ROIs), the trial with the highest response was identified and the orientation presented within this trial was deemed to be the preferred one. To identify ROIs which responded to a specific location in visual space, data for each location was extracted for the preferred orientation and then fitted with a two-dimensional Gaussian model with the formula:

$$f(x,y) = Ae^{-\left(\frac{(x-x_o)^2}{2\sigma_x^2} + \frac{(y-y_o)^2}{2\sigma_y^2}\right)}$$

Here, A represents the highest amplitude of response, x_0 and y_0 are the coordinates of the centre of the peak and σ_x and σ_y are the spread of the peak in the x and y directions. The fit was then manually checked to confirm the receptive field centre (RFC) was at a peak (Figure 3.5).

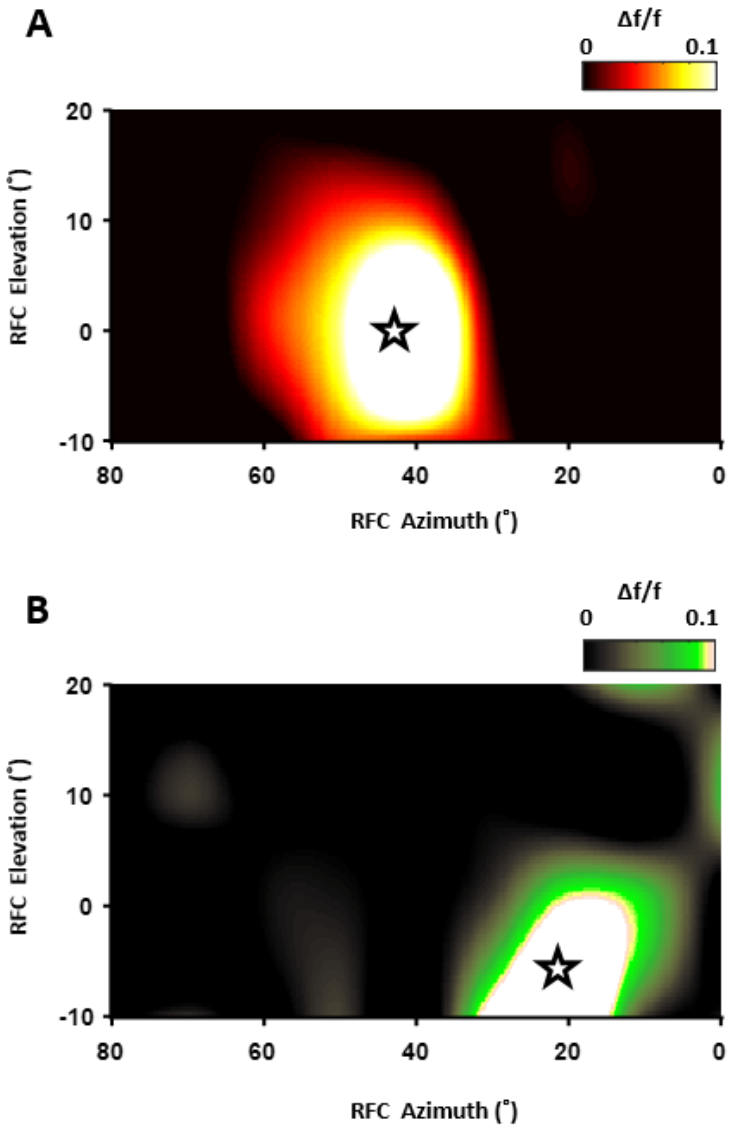

Figure 3.5: Example of neuronal responses and the two-dimensional Gaussian fit

A: The response of each V1 pyramidal neuron that showed a location preference and then fitted with a two-dimensional gaussian was visualised. Responses to the 36 locations were smoothed and the star indicates the two-dimensional gaussian fit. **B:** As in A, but an example of an ACC axon which exhibited a spatially specific response.

To identify ROIs which showed an orientation or direction preference, data for each orientation was extracted at the preferred location. From this the orientation selective index (OSI) could be calculated using the formula below using preferred (pref) and orthogonal (orthog) values:

$$\frac{Orientation_{pref} - Orientation_{orthog}}{Orientation_{pref} + Orientation_{orthog}}$$

To analyse whether RFCs of axons were organised in patterns around RFCs of somas, the mean RFC of V1 somas was subtracted from each axonal RFC resulting in offset values in azimuth and elevation. These could then be plotted in 'relative visual space' encircling a centre that represented V1 somas mean RFC. This relative visual space was then divided up into segments to investigate how many axons were offset in each direction from the V1 somas. This was achieved by counting the number of offset values in each segment and generating a percentage for each segment per experiment. In the case where these groups were further divided by orientation preferences, these counts were normalised to the number of offset values in each segment from axons which did not show orientation specificity. In these cases, it was important to control for a general over-representation of offset values in particular segments. For all of these experiments, relative visual space was limited to 30˚ in each direction to control for stimuli being presented over a greater amount of visual space in azimuth (80˚) compared to elevation (30˚).

3.3 Results

To explore the functional organisation of the top-down ACC and LM projections into V1 compared to that of layer 2/3 V1 somas in the same location, RFC preferences of ACC and LM axons were examined in relation to those of V1 somas. It was asked whether ACC/LM axons and V1 somas in the same area of V1 had matching retinotopic preferences and, if not, whether there was any consistent offset. This was then examined for ACC axons and V1 somas which also exhibited orientation preferences to determine whether any organisation was dependent upon orientation selectivity. To do this, the visual cortex in the right hemisphere of mice was recorded from while drifting gratings were presented to the contralateral eye (Figure 3.1). These gratings were 15°x15° in size and appeared pseudo-randomly in thirty-six locations consisting of four rows and nine columns beginning directly in front of the mouse and ranging through both binocular and monocular fields of visual space. Four orientations were tested (0˚, 45˚, 90˚, 135˚).

3.3.1 Receptive Field Properties of ACC Axons Compared to V1 Somas

Initially, the receptive fields of ACC axons and layer 2/3 V1 somas were compared. This study involved eight mice and 14 experimental sessions where 5087 axons and 1622 V1 somas were identified. By considering the response profile for each stimulus type, it was found that 8.49 ± 0.84% of ACC axons terminating in L1 V1 were visually responsive (Figure 3.6)

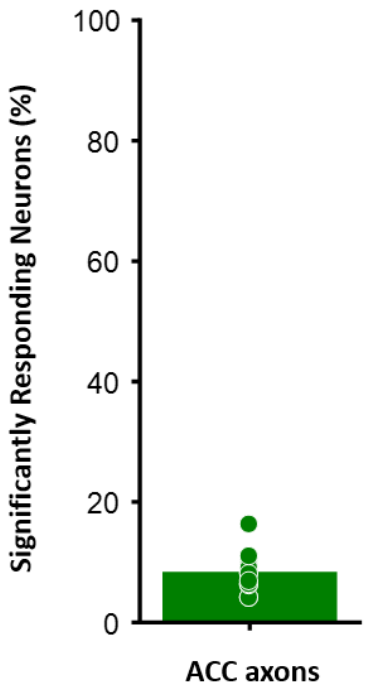

Figure 3.6: A proportion of ACC axons are visually responsive

On average, 8.49 ± 0.84% of ACC axons terminating in L1 V1 were visually responsive. This data was taken from 14 experimental sessions involving 8 mice. The average number of axons per experimental session was 210.86 ± 56.36 and per mouse was 466.11 ± 164.79.

The orientation with the highest response amplitude from each identified axon and soma was detected and, if this response was greater than that to the blank, data were extracted from each location for this preferred orientation. A one-way ANOVA was then carried out to find neurons that had significantly different responses depending on location. Neurons that showed this preference were fitted with a two-dimensional Gaussian to identify their receptive field centre (RFC), as well as receptive field size, and manually checked to confirm the fit was at a peak. Somas and axons which met these criteria were then taken forward in the analysis.

Both layer 2/3 V1 somas and ACC axons contained a fraction of neurons which responded to a specific location in visual space (Figure 3.7A). An average of 18.58 ± 0.95% ACC axons showed this retinotopic preference, which was significantly less than the 52.32 ± 4.73% that observed for the V1 somas ($p < 0.001$, Mann Whitney-U Test; Figure 3.7B).

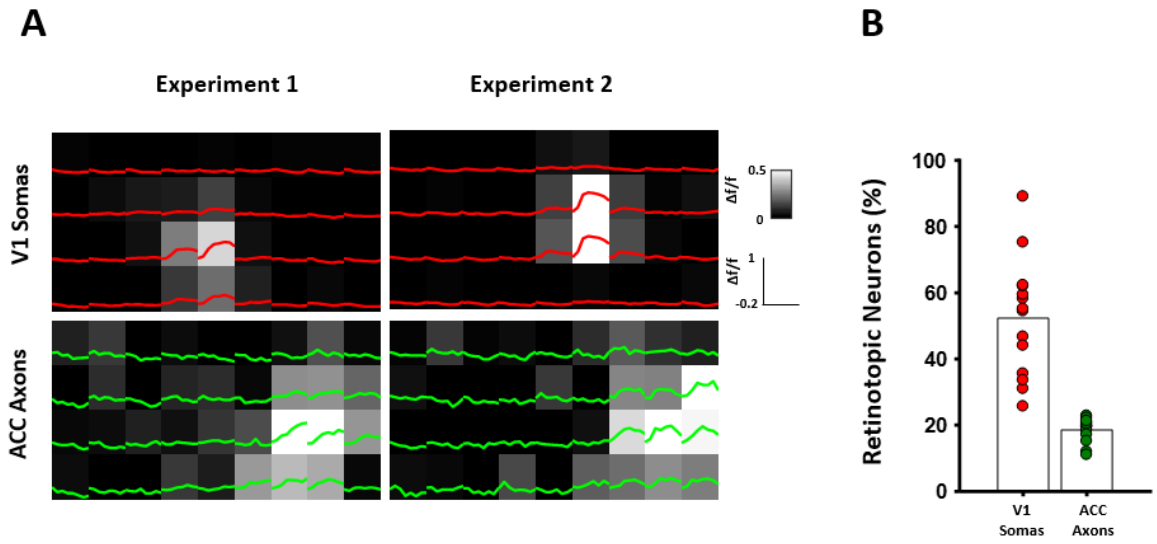

Figure 3.7: ACC axons show retinotopic preferences

A: Examples of neural responses to each of the 36 locations in which visual stimuli were presented. **B:** Although a fraction of ACC axons show retinotopic preferences, the percentage is significantly less than V1 somas. This data was taken from 14 experimental sessions involving 8 mice. The average number of axons per experimental session was 210.86 ± 56.36 and per mouse was 466.11 ± 164.79. The average number of somas per experimental session were 20.42 ± 5.46 and per mouse was 130.39 ± 46.10. Standard errors were calculated per experimental session.

After establishing the existence of spatial specificity in ACC axons, the size of the scatter of RFCs were compared. RFCs for each axon and soma in four example experiments in which somas preferred a different area of visual space suggested that ACC axons RFCs are more scattered than those of the somas (Figure 3.8A). To investigate this, the distance between each of the individual RFCs and the mean RFC for the population was calculated independently for the soma and axon neuronal populations (Figure 3.8B). ACC axon RFCs were consistently significantly further away from their mean ($p < 0.001$, Mann Whitney-U Test; Figure 3.8C), and this was true for spread in both azimuth ($p < 0.005$, Mann Whitney-U Test; Figure 3.4D) and elevation ($p < 0.001$, Mann Whitney-U Test; Figure 3.7E).

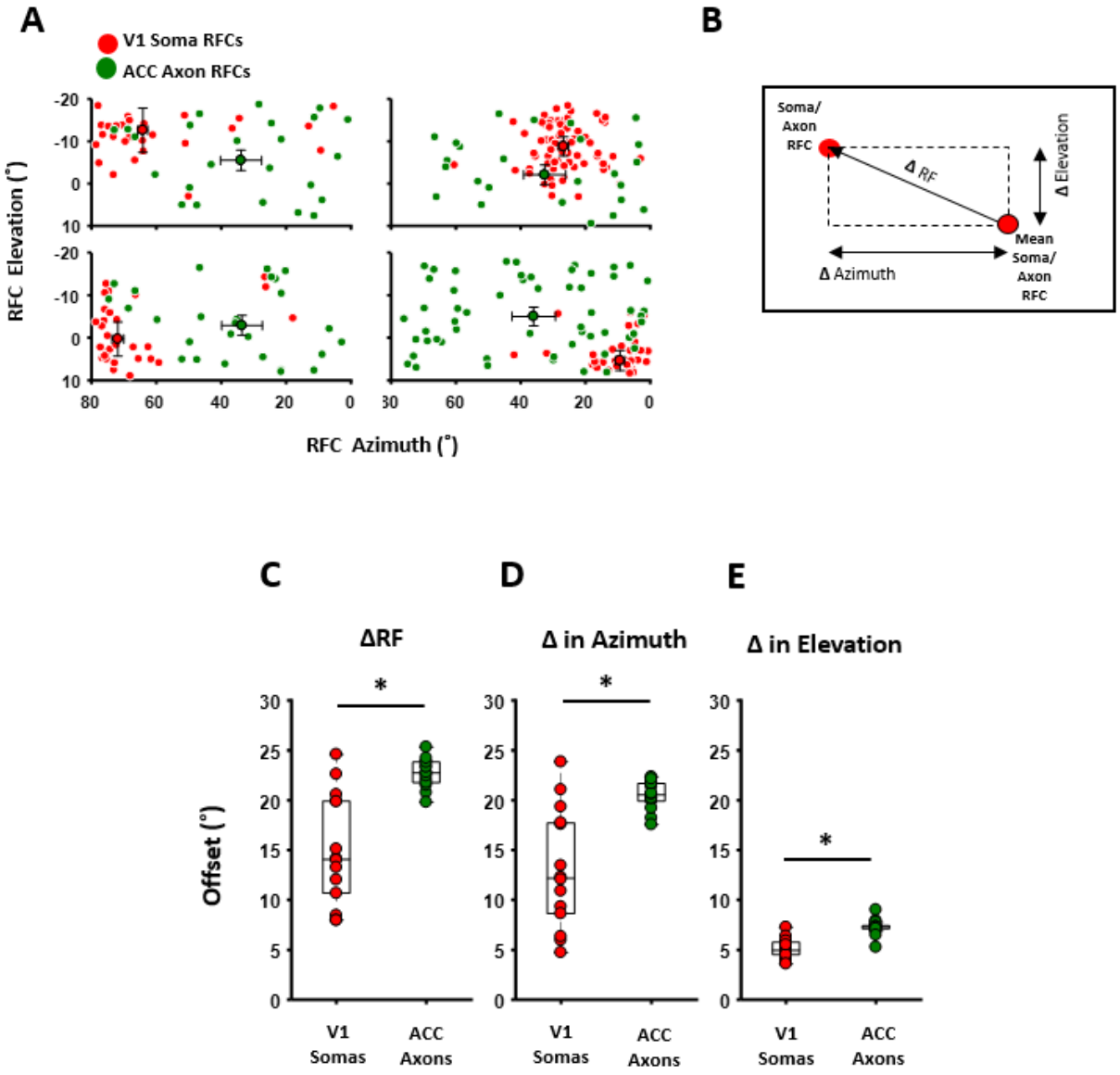

Figure 3.8: ACC axons carry signals from a wider area of visual space than V1 somas process in the same area of visual cortex.

A: Examples of RFCs for four experiments where V1 somas preferred different visual locations **B:** Schematic of the normalisation of soma and axon RFCs to their mean in order to compare RFC scatter size. The distance between each point was referred to as ΔRF, and this was then divided into Δ azimuth and Δ elevation **C:** The comparison between scatter sizes of RFCs in V1 somas and ACC axons **D/E:** As in C, but specifically for Δ in azimuth (D) and Δ in elevation (E). The average number of axons per experimental session was 49.00 ± 5.81 and per mouse was 85.75 ± 19.14. The average number of somas per experimental session were 35.86 ± 4.43 and per mouse was 62.75 ± 16.94. Standard errors were calculated per experimental session.

An average scatter distance greater in azimuth (20˚) than in elevation (7.5˚) could have resulted for two reasons. The first was that ACC axon RFCs were consistently offset by this distance from each other in azimuth and elevation respectively. On the other hand, these values represent the average limit of spread dictated by the size of visual space in which the visual stimuli were presented. It was therefore possible that ACC axon RFCs were arranged randomly or in a pattern that covered the whole of the available visual scene. To investigate this further, the distribution of offset values in azimuth and elevation were examined by splitting them up into bins of size 2˚ and counting how many RFCs were in each bin (Figure 3.9). It was found that, in both azimuth and elevation, the soma RFC count peaked at approximately the RFC mean. On the other hand, RFCs for ACC axons were consistently spread across the visual scene in both azimuth and elevation (Figure 3.9B/C).

Taken together, this suggested that a proportion of ACC axons responded to specific areas of visual space, but that the relay of this information back to V1 is not organised retinotopically. Information about a much wider area of visual space is converging on V1 than what the somas in that area selective for.

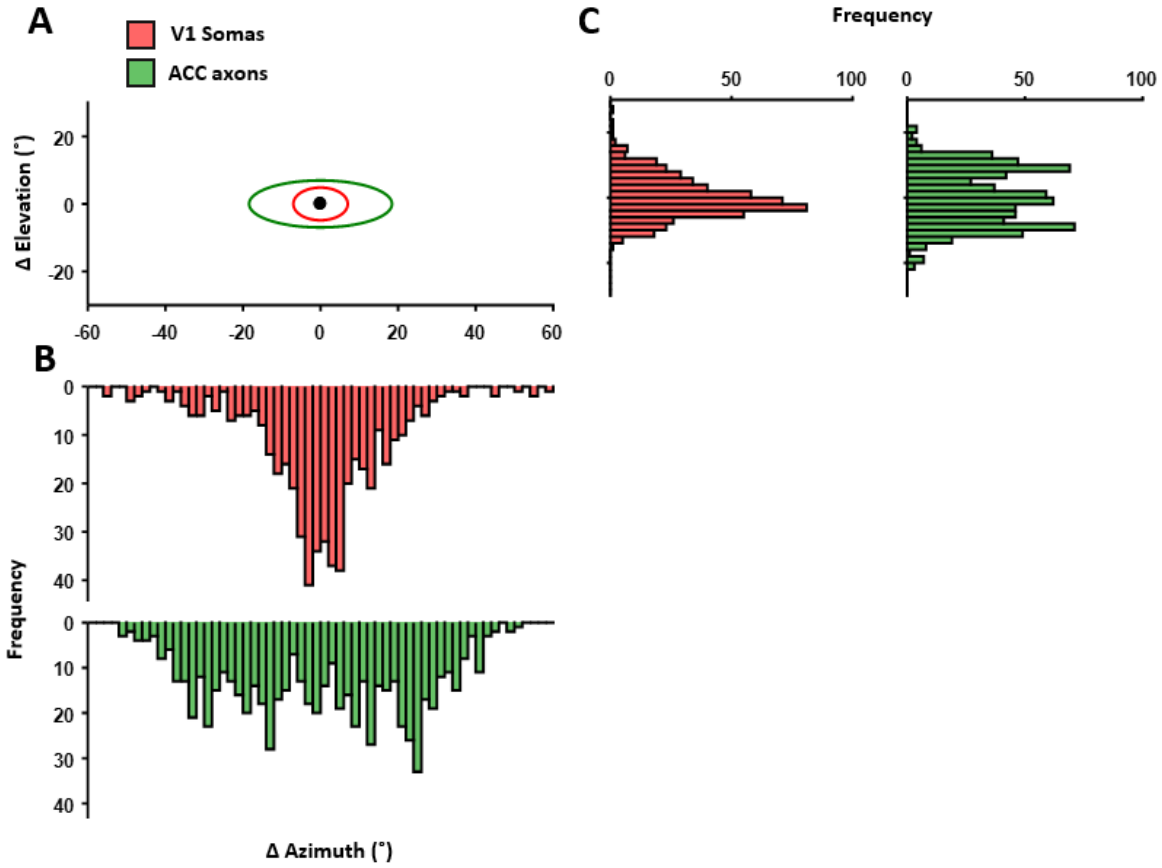

Figure 3.9: The distribution of V1 soma and ACC axon RFCs across visual space in which visual stimuli were presented

A: Mean offset of RFCs of V1 somas and ACC axons from their respective mean RFCs in azimuth and elevation. **B:** Frequency distribution of RFCs across visual space in which stimuli were presented for V1 somas (red) and ACC axons (green). Each bin refers to 2˚ of visual space. **C:** As in B but for elevation. The average number of axons per experimental session was 49.00 ± 5.81 and per mouse was 85.75 ± 19.14. The average number of somas per experimental session were 35.86 ± 4.43 and per mouse was 62.75 ± 16.94. Standard errors were calculated per experimental session.

3.3.2 Receptive Field Scatter of LM Axons Compared to V1 Somas

It has been established that the somas located in the LM area of visual cortex exhibit some classical visual response properties such as orientation and spatial specificity (Glickfeld *et al.*, 2013). Furthermore, axons belonging to neurons projecting from LM and terminating in V1 show retinotopic organisation similar to V1 (Marques *et al.*, 2018). To further investigate the organisation of visual properties in axons projecting from LM to V1, the same experiment and analysis detailed above was carried out, but in this case LM axons were labelled with GCaMP6s. This study involved five mice and six experimental sessions where 997 axons and 558 V1 somas were identified. Both layer 2/3 V1 somas and LM axons contained a fraction of neurons which responded to a specific location in visual space (Figure 3.10A), and the 35 ± 5.52% of axons that were retinotopically specific was not significantly different from the 49.36 ± 9.36% of V1 somas (Figure 3.10B).

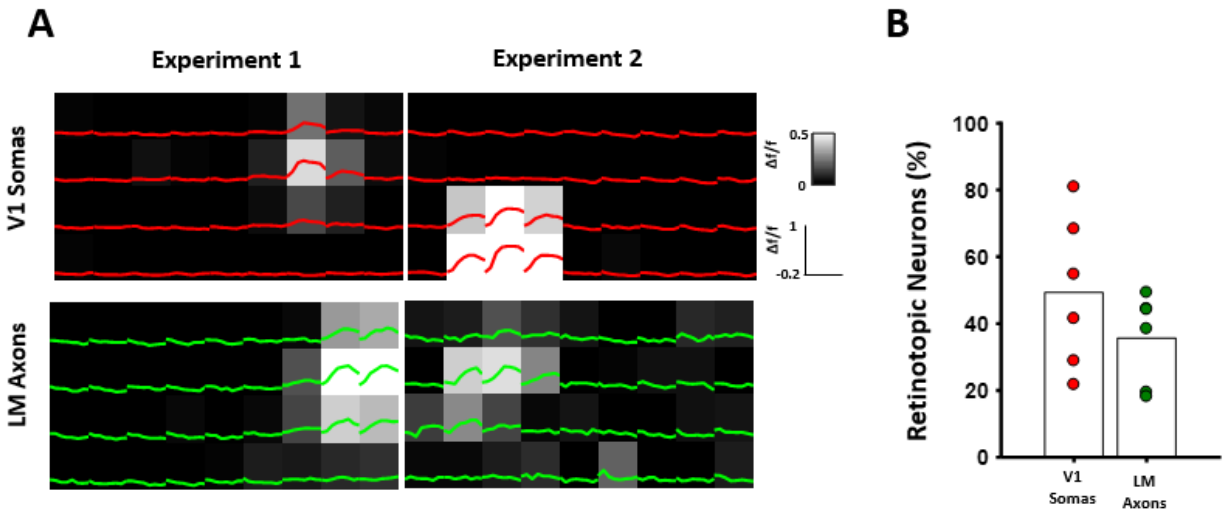

Figure 3.10: LM axons show retinotopic preferences

A: Examples of neural responses to each of the 36 locations in which visual stimuli were presented. **B:** Although a fraction of LM axons show retinotopic preferences, the percentage is not significantly different from that of V1 somas. This experiment consisted of 6 experimental sessions and 5 mice. The average number of axons per experimental session was 166.17 ± 47.87 and per mouse was 199.4 ± 66.43. The average number of somas per experimental session were 93.00 ± 13.57 and per mouse was 111.60 ± 27.36. Standard errors were calculated per experimental session.

Example experiments suggested that the mean LM RFCs mirrored the properties of V1 somas in the area of the V1 retinotopic map into which they projected more closely than those of ACC axons (Figure 3.11A). RFCs of each spatially specific V1 soma and LM axon were normalised to the mean soma RFCs and compared to investigate the size of RFC scatter (Figure 3.11B). LM axons were significantly more offset in elevation ($p < 0.05$, Mann Whitney-U Test; Figure 3.11D), but not in azimuth (Figure 3.11E). Overall analysis indicates that signals carried by a subset of LM axons are driven by spatially specific stimuli, and that these axons carry information covering a comparable area of visual space to V1 somas in the same retinotopic area in azimuth, but represent a larger area of visual space in elevation.

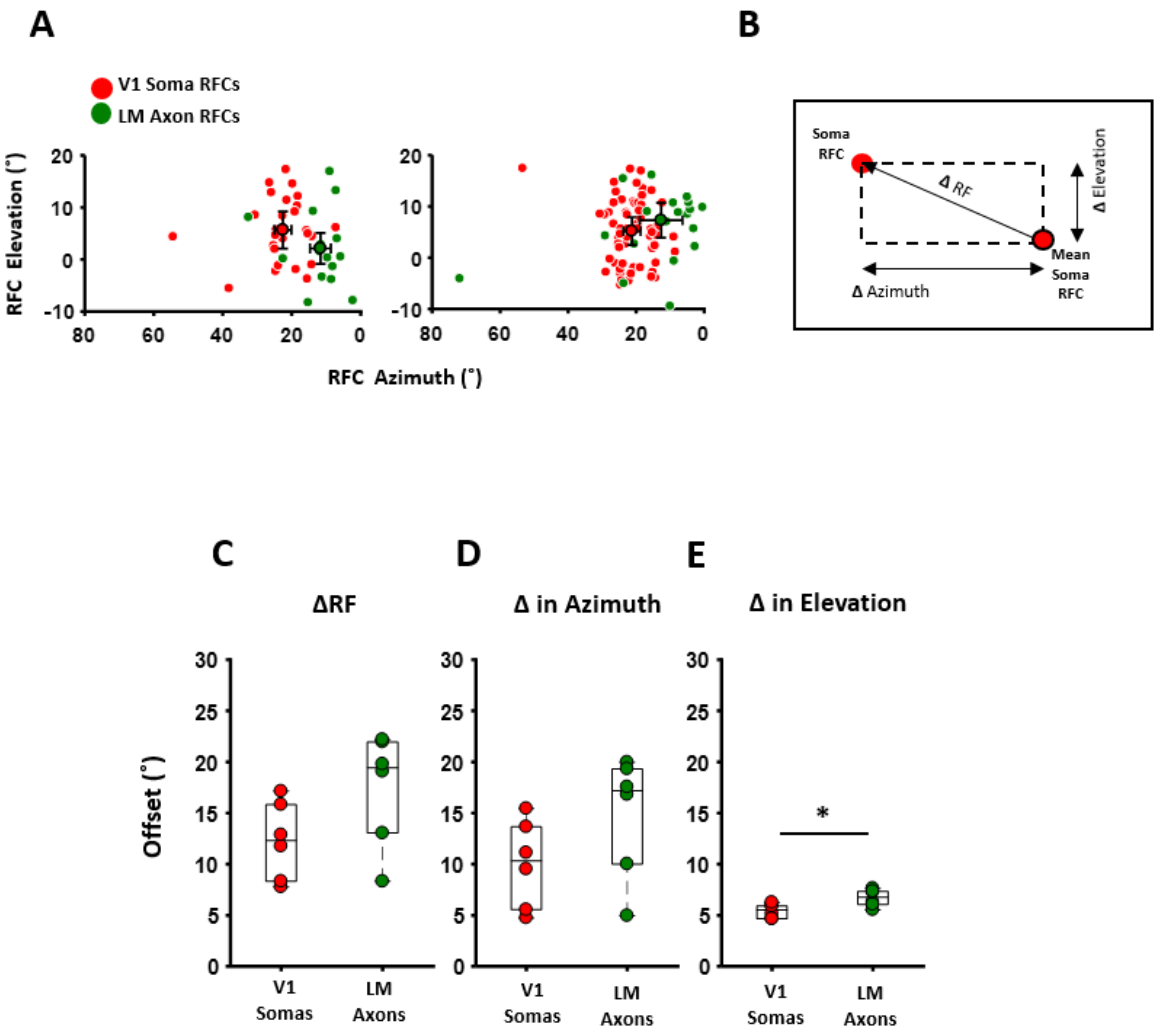

Figure 3.11: LM axons carry signals from a wider area of visual space in elevation than V1 somas process in the same area of visual cortex

A: Examples of RFCs for four experiments where V1 somas preferred different visual locations **B:** Schematic of the normalisation of soma and axon RFCs to their mean in order to compare RFC scatter size. The distance between each point was referred to as ΔRF, and this was then divided into Δ azimuth Δ elevation **C:** The comparison between scatter sizes of RFCs in V1 somas and LM axons **D/E:** Same as in C, but specifically for Δ in azimuth (D) and Δ in elevation (E). The average number of axons per experimental session was 40.67 ± 9.38 and per mouse was 48.8 ± 12.37. The average number of somas per experimental session were 30.83 ± 6.54 and per mouse was 37.00 ± 7.01. Standard errors were calculated per experimental session.

3.3.3 Receptive Field Offset of ACC and LM Axons from V1 Somas

ACC modulation of V1 is thought to be spatially specific (Zhang *et al.*, 2014; Fiser *et al.*, 2016). An involvement in attention (Zhang *et al.*, 2014) would suggest that ACC axons would enhance the response of V1 neurons to relevant stimuli and so if this stimulus is spatially specific then ACC axons need to be arranged closely to V1 neurons that respond to the same location in the visual field in order to have this effect. LM axons projecting to V1 are believed to be involved in the processing of moving objects, including that which occurs when the animal itself is moving (Marques *et al.*, 2018). In this case an offset may be expected as a prediction of where the stimulus is likely to move to.

To explore this, the offset of ACC and LM axonal RFCs were compared with those of the V1 somas in the same imaging region. Initially ACC axons were examined. Imaging regions encompassed V1 somas that were responsive to stimuli across the visual field and RFCs of ACC axons tended to the centre of the visual field regardless of the location of the equivalent V1 soma mean RFC (Figure 3.12A). These were then compared by normalising ACC axon RFCs to the mean soma RFC for each experiment (Figure 3.12B), resulting in an offset value. Each offset value represented a relative distance in visual space. To explore whether the offset values were biased towards a particular location compared to the V1 somas, this relative visual space was divided up into eight segments. ACC axon offset values scattered across all eight segments (Figure 3.12C). The number of offset values in each segment was counted and converted to a percentage for each experiment. Offset values were limited to 30° either side of the V1 soma mean to account for a horizontal bias arising from stimuli being presented over a wider area of visual space in azimuth compared to elevation. It was found that there were significantly more offset values in segments four, seven and eight than two and three (P Values

reported in Table 3.1; Figure 3.12D), suggesting that ACC axon RFC offset is biased to a horizontal alignment with V1 somas.

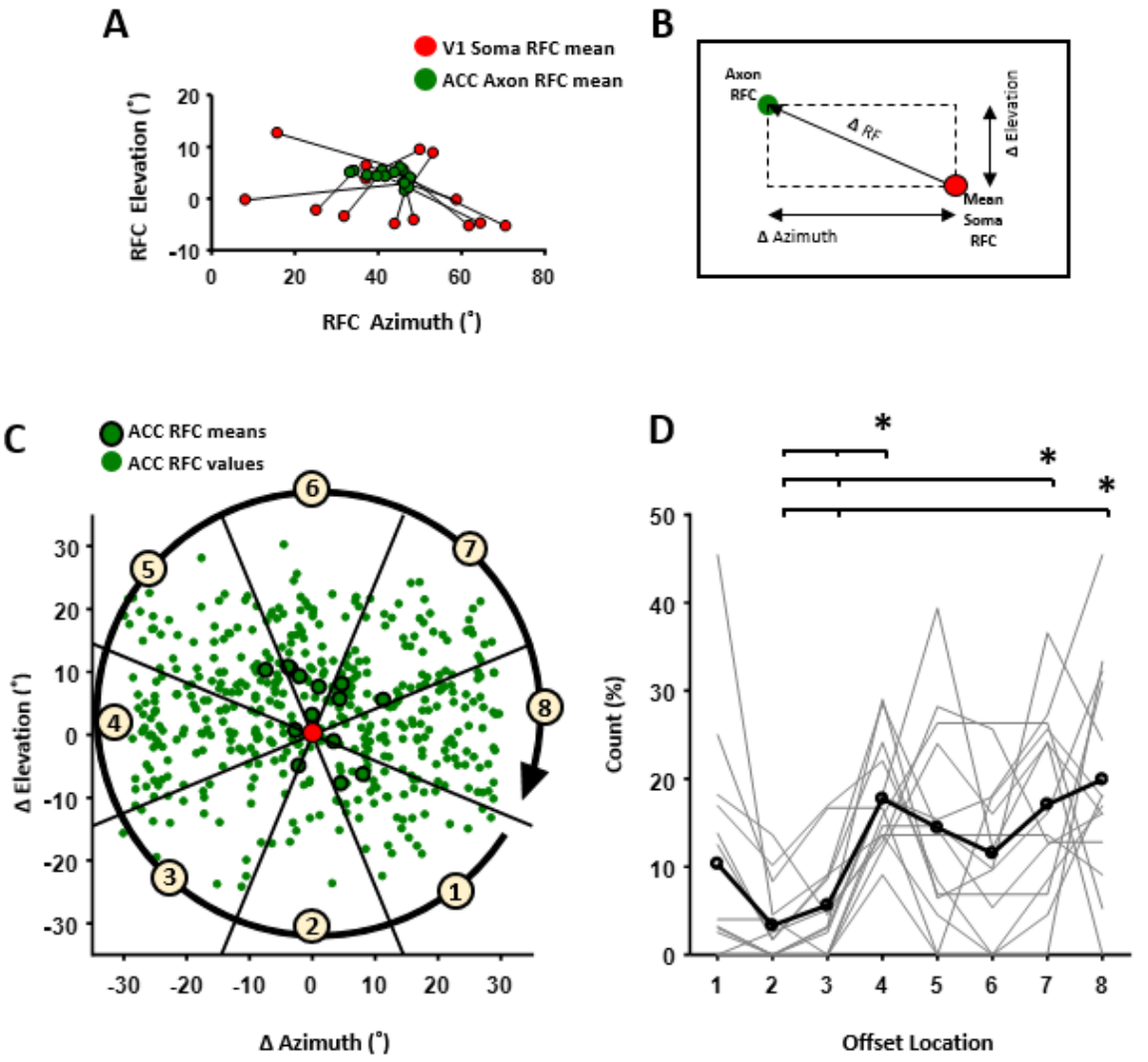

Figure 3.12: ACC axon RFCs are offset in the horizontal plane compared to V1 somas RFCs

A: Mean V1 soma and ACC axon RFCs. Each independent experiment was connected **B:** Schematic showing the normalisation of ACC axon RFCs to their respective V1 soma RFC mean. This resulted in offset values that could be plotted in visual space relative to V1 soma RFC means, where those means were represented by the centre coordinate (0˚,0˚) **C:** Visual representation of ACC axon RFC values described in B. Visual space relative to V1 somas mean RFCs was divided into 8 surrounding segments and the number of offset values in each were counted. The red circle in the centre represents the mean RFC of V1 somas. **D:** Counts for each segment shown in C. Grey lines represent each experiment and black represents to mean. The average number of axons per experimental session was 49.00 ± 5.81 and per mouse was 85.75 ± 19.14. The average number of somas per experimental session were 35.86 ± 4.43 and per mouse was 62.75 ± 16.94. Standard errors were calculated per experimental session.

This was then repeated for LM axons. Mean somas RFC preferences spanned across azimuth from the monocular to binocular region of visual space. In each case, it appeared that LM axons were offset towards binocular visual space (Figure 3.13A). To examine this further, LM axon RFCs were normalised to V1 somas in the same imaging area as described for ACC axons (Figure 3.13B). The offset values of LM axons were also scattered across each of the eight segments dividing up relative visual space, but with a possible bias towards stimuli that appeared above and towards the binocular field of view compared to V1 soma preferences (Figure 3.13C). This was again compared using percentage counts as described earlier, and it was found that there were significantly more axons offset in segment 8 than 1-6 (P Values reported in Table 3.2; Figure 3.13D), confirming the bias towards the binocular direction. No significant difference between segments 8 and 7 suggested that this bias could also be directed above.

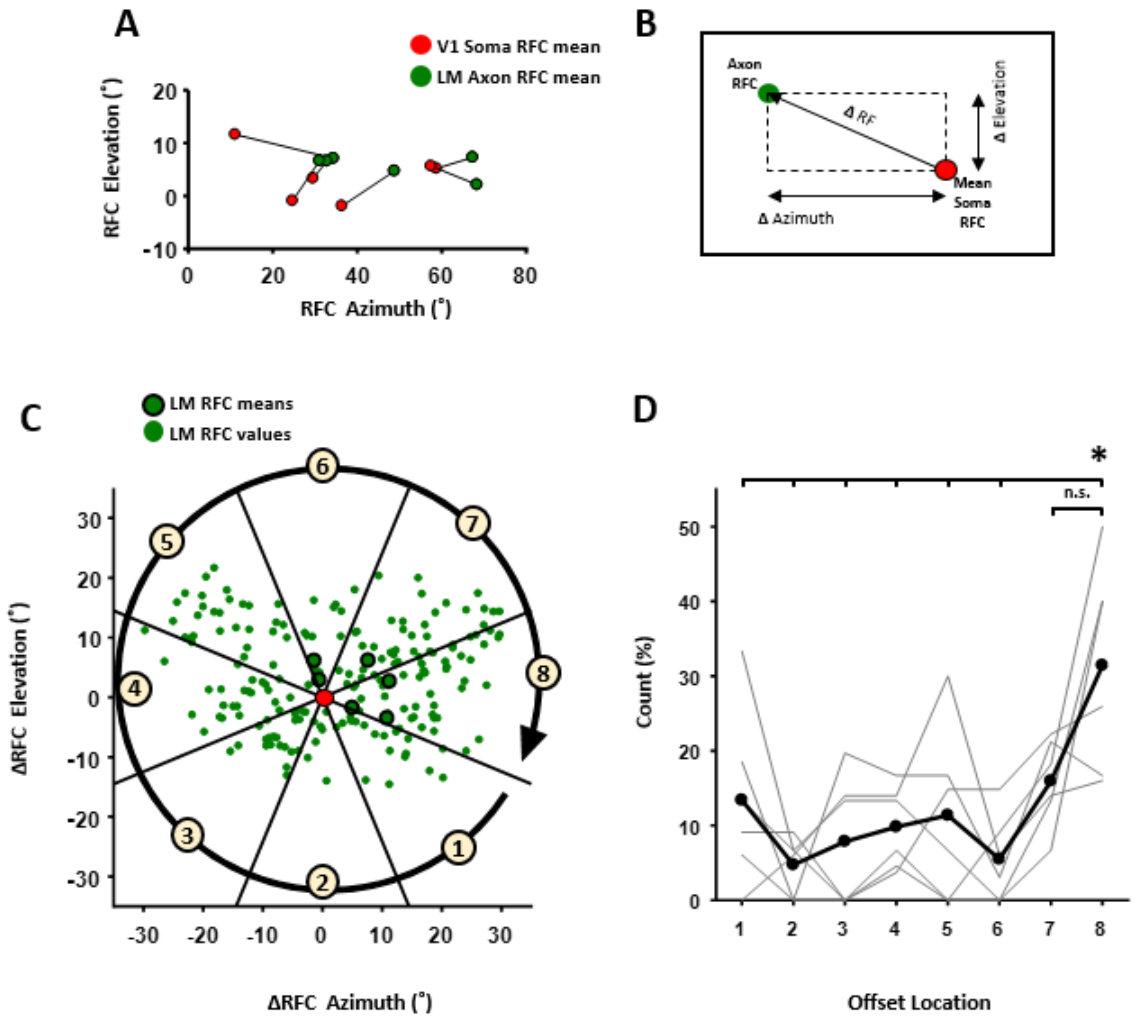

Figure 3.13: LM axon RFCs are offset in the binocular direction compared to V1 somas RFCs

A: Mean V1 soma and LM axon RFCs. Each independent experiment was connected **B:** Schematic showing the normalisation of LM axon RFCs to their respective V1 soma RFC mean. This resulted in offset values that could be plotted in visual space relative to V1 soma RFC means, where those means were represented by the centre coordinate (0˚,0˚) **C:** Visual representation of LM axon RFC values described in B. Visual space relative to V1 somas mean RFCs was divided into 8 surrounding segments and the number of offset values in each were counted. The red circle in the centre represents the mean RFC of V1 somas. **D:** Counts for each segment shown in C. Grey lines represent each experiment and black represents to mean. The average number of axons per experimental session was 49.00 ± 5.81 and per mouse was 85.75 ± 19.14. The average number of somas per experimental session were 35.86 ± 4.43 and per mouse was 62.75 ± 16.94. Standard errors were calculated per experimental session.

Segment A	Segment B	P Value
4	2	0.0028
4	3	0.023
7	2	0.0053
7	3	0.038
8	2	0.00029
8	3	0.0031

Table 3.1: List of p values for relative offset of ACC RFCs from their respective V1 somas

Segments refer to the area of visual space relative to V1 soma RFC means, shown in Figure 3.9C

Segment A	Segment B	P Value
8	1	0.026
8	2	0.00021
8	3	0.0013
8	4	0.0040
8	5	0.0092
8	6	0.00033

Table 2.2: List of p values for relative offset of LM RFCs from their respective V1 somas

Segments refer to the area of visual space relative to V1 soma RFC means, shown in Figure 3.10C

3.3.4 Experience-dependent properties of LM axon organisation

LM axon RFCs appeared to be biased towards binocular visual space compared to V1 somas in the same location in V1. Studies have shown that the formation of the retinotopic map in V1 occurs without visual experience. It is guided both by the expression of receptors such as the EphA-ephrin-A signalling family (Cang *et al.*, 2005) which are arranged in a gradient across V1 (Feldheim and O'Leary, 2010), as well as through cholinergic mechanisms that create waves of ganglion cell discharge propagating across the retina (Wong *et al.,* 1993) before these cells are driven by rods and cones. It is not known, however, whether this would be sufficient to allow the retinotopic organisation of LM inputs into V1 without visual experience. Therefore, to understand this, the study was repeated in mice that had been dark reared. This consisted of placing animals into the dark before eye opening and then recording from LM axons in layer 1 V1 as well as layer 2/3 V1 pyramidal neuron somas as described earlier in this chapter. Dark reared mice were imaged over three sessions, once immediately after removal from the dark, then at 7 and 28 days after this (Figure 3.14A). Light reared control animals were imaged at session one. The imaging protocol was the same as previously described and consisted of presenting visual gratings in 36 locations using 4 orientations and 8 directions (Figure 3.14B). The light reared control group consisted of five mice, six experimental sessions, 997 identified LM axons and 558 identified V1 somas. Session one, two and three after dark rearing consisted of six, seven and six mice, six, seven and seven experimental sessions, 2591, 2999 and 4744 identified axons and 615, 813 and 837 identified somas respectively.

It appeared as though visual responsiveness of V1 neurons and LM axons was reduced when mice were dark reared compared to light reared controls, but this did not reach significance (Figure 3.14C).

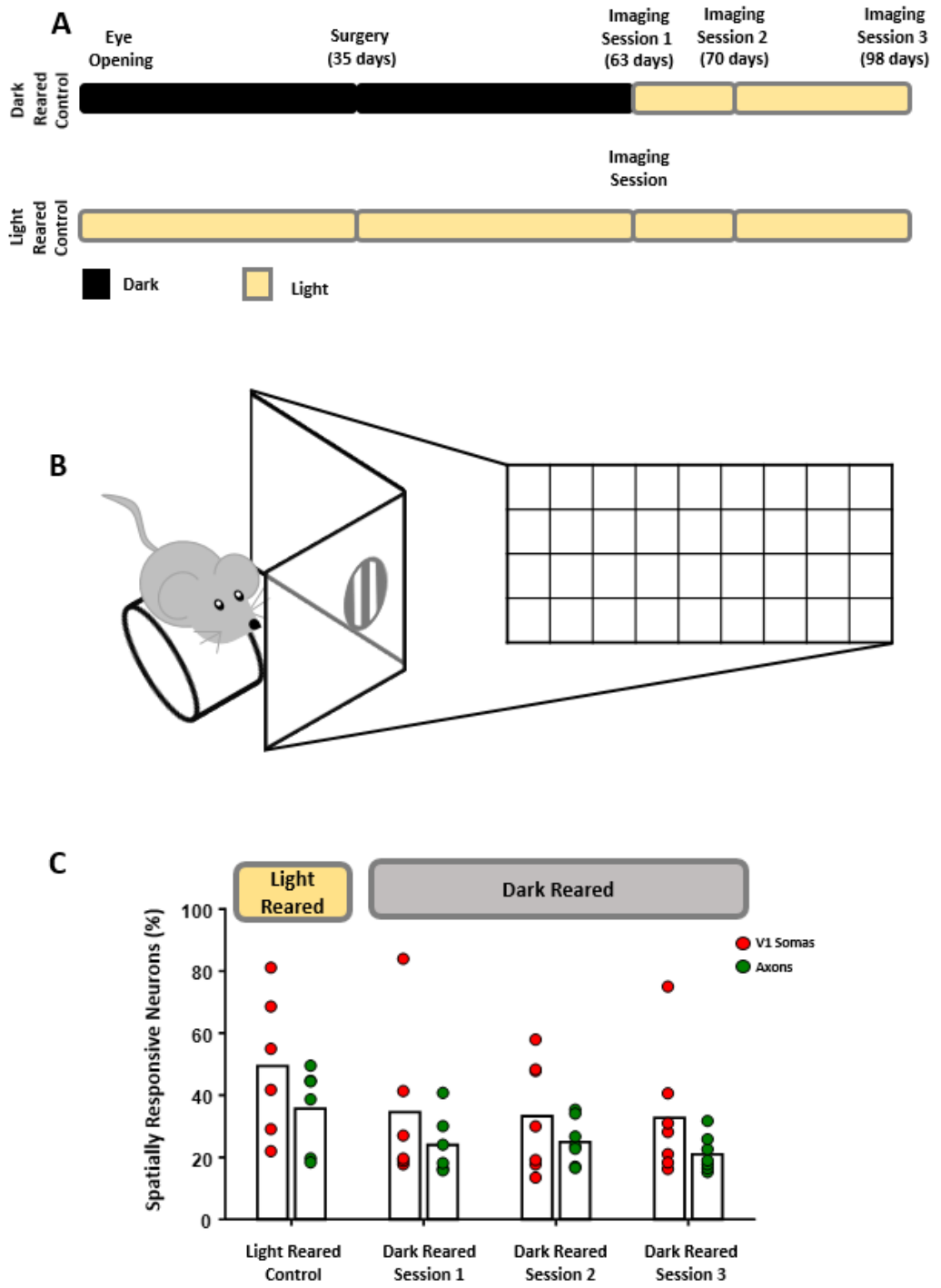

Figure 3.14: Dark reared experiment

A: Schematic of the dark rearing experiment **B:** Schematic of the experimental set-up. Mice were shown visual stimuli as described previously **C:** The percentage of V1 somas and LM axons which exhibited spatially specific activity. Light reared data is from the same cohort as used previously. The light reared control involved 6 experimental sessions and 5 mice. Dark reared session 1 involved 6 experimental sessions and 6 mice; dark reared session 2 involved 7 experimental sessions and 7 mice and dark reared session 3 involved 7 experimental sessions and 7 mice. The number of axons or somas per experimental session and per mouse are shown in Table 3.3

Session	Exp No	Mouse No	Mean ROI per exp/mouse
1	6	6	431.83 ± 203.79
2	7	7	165.57 ± 53.65
3	7	7	525.71 ± 208.55
1	6	6	102.50 ± 7.86
2	7	7	104.57 ± 8.32
3	7	7	109.00 ± 5.98

Table 3.3: The number of experimental sessions and mice used for each dark reared session.

Sessions refer to dark rearing session with session one being immediately after removal from the dark, session two one week after this and session three four weeks after session two. The exp no refers to the number of experimental sessions for each experiment. The mouse number refers to how many mice were used for each dark rearing session. The mean ROI per experiment or mouse is the same in this case as only one area was imaged per mouse. Green highlighted rows indicate information for LM axons and red highlighted rows indicate information for V1 somas.

After this, RFC scatter was then examined for V1 somas and LM axons in dark reared animals and compared to those of light reared controls. Example experiments for each of the three imaging sessions taken from one animal indicated that LM axon RFCs of dark reared animals are scattered across visual space (Figure 3.15A-C). In these experiments the axons were not specifically tracked, but the imaged area was the same and so there was likely to be overlap in axon populations across imaging sessions. LM axon and V1 soma RFCs were then normalised to their respective means to examine the scatter of the receptive fields. There was no significant difference between the scatters for the overall change in receptive field (Figure 3.16A-C). It could be noted, however, that dark reared axon means are clustered around 20˚ for a change in azimuth (Figure 3.16B) and 7.5˚ (Figure 3.16C) for change in elevation, reminiscent of ACC axon arrangement which was shown to feed information from across visual space to V1 somas.

To examine further whether LM axons of dark reared mice projecting to V1 showed a bias to RFC locations towards the binocular area of visual space, LM RFCs were normalised to their equivalent V1 soma RFC as described previously. For each session after dark rearing, LM axon RFCs tended towards the centre of visual space in which stimuli were presented, suggesting the binocular bias was not apparent (Figure 3.17A-C). After normalisation, relative visual space was again divided into 8 segments and offset values were analysed as previously described (Figure 3.18A/C). As session one only had mean soma RFCs covering one half of the visual space in which stimuli were presented, it was discounted from this analysis. In session two, it was found that there was no significant difference between the number of offset values in any of the segments (Figure 3.18B). In session three, there were significantly more offset values in segment 4 than segments 2 and 3 (P values reported in Table 3.3; Figure 3.18D). This suggested

that not only was there no bias towards the binocular area of visual space, but that the bias which did emerge was in the opposite direction. Taken together, these data suggest that visual experience is required for the development LM axonal functional organisation in V1 observed in light reared mice.

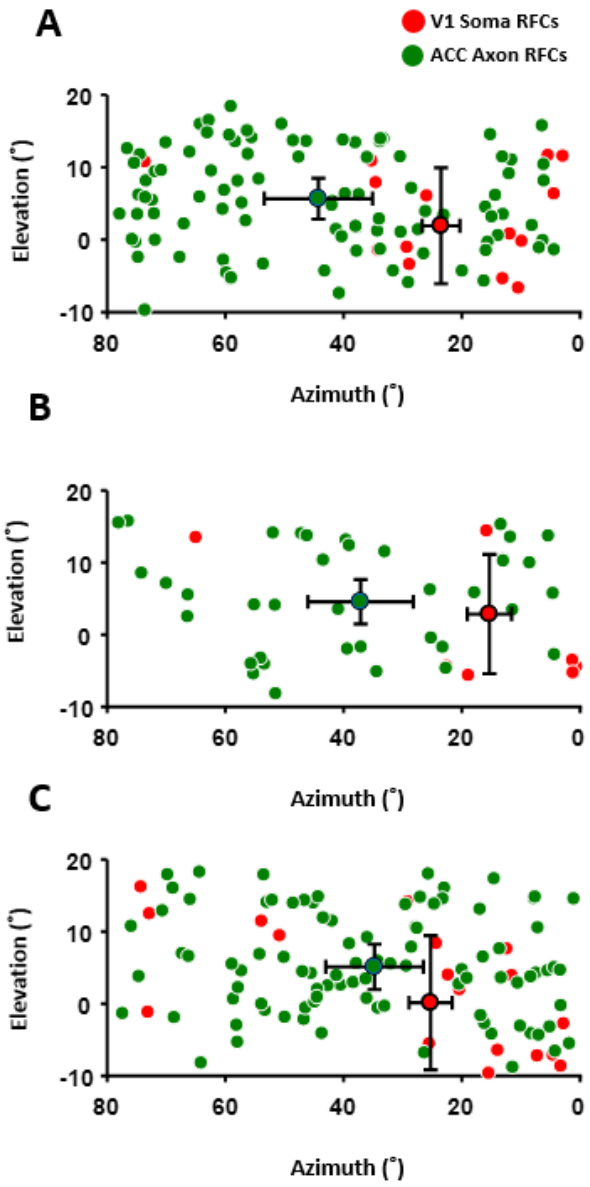

Figure 3.15: Example RFCs for one dark reared mouse for each imaging session

A: RFCs of LM axons and V1 somas in imaging session 1. Data points with black borders indicate the mean RFC for LM axons (green) and V1 somas (red). This experiment recorded one experimental session from one animal with a mean of 74.50 ± 13.82 axons and 20.83 ± 6.88 somas per experimental session and animal **B:** As in A but for session 2. There was a mean of 34.5 ± 7.25 axons and 20.5 ± 5.55 somas per experimental session and animal **C:** As in A but for session 3**.** There was a mean of 95.67 ± 7.75 axons and 16.33 ± 4.77 somas per experiment and per animal.

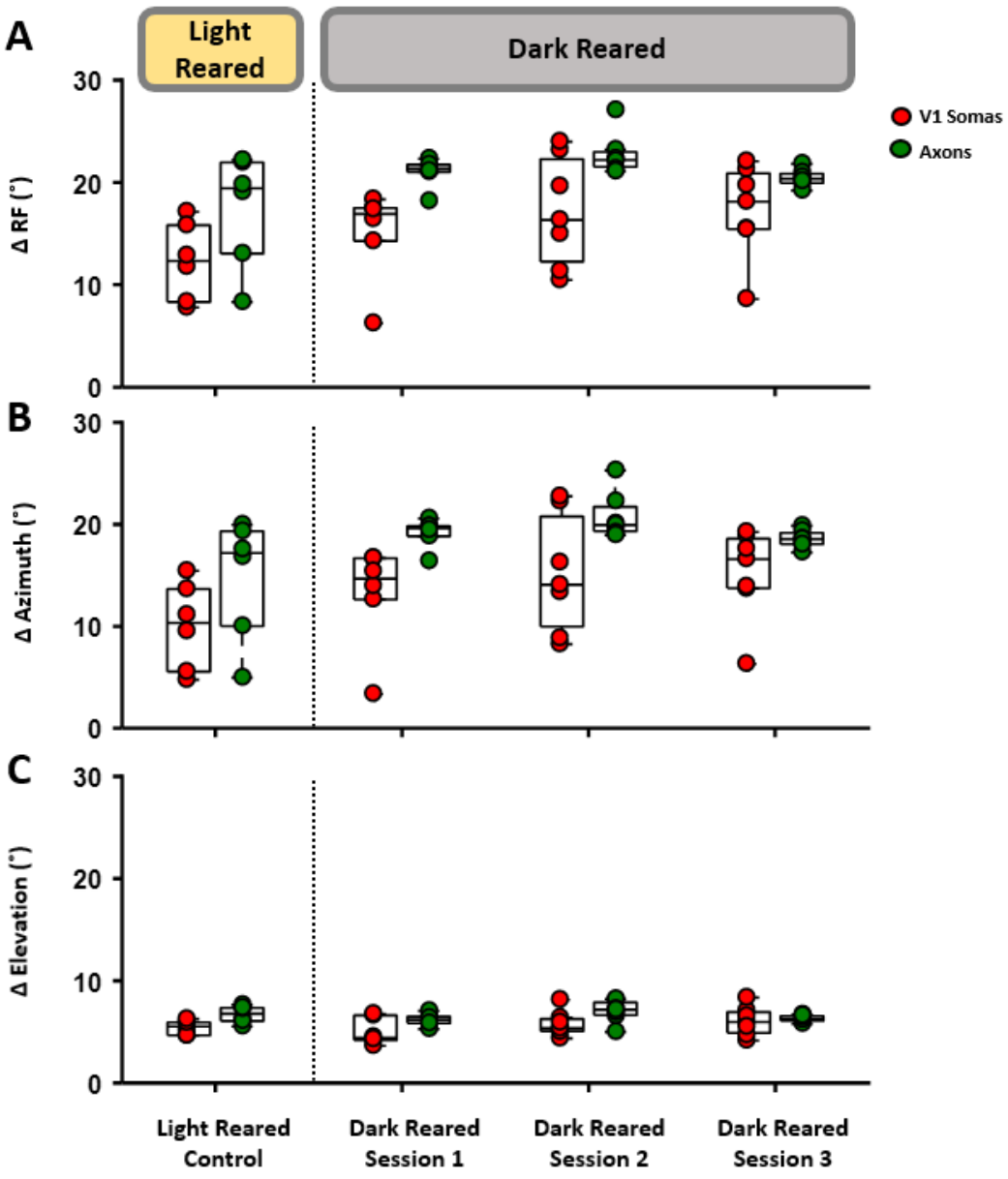

Figure 3.16: Scatter of LM axons and V1 soma RFCs after dark rearing

A: The scatter of V1 somas and LM axon RFCs for the light reared control (left), and for each of the imaging sessions after dark rearing for ΔRF. Each data point indicates the mean for an experimental session **B:** As in A but for Δ Azimuth. **C:** As in A but for Δ Elevation. Light reared data is from the same cohort as used previously. The number of axons and somas per experiment and per mouse were described in Figure 3.14

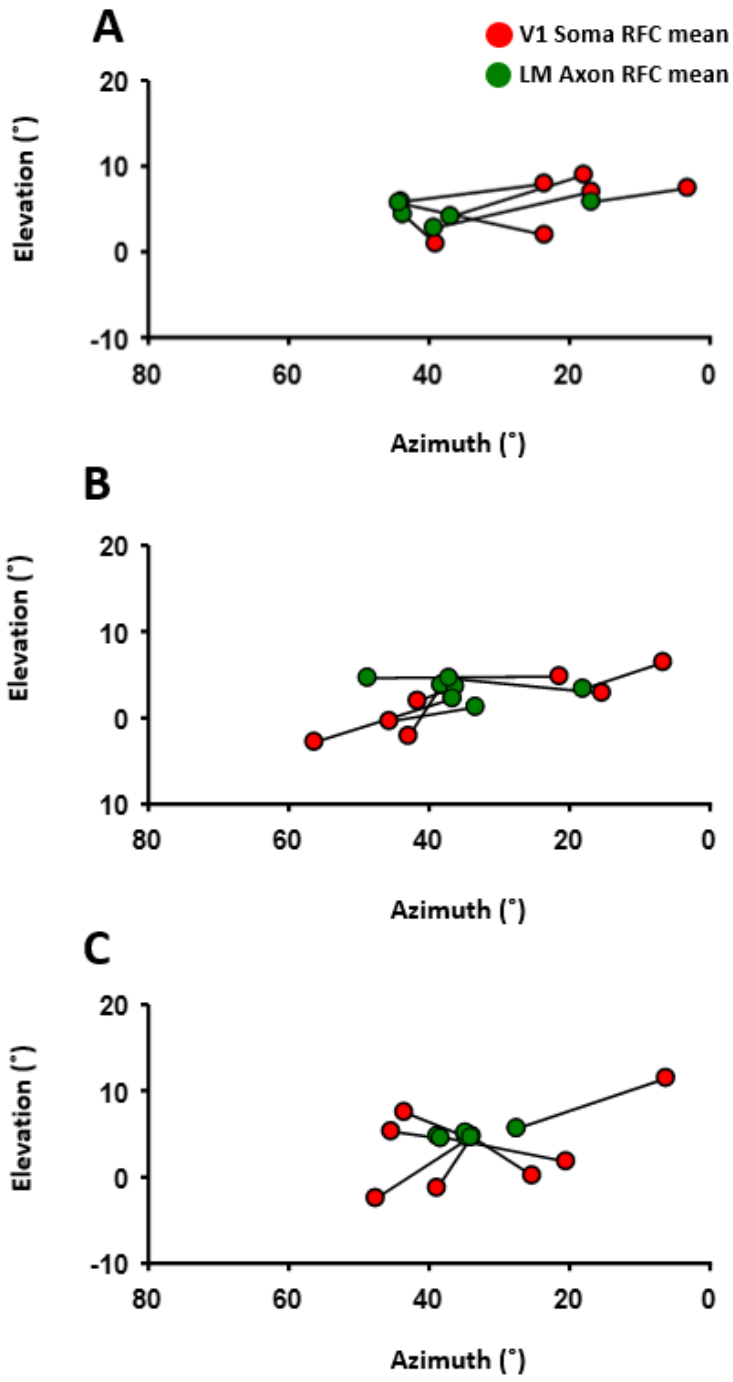

Figure 3.17: Mean V1 soma and LM axon RFCs for dark reared mice

A: RFCs from imaging session 1. Each independent experiment is connected. **B:** As in A, but for imaging session 2. **C:** As in A but for imaging session 3. The number of axons and somas per experiment and per animal were as described in Figure 3.14.

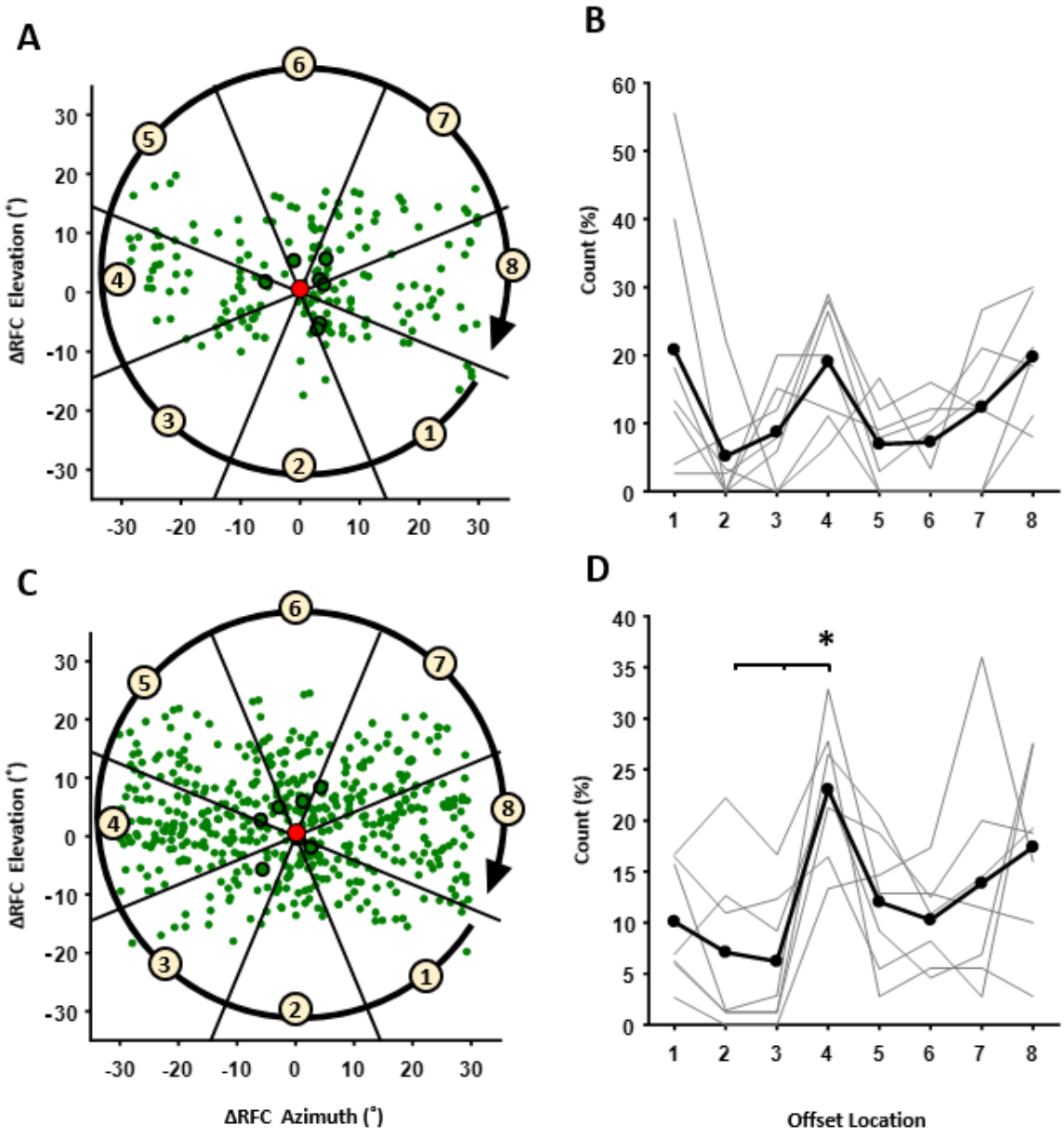

Figure 3.18: LM axon RFC offset from V1 soma mean RFCs is not in the direction of the binocular zone after dark rearing

A: Visual representation of LM axon RFC offset values as described in figures 3.9C and 3.10C but for the second session after mice were dark reared. **B:** Counts for each segment. Grey lines represent each experiment and black represents to mean. **C/D:** As in A/B respectively but for session 3 after dark rearing. Numbers of mice, experimental sessions and average number of axons and somas identified are given in Table 4.

Segment A	Segment B	P Value
4	2	0.0067
4	3	0.0035

Table 3: List of p values for relative offset of LM RFCs from their respective V1 somas for dark reared mice

Segments refer to the area of visual space relative to V1 soma RFC means, shown in Figure 3.15C. P values reported here are for session 3.

3.3.5 Functional organisation of ACC RFCs compared to V1 somas RFCs is not dependent on orientation selectivity

ACC axons appear to have RFCs biased somewhat to the horizontal axis of visual space relative to RFCs of V1 somas in the same imaging area. It remains unknown, however, whether there is any functional organisation of ACC axons dependent on orientation selectivity. It has been shown previously that LM axons projecting to V1 respond preferentially to areas of visual space located orthogonally from their orientation of preference (Marques *et al.*, 2018). It might be the case that the spatial functional organisation of ACC axons is dependent on orientation preferences of axons.

First, orientation preference was explored in V1 somas and ACC axons in the same location within V1. To examine this, the Orientation Selectivity Index was calculated for each neuron (see methods). A significantly higher percentage of V1 somas, at 33.67 ± 2.44 preferred 90˚ to other orientations with 25.00 ± 2.12%, 17.33 ± 2.26% and 24.00 ± 1.26 preferring 0˚, 45˚ and 135˚ respectively. This was in line with V1 somas preferring cardinal rather than oblique orientations. (Xu et al., 2006; Drager 1975) (Figure 3.19A). Proportions of ACC axons also showed orientation selectivity, although the number of neurons that responded to each orientation were comparable at 25.71 ± 1.89%, 23.21 ± 1.35%, 25.09 ± 1.48% and 26.00 ± 1.91% responding to 0˚, 45˚, 90˚ and 135˚ respectively (Figure 3.19B).

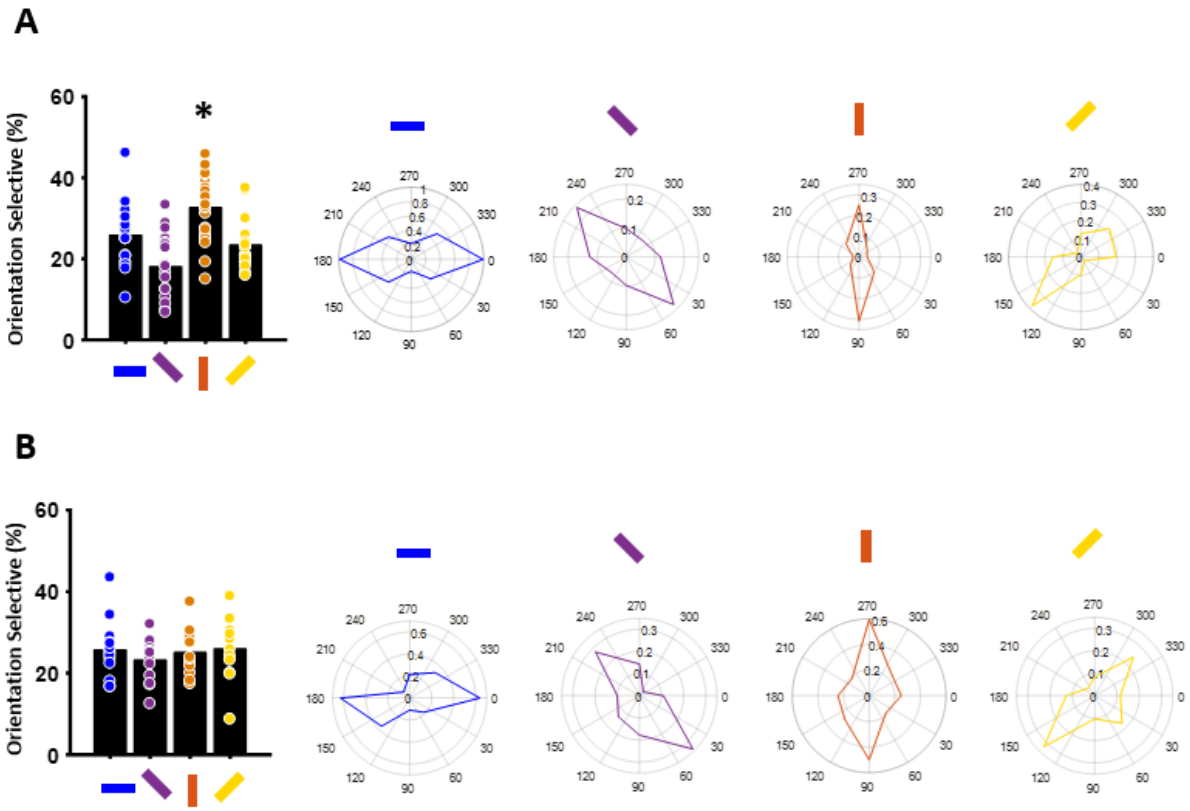

Figure 3.19: ACC axons show orientation selectivity but there is not an over-representation of cardinal orientation preference

A: The percentage of V1 somas, out of all those that exhibited orientation preferences, that preferred each of the four orientations presented (left). Examples of somas which preferred each orientation (right). **B:** As in A but for ACC axons. This involved a mean of 51.64 ± 8.84 axons and 24.21 ± 2.51 somas per experimental session.

After establishing that some ACC axons exhibited orientation preferences, it was investigated whether there was any organisational pattern of RFCs dependent on orientation specificity. To explore this, ACC axons and V1 somas that showed both spatial and orientation preferences were considered. This included 61, 54, 71 and 70 ACC axons that preferred 0°, 45°, 90° and 135° oriented stimuli respectively. Initially, axon RFCs were normalised to the mean soma RFC of the V1 somas in the same imaging area to calculate a change in RF (Figure 3.21A) resulting in offset values as described previously. These offset values were also calculated for axons that were spatially specific but did not exhibit an orientation preference (Figure 3.21B) for later normalisation of the percentage counts. The relative visual space around the mean soma RFC was then split into four segments (Figure 3.21C) in which the offset axonal RFCs could lie. The RFC pattern of each orientation was taken into account individually and so there were three populations of axonal RFC within each segment – those of the current orientation, those of the other three orientations, and those that only show spatial specificity (Figure 3.21D). The organisation of ACC axon RFC offset values was explored for each orientation independently and the positioning of each segment in visual space depended upon the orientation under investigation. The parallel segment would always be the area of relative visual space along the long axis of the orientation in question, and the perpendicular would be along the short axis (Figure 4.21E). RFCs for each orientation in each segment were counted within a radius of 30˚ and normalised to the number of RFCs in that segment that did not show an orientation preference. This was to control for stimuli being presented over a larger degree of visual space in azimuth. For each orientation within each experiment, a percentage was calculated for how many offset values were in each relative segment compared to the other three. These values were then compared using an n-way ANOVA. There was no significant different between the number of RFCs in each of the relative segments for any of the four orientations tested. This suggested that there was no

organisation of ACC axon RFCs dependent on orientation preference (Figure 3.21B).

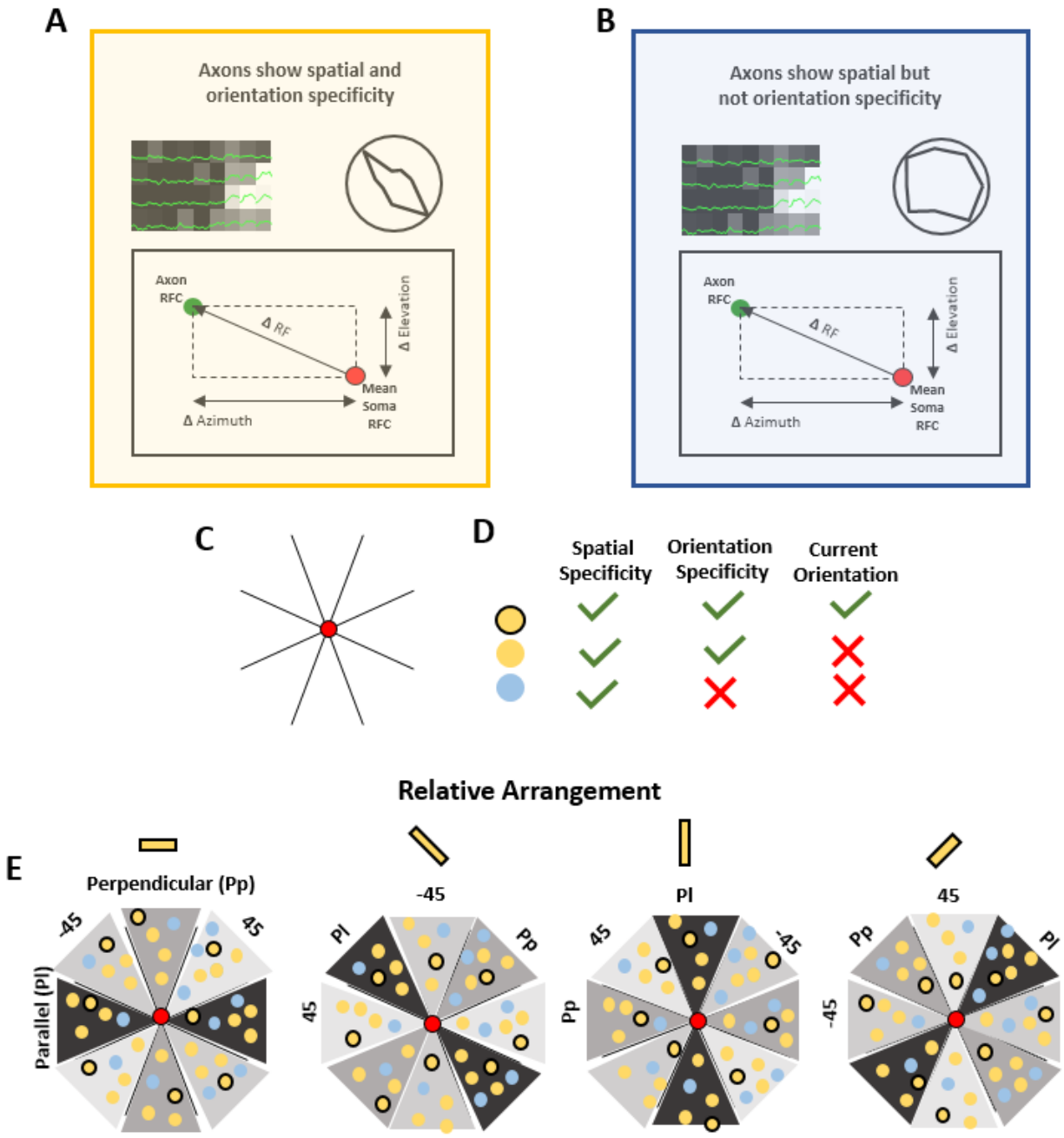

Figure 3.20: Orientation-dependent organisation of ACC axon RFC offset from V1 somas

A: Schematic showing the calculation of ACC axon RFC offset values for axons which responded to both a specific location and orientation of visual stimulus. **B:** As in A but for axons that did not show an orientation preference **C:** The relative visual scene where the centre coordinate represented V1 soma RFC means was divided into four segments **D:** Each of the different groups of ACC axon that were present in each segment. **E:** The relative arrangement of each of the segments of visual space relative to V1 soma RFC means. Segments were arranged depending on the orientation under investigation. Parallel segments were always arranged along the long plane of the orientation, and perpendicular segments were always orthogonal. For example, for axons that preferred 0˚ (left diagram), the parallel segment was on the horizontal plane, and for axons that preferred 90˚, the parallel segment was on the vertical plane.

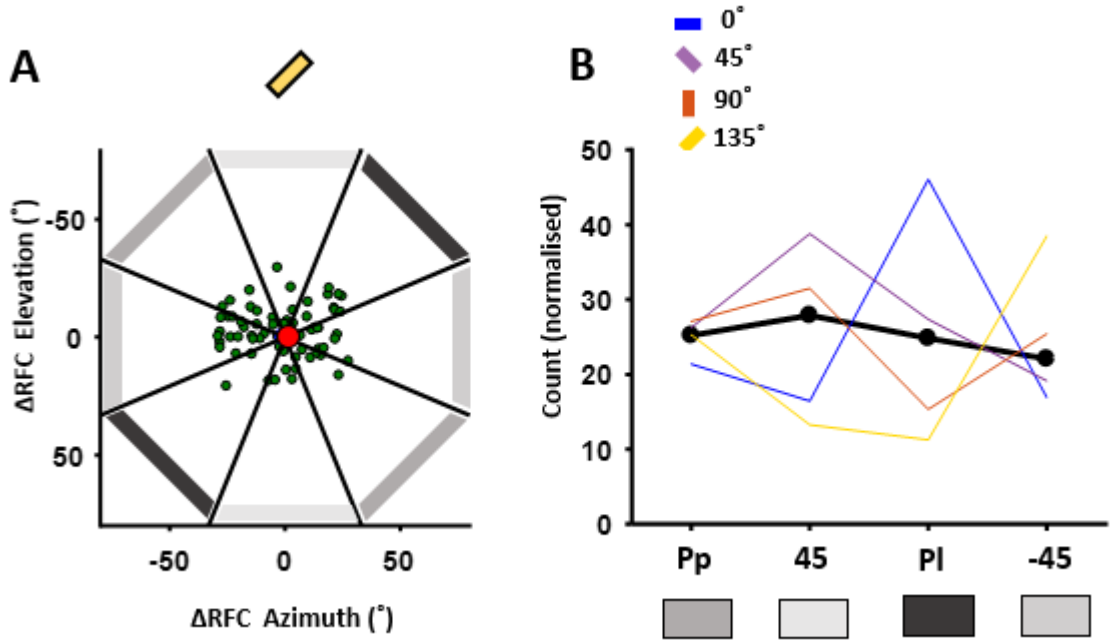

Figure 3.21: Organisation of ACC axon offset values relative to their orientation preferences

A: An example of the distribution of ACC axon offset values for ACC axons preferring visual stimuli of orientation 135˚. Green dots indicate the relative offset of ACC axon RFCs from the mean of the V1 soma RFC, indicated by the red dot in the centre. **B:** There was no preferences for any area of visual space depending on orientation preference. This involved a mean of 51.64 ± 8.84 axons and 24.21 ± 2.51 somas per experimental session.

3.4 Summary of Findings

1. A fraction of ACC axons have spatially selective responses, but the proportion showing these was significantly lower than for V1 somas.
2. A fraction of LM axons have spatially selective responses, and the proportion showing these was comparable to that for V1 somas.
3. ACC axon RFCs were significantly more scattered in both azimuth and elevation compared to V1 soma RFC scatter.
4. LM axon RFCs were significantly more scattered only in elevation compared to V1 somas.
5. ACC axon RFCs were offset towards the horizontal plane compared to V1 soma RFCs.
6. LM axon RFCs were offset towards the binocular field of view, and this appears to be dependent on visual experience.

4 The Involvement of Anterior Cingulate Cortex Axons Terminating in Primary Visual Cortex in Visually Guided Tasks

4.1 Introduction

The sensory environment has a plethora of stimuli which the brain is unable to process at once. To successfully navigate this world, the brain must be able to focus attention amongst competing stimuli onto those which are important (Desimone and Duncan, 1995) and coordinate relevant responses. This is apparent, for example, when searching for food or when evading predators. To achieve this, two processing streams are used, known as bottom-up and top-down projections. In the visual system, bottom-up projections faithfully relay information about particular visual stimuli such as their location and orientation. They are most crucial in directing attention in unfamiliar scenarios to visual features of potential importance such as the movement of a predator or a car. As scenarios gain familiarity, bottom-up projections are believed to dynamically interact with top-down influences (Makino and Komiyama, 2015) that use previous experience to guide attention to specific stimuli. These are believed to be internal projections originating primarily from the frontal (Miller and Cohen, 2001) and parietal regions (Kastner and Ungerleider, 2000; Bisley and Goldberg, 2010), such as the frontal eye field (Zhou and Desimone, 2011; Squire *et al.*, 2013), and have been implicated not only in the direction of attention (Zhang *et al.*, 2014), but also in the development of spatial maps (Fiser *et al.*, 2016) as well as influencing processing during motion (Niell and Stryker, 2010; Keller *et al.,* 2012; Bennett *et al.,* 2013; Saleem *et al.*, 2013; Erisken *et al.*, 2014).

Where various stimuli are competing for finite processing resources, learning to direct attention towards stimuli that are behaviourally relevant and can be associated with a reward or avoiding an aversive stimulus will be favoured. Using previous experience to

focus attention upon a stimulus that holds behavioural relevance appears to involve a strengthening of top-down activity coupled with the weakening of bottom-up signals, something that has been implicated during learning (Makino and Komiyama, 2015) and perceptual memory consolidation (Miyamoto *et al.*, 2016). This would require an integrated system able to identify the visual stimulus, make a decision based upon it, process the consequences of that decision and use that information to inform subsequent choices based on what has been learned.

It has been extensively reported that neurons in V1 respond more to visual stimuli that are being attended to compared to those which are not (Moran and Desimone, 1985; Corbetta *et al.*, 1991; Treue and Maunsell, 1996) and that paying attention to a stimulus that is behaviourally relevant in particular works to strengthen the corresponding neuronal representation (Poort *et al.*, 2015; Daliri, Kozyrev and Treue, 2016; Keller *et al.*, 2017). Attending to specific stimuli in the environment requires a decision to be made and this will be influenced by association of a stimulus with a rewarding or aversive outcome. Therefore, processing of reward and subsequent decision making are essential in deciding where to direct attention. The anterior cingulate cortex (ACC) has been strongly implicated in decision making, especially when influenced by reward. Rats with lesions at the ACC tend to always choose a lower reward when greater effort is needed to obtain a larger reward, whereas rats with an intact ACC go for the higher reward (Schweimer and Hauber, 2005) suggesting an importance in choosing the appropriate option when responses have competing outcomes (Cocker *et al.*, 2016). Located within the prefrontal cortex, a structure implicated in goal-directed activity (Miller and Cohen, 2001), the ACC is also the source of many long-range top-down projections. In the mouse, it projects extensively to multiple sensory cortices including the auditory cortex, somatosensory cortex and visual cortex (Zhang *et al.*, 2016). This suggests that an interaction between ACC and

V1 is a prime candidate for controlling visual attention in tasks that involve detecting and subsequently making a decision based on a stimulus in order to obtain a reward.

One such projection originating at ACC and terminating predominantly in layer 1 of V1 has been identified (Zhang *et al.*, 2014). Recent studies have, however, highlighted discrepancies in its believed functionality. One idea is that this circuit is involved in aiding visual attention. Optogenetic activation of this projection not only sharpened orientation tuning of neurons in V1, but also improved performance in a visual discrimination behavioural task suggesting an involvement in selective attention as well as exhibiting spatially specific responses. This projection is believed to act through local inhibitory circuits with somatostatin positive GABAergic interneurons contributing preferentially to surround suppression and vasoactive intestinal peptide-positive interneurons critical for centre facilitation (Zhang *et al.*, 2014). Other evidence, from another recent study, has suggested it instead has a key role in developing an internal representation of the visual environment based on spatial location. In this study, head-fixed mice were allowed to explore a virtual tunnel where the presentation of four stimuli in a specific order was coupled to the movement of the mouse on a rotating spherical treadmill. Under these conditions initially axons projecting from ACC were only responsive to the visual stimuli when on the screen but as the mouse was exposed to more trials, these responses occurred just before the stimuli appeared. This suggests that temporal tuning of activation of the projection becomes predictive as a visual stimulus gains spatial relevance while mice learn to navigate an environment (Fiser *et al.*, 2016).

Following on from the work of Zhang *et al.* (2014), I asked the question of whether the ACC→V1 top-down circuit is endogenously recruited to improve performance in a visually guided discrimination task. To address this question, two-photon microscopy was used to image axons originating from ACC in layer I of V1 while animals performed

the same go/no-go visual discrimination task employed by Zhang *et al* (2014). It was hypothesised that, once mice learned the task and exhibited high performance, ACC activity would be apparent, and specifically elevated during correct trials. Furthermore, as ACC activity would be influenced by the retinotopic location of the visual stimulus presented.

4.2 Materials and Methods

4.2.1 Mice

All procedures performed on animals were carried out in accordance with institutional and UK welfare guidelines as previously stated. Mice were kept in standard laboratory conditions which involved cycles of 14 hours of light and 10 hours of darkness at 24°C. They were provided with a standard diet and water ad libitum unless on water restriction. Water restriction was implemented during the course of the behavioural tasks, beginning approximately three days before studies commenced. A daily allowance of water was calculated for each mouse individually based on weight. Mice were able to obtain this during the behavioural task each day, and if they did not reach the allowance limit then the rest was given directly after. The weight of each mouse was monitored daily to ensure it did not drop below 80% of the original baseline weight of the mouse. Experiments involved both wildtype (WT) mice and those in which parvalbumin positive (PV+) interneurons were labelled with the red marker tdTomato, achieved by crossing B6.Cg-Gt(ROSA)26Sortm14(CAG-tdTomato)Hom/J and B6;129-Pvalbtm1(cre)Arbr/J (Jackson Laboratory, JAX Stock 007914 and 008069, respectively). Wildtype mice were ordered from Charles River and PV-CRE mice were bred in-house. All mice were housed with same sex littermates and were provided with running wheels.

4.2.2 Viral Injection and Cranial Window Implant

Experiments involved mice where just ACC axons were labelled with a calcium-sensitive indicator, as well as mice where both ACC axons and layer 2/3 V1 somas were labelled. To achieve this, methods previously described in the general methods and previous result chapter were used. Mice used in the detection task were injected with a type of gCaMP6s that was preferentially transported to axons (Broussard *et al.*, 2018).

4.2.3 Intrinsic Signal Imaging

Intrinsic signal imaging was used to identify the area in monocular V1 to image from. This was achieved using methods previously described in the general methods.

4.2.4 Visual Discrimination Task

Mice were placed on water restriction and behavioural training commenced after they reached 80% of their initial weight. They were headfixed and the custom-designed fixed axis treadmill was locked to prevent locomotion. Behavioural training for the go/no-go visual discrimination task consisted of three stages, including stage one, two and the testing stage. Each stage was controlled by custom-written code in MATLAB that automatically progressed the mice to the next stage after reaching a pre-defined threshold. On correct go trials mice were rewarded with KoolAid® (Craft Foods).

Stage one (Figure 4.1) consisted of building an association between licking the reward spout and obtaining a reward. At this point, no visual stimuli were presented to the mice. Each trial could last up to 60s, but if the mouse licked the spout then it was immediately given a reward and moved into a variable quiescent period (Figure 4.1B). During the quiescent period of the task, a lick of the spout would not result in a reward. This was to reinforce that rewards could not be obtained at all times. The quiescent period was temporally variable so that mice could not predict when to lick the spout to obtain a reward based on time. This was important for later stages where mice were required to lick the spout at certain times and withhold at others. Mice were able to consistently lick the spout throughout the session, as well as complete trials with a minimum of a two second quiescent period prior (Figure 4.1C/D). Once mice were consistently licking the spout with a median response time of less than 5s over a period of 20 trials, they were progressed to stage two.

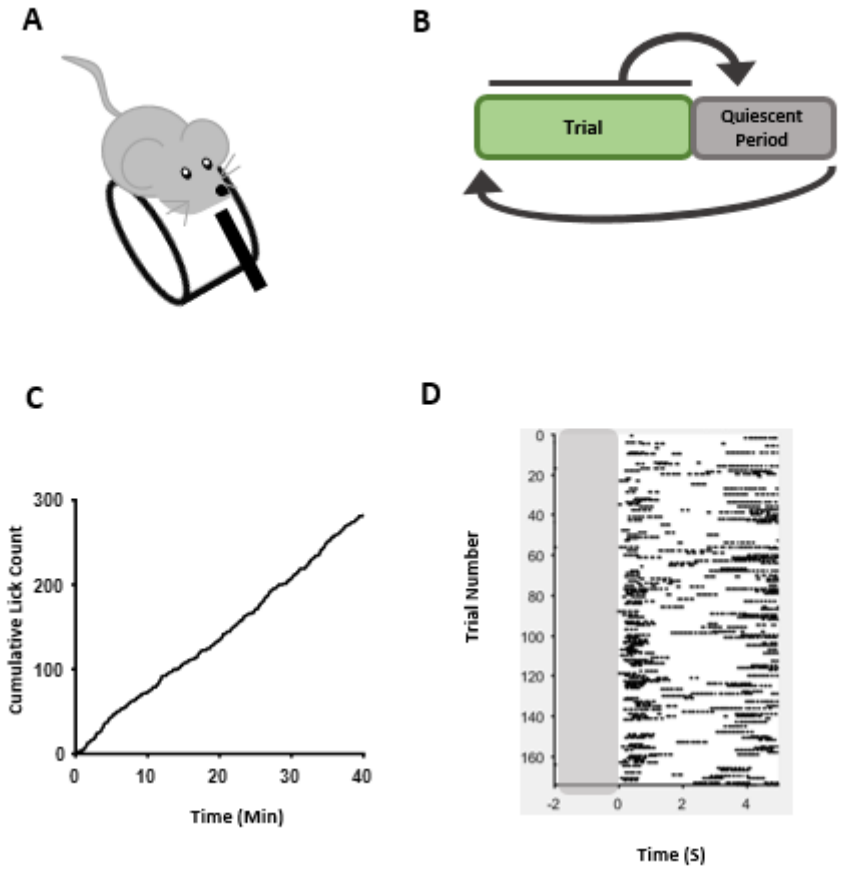

Figure 4.1: Stage one of the visual discrimination task

A: Schematic of stage one of the task. This stage was used to associate licking the spout with gaining a reward. As in later stages of the task the reward would only be given under certain circumstances, a reward was not given for every lick. Instead, if the animal licked within the trial then it would immediately receive the reward and be shifted into the quiescent period. Licking during this quiescent period did not result in a reward, and mice had to refrain from licking for at least two second before beginning the next trial. This was important to reduce continuous repetitive licking. No visual stimuli were shown at this stage **B:** Diagram of stage one of the task. The top arrow shows that after the mice lick at any point during the trial, they are immediately shifted into the quiescent period. The lower arrow indicates that after the quiescent period, mice are shifted to the next trial as described in A. **C:** Mice lick consistently throughout the course of this stage **D:** Lick raster plot shows that mice do not continuously lick the spout. The grey section indicates the quiescent period.

Stage two (Figure 4.2) consisted of introducing the go stimulus and pairing it with the lick response to obtain a reward. An auditory tone occurred 0.5s prior to the onset of the trial. The visual stimulus was then presented to the mouse for a period of four seconds (Figure 4.2A/B). The response of the mouse was disregarded during the first two seconds of stimulus presentation as mice were likely to exhibit impulsive licking when the visual stimulus appeared and contributed to the outcome of the trial in the latter two seconds of presentation, referred to as the response window. The go stimulus was paired with the reward by having a mix of 'free reward' and 'normal' trials. In the 'free reward' trials, the reward would be given at 3.5s if the animal did not lick the spout during the response window and the trial was classed as incorrect. If the mouse licked the spout in the response window prior to 3.5s then it immediately obtained the reward and this was classed as a correct trial. In 'normal' trials, a correct trial was recorded if the mouse licked and obtained a reward in the response window. If the animal did not lick the spout throughout the response window then it would not receive the KoolAid® and the trial was deemed incorrect. Stage 2 began with 90% 'free reward' trials and 10% 'normal' trials. These proportions changed by 10% if the mouse achieved a performance of 70% correct until 100% of trials were 'normal' (Figure 4.2C). Mice improved in performance across this stage (Figure 4.2D) and once their performance at 0% 'free reward' trials reached 70%, they were progressed to the testing stage of the task.

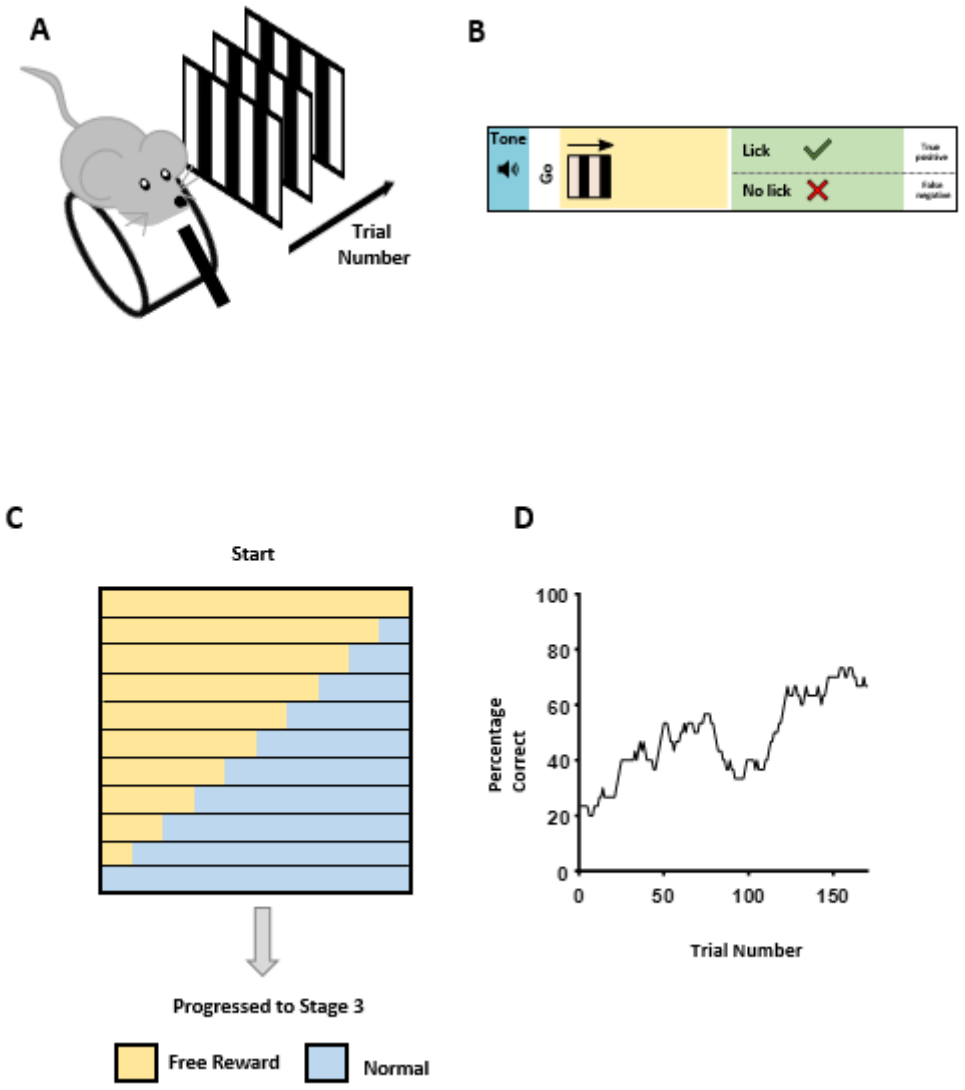

Figure 4.2: Stage two of the visual discrimination task

A: Schematic of stage two of the task. This stage was used to associate licking the spout in response to the presentation of the go stimulus with a reward. **B:** Diagram of the visual discrimination task. **C:** Diagram of the progression through stage 2 where mice are given a changing proportion of 'free' and 'normal' trials. This begins at 100% 'free' trials and 0% 'normal' trials. Mice progress if they complete over 70% of trials correctly in 10% percentage intervals to 100% 'normal' trials and 0% 'free' trials, and then subsequently onto stage three. **D:** An example experiment indicating that mice increase in performance (calculated by percentage correct) over the course of stage two and reach the 70% threshold.

The testing stage introduced the no-go stimulus, a grating of orientation 0˚ which drifted upwards. If the mouse licked the spout during the response window of a no-go trial then it received an air puff, white noise and a ten second time-out. This encouraged licking the spout only in response to the go stimulus. Performance was calculated use d' (d' = ZFA - ZHit). High performance was considered to be a d' of greater than 1.5 and a HR-FA rate of greater than 0.5.

Two forms of the visual discrimination task were used. The first involved the go and no-go visual stimuli being presented in the same spatial location in each trial, and to the contralateral eye to imaging. This version was referred to as the retinotopically predictable format. The second design comprised the visual stimuli being presented in the monocular field of either the contralateral or ipsilateral eye in a pseudorandom way, and thus the mice were not able to predict exactly where the stimulus would appear. This was referred to as the retinotopically unpredictable format. This allowed the investigation into whether ACC activity was retinotopically specific, as well as examining ACC activity in an arguably more difficult visual discrimination task.

4.2.5 Visual Detection Task

Studies have shown that the ACC projection to V1 is retinotopic and may exhibit properties similar to surround suppression (Zhang et al., 2014), something that is characteristic of top-down modulation. It was therefore possible that ACC activity properties would be overlooked in the visual discrimination task due to the large stimulus required. To address this in this study, a visual detection task was developed which allowed for a smaller stimulus. Mice that had both ACC axons and layer 2/3 V1 somas labelled were used in this experiment so that it was possible to image locations in V1 that were retinotopically matched to the stimulus, and then move the stimulus outside of this area. Mice were placed on water restriction and behavioural training commenced after they reached 80% of their initial weight. Behavioural training for the detection task was based on the same three stages already described in the visual discrimination behaviour. Stage one was identical with the same aim of associating licking the spout with gaining a liquid reward of KoolAid®. Stage two introduced the go stimulus, but the response window lasted the entire length of the presentation rather than just the second half. Mice again progressed through trials where there were a high proportion of 'Free Rewards' relative to 'Normal' trials, which reversed as performance improved and entered a variable quiescent stage in between trials. The testing stage consisted of a go/no-go structure where a blank was shown in the no-go trials, but the incorrect response of licking during this time did not result in an air-puff, white noise or time-out. This design made it possible to investigate ACC axonal responses to a visual stimulus both inside and outside of the matched receptive field of the layer 2/3 V1 somas directly ventral in the cortex. Furthermore, it was possible to begin to separate axon activity levels at the visual stimulus onset and when the mouse licked the spout to gain a reward due to reaction time causing a slight temporal delay between the two.

4.2.6 Perfusion and Histology

Mice were given a lethal intraperitoneal injection of sodium pentobarbital (Euthatal; Merial Animal Health). After there was no response to tail pinch and the mouse had stopped breathing, it was perfused. This consisted of opening the chest cavity to expose the heart. A needle attached to a pump was inserted into the left ventricle and the right atrium was snipped. This allowed 0.1M phosphate-buffered saline (PBS) to be fed through the circulatory system in order to remove the blood. Once the blood had been cleared, 4% paraformaldehyde (PFA) in PBS was pumped through to fix the tissue. The brain was then dissected out and submerged in PFA for another four hours.

Each mouse brain was sliced at 80 µm using a vibratome. Slices were mounted onto gelatin-covered microscope slides, left to adhere and dry, re-hydrated and then coverslipped using Fluoromount Aqueous Mounting Medium. Mounted slices were imaged using a confocal microscope.

4.2.7 Data Analysis of Neuronal Activity

Analysis was carried out using Python and MATLAB. Images were extracted and registered using Suite2p (Pachitariu *et al.*, 2017). To analyse neural activity on a trial-by-trial basis, fluorescence timecourses of gCaMP6s or jrGECO1a representing ACC axon and V1 soma activity within individual experiments were broken up by aligning to an element of the behaviour, for example the onset of the visual stimulus or the timing of the rewarded lick. Neurons were considered to be responsive to a particular stimulus if there was a significant change in activity compared to a baseline time calculated for each trial independently across an experimental session using a repeated measures ANOVA test. In some cases, this was done for a specific time window within the trial such as the visual stimulus onset or response window of the visual discrimination task. In other cases, significantly increased responses were examined at 0.2s time intervals

after the defined baseline time before the start of the trial. This was to identify when axons or somas began to respond during the tasks, and to make sure responses were not discounted because the occurred prior to a specific relevant time window, something that may occur otherwise if predictive or preparatory responses were exhibited.

Where data was not extracted as trials, correlational analysis and permutation tests were used. This involved comparing fluorescence data to lick frequency and locomotion data. Lick data was collected at 1000 Hz in binomial form. It was converted to rate over a time kernel of 1s and then resampled to 5 Hz to match the fluorescence data timings. A permutation test was then carried out by correlating the resulting lick data with the fluorescence trace, before incrementally shifting the fluorescence trace circularly and calculating a correlation coefficient for each shift. The 100 coefficient values for each individual session were ranked, and if the original value was in the top fifth percentile then calcium activity was considered to be significantly associated with lick frequency. The same method was used to examine the association of locomotion and neural activity, although in this case wheel velocity (i.e. running speed of the animal) was used in place of lick frequency. Values are given as mean ± SEM unless otherwise stated.

4.3 Results

4.3.1 Learning a retinotopically predictable go/no-go visual discrimination task

Mice are able to learn a range of visually guided tasks when head-fixed, including those where different stimuli are passively presented, as well as those using virtual reality corridors linked to the movement of the mouse (Chen *et al.*, 2013; Poort *et al.*, 2015). In this study, the endogenous activity of ACC axons was explored while animals performed a go/no-go visual discrimination task while stationary to investigate whether ACC axons exhibited elevated activity at specific time windows within the task; as well as whether ACC axon activity was generally elevated when the task was being performed successfully. The go/no-go visual discrimination task was implemented based on that used in Zhang *et al*., (2014) and Andermann *et al*., (2010). Head-fixed animals were trained to discriminate between the go stimulus, a vertical grating drifting forwards, or the no-go stimulus, a horizontal grating drifting upwards, by licking a spout to receive a liquid reward in response to the go stimulus. Animals were positioned on a spherical treadmill which was locked in place to prevent locomotion. Each stimulus was presented for four seconds and the lick response of the mouse was recorded in the final two seconds, known as the response window. High performance on this task was achieved by training animals through three stages (see methods).

During the testing stage, trials consisted of presenting the mouse with either the go or the no-go stimulus in a retinotopically predictable location in the monocular region of the contralateral eye (Figure 4.3A). Each trial (Figure 4.3B) was preceded by an auditory tone sounded 0.5s before the onset of the visual stimulus. The go or no-go stimulus would drift for four seconds, and the lick response of the animal would only lead to correctly or incorrectly completing the trial in the latter two seconds to reduce the impact of impulsive licking. Licking the spout was only reinforced during the go trials, and if the mouse licked the spout during the response window of the no-go trial it

received an air puff, white noise and a 10s time-out. Performance was quantified by calculating d' (see methods) which measured the difference in proportions of hit and false alarm trials. A higher d' indicated a higher level of performance. The following study included six mice, 16 experimental sessions and 2007 identified axons.

Over the course of training, the lick responses of the mice aligned to specific elements of the task including the sounding of the tone and the response window of go trials, the latter being indicative of an improvement in performance. (Figure 4.3C). On average, mice were able to achieve a high level of performance (defined as d' > 1.5) after 8 days of training during this stage (Figure 4.3D); and were generally able to perform this behaviour consistently over days with only rare drops in performance (Figure 4.3E). The performance of each animal was considered independently.

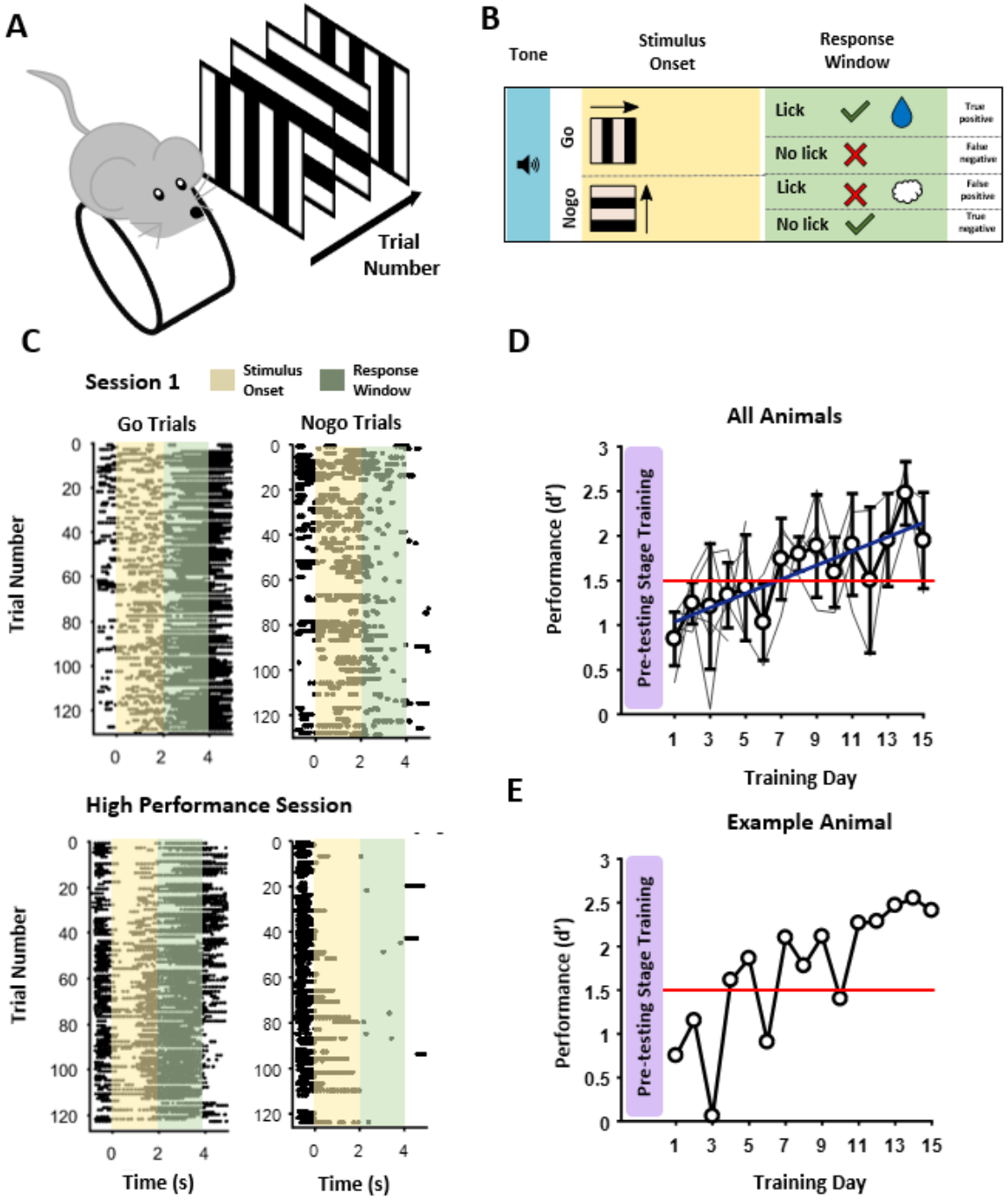

Figure 4.3: Mice can perform a go/no-go visual discrimination task

A: Schematic of the retinotopically predictable discrimination task. **B:** Diagram of the visual discrimination task. **C:** Lick raster plots: top – early training session before the mouse has learned the task; bottom – training session where the mouse exhibits high performance. **D:** Mean performance of all mice. Lines indicate the best fit (blue) and the high performance threshold (red) **E:** Example performance of an individual mouse. The red line shows the high performance threshold.

4.3.2 The activity of ACC axons was elevated during specific time windows during the go/no-go discrimination

To label ACC axons projecting to V1, GCaMP6s was injected into ACC (Figure 4.4A). This injection site is shown in Figure 4.4B. After approximately four weeks GCaMP6s filled axon terminals could be visualised both at the site of injection at ACC and throughout the depth of V1, with the highest density in layer 1 (Figure 4.4C). A cranial window was implanted above V1 of the right hemisphere and intrinsic signal imaging was used to localise V1 (see general methods) before using two-photon microscopy to functionally measure activity of the axons.

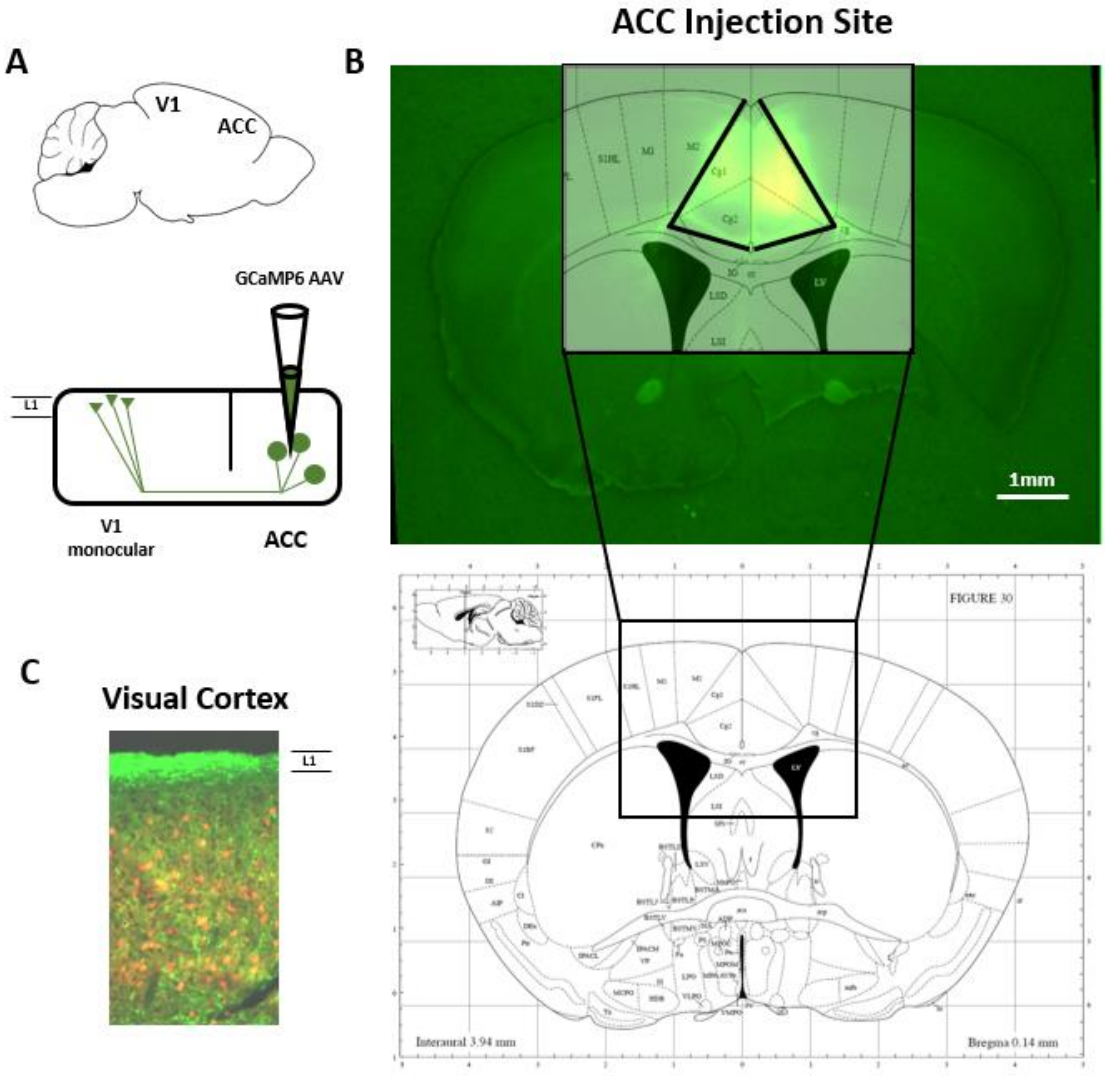

Figure 4.4: ACC injection and cranial window implant

A: Top: Approximate position of ACC and V1; bottom – ACC injection schematic. **B:** Histology of ACC injection. Top - injection site at ACC where GCaMP6s transfected neurons appear green/yellow. This image is superimposed by a schematic of the mouse brain atlas (also shown below the image) to confirm the injection was made in ACC. **C:** visual cortex where the green colour in layer I indicates axons labelling.

Initially the question of whether ACC axon activity increased during the task as the mice learned was addressed. To do this, ACC axonal responses from the first session in which the mouse was exposed to either the go or no-go stimulus were compared with when the mouse exhibited high performance on the task. Axons were not specifically tracked but were sampled from the same location in V1 and so were likely to be made up of a similar population. A percentage of 39.16 ± 3.54% of ACC axons responded during the presentation of the go stimulus once the task had been learned, significantly higher than the 18.29 ± 5.26% that responded the first time the go stimulus was shown to the mice. No significant difference was observed during no-go trials with 23.62 ± 8.52% responding the first time the no-go stimulus was shown and 31.65 ± 4.22% responding when performance was high (Figure 4.5A/B).

After this, the responsiveness of 2007 axons was measured during behavioural sessions where the mice exhibited high performance. Axons were divided into go and no-go conditions before sorting trials by the time of peak activation. It was observed that subsets of axons were active at time points spanning the entire trial in both conditions (Figure 4.5C). Although axons were observed to respond exclusively to either go or no-go trial types, it was clear that overall activity levels were significantly higher during go trials as compared to no-go trials with 29.68 ± 3.04% and 11.52 ± 1.20% of axons showing activity over the entire trial respectively ($p < 0.001$, one-way ANOVA). It was also noted that 6.33 ± 1.80% of axons responded indiscriminately to both types of trial, which was significantly less than those exclusively responding to go trials ($p < 0.001$, one-way ANOVA), but comparable to those responding to no-go trials (Figure 4.5D).

Each trial was made up of two main elements, namely the presentation of the visual stimulus and the response window, and further investigation was carried out to find out

which of these the axons were active in. When the visual stimulus was presented, 24.29 ± 3.18% of axons responded exclusively to the go stimulus which was significantly more than the 8.15 ± 1.87% to the no-go stimulus ($p < 0.001$, one-way ANOVA). This was also significantly more than the 5.79 ± 1.19% that responded to both stimuli ($p < 0.001$, one-way ANOVA). Additionally, significantly more axons were active during the response phase of task during go trials with 26.56 ± 3.68% compared to 10.57 ± 1.64% in the no-go trial ($p < 0.001$, one-way ANOVA). Furthermore, significantly more axons were active exclusively in either the go ($p < 0.001$, one-way ANOVA) or the no-go ($p < 0.05$, one-way ANOVA) trials during this phase of the trial compared to indiscriminately active axons (Figure 4.5D).

This analysis indicated that axons were active during each phase of the task when it was performed correctly, but that there were a significantly higher percentage of axons that responded to the go stimulus in comparison to the no-go stimulus. Additionally, when the mice were required to make a response, significantly more axons responded exclusively to either the go or no-go stimulus than indiscriminately to both.

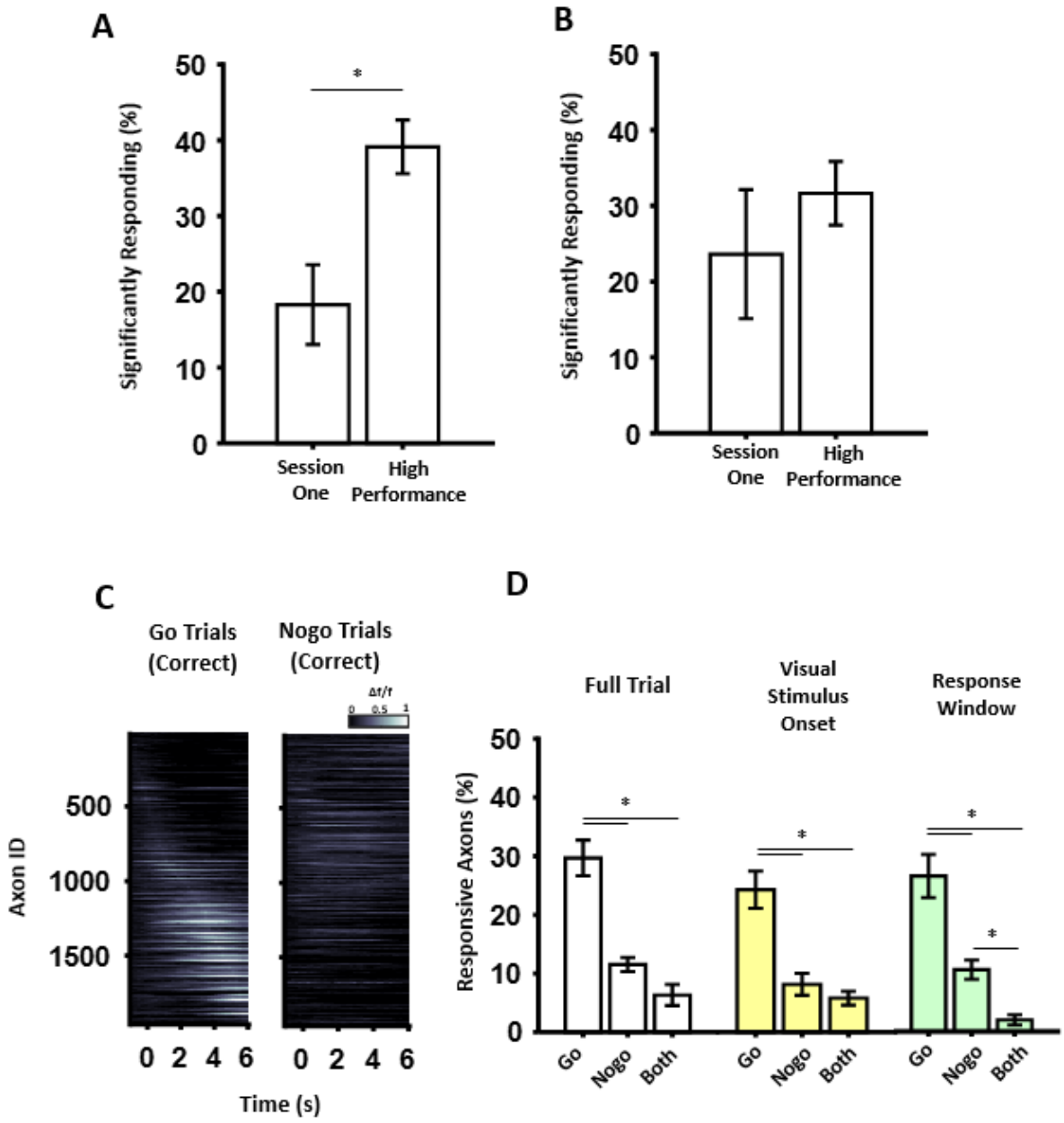

Figure 4.5: ACC axon activity during the retinotopically predictable version of the task

A-B: The percentage of ACC axons that were significantly activated during the first presentation of the go stimulus (A) or the no-go stimulus (B) relative the percentage active during high performance trials **C:** Heatmaps of all identified axon activity across go (left) and no-go (right) trials, sorted by activity in go trials. **D:** The percentage of ACC axons that exhibit increased activity relative to prior baseline of 0.5s during the trial (left), the visual stimulus onset period (middle) and the response window (right). This experiment involved 16 experimental sessions and 6 mice. The mean number of ACC axons identified per session was 126.44 ± 10.83 and per animal was 337.17 ± 72.33.

4.3.3 Elevated activity in ACC axons is not linked to improved performance

It has been asserted that this long-range projection from ACC to V1 is involved in directing visual attention and that its activity can influence performance in a visual discrimination task. Zhang *et al.,* (2014) have provided evidence that optogenetically stimulating ACC axon terminals in V1 led to significant increases in performance compared to non-stimulated trials in the same behavioural session (Zhang *et al.*, 2014). To investigate whether increased elevated endogenous ACC axonal activity was associated with improved discriminability, I examined it for each trial type across all identified axons. In high performance behavioural sessions there was a fluctuation in performance throughout, but this did not appear to be associated with equivalent fluctuations in ACC activity (Figure 4.6A). Additionally, when the mean neural activity across the four different trial types was examined, it was apparent that, as predicted, the highest levels of activity during go trials occurred when completed correctly; however, this was not the case during no-go trials. For these trial types, neural activity was elevated more during incorrect iterations (Figure 4.6B).

This projection from ACC to V1 is thought to terminate on a variety of different neuronal types including PV+, SST+ and VIP+ interneurons, as well as the apical dendrites of excitatory pyramidal neurons in V1 (Zhang et al., 2014). It is possible that there are different subsets of axons projecting from ACC that transmit an assortment of information and, by including all identified axons in the sample, the activity of individual axons had been masked. To understand whether a subset of ACC axons showed a general elevation in activity while mice performed well in the visual discrimination task, axons exhibiting significantly different activity in correct trials compared to incorrect trials were selected. It was hypothesised that, if endogenous activation of ACC axons enhances visual discrimination, as has been shown with optogenetic activation, then an increase in activity would be observed in correct trials regardless of whether the trial type was go or no-go. The trials were split into 0.2s bins and the activity of each axon

was compared to a baseline activity 0.5-1s before the sounding of the tone for each time epoch. Animals did not lick the spout and were not able to predict the starting time of the trial during this baseline time. It was found that, in general, the percentage of axons that had a significantly elevated activity compared to the baseline increased over the course of the trial with a peak of 12.95 ± 3.15% and 29.95 ± 2.94% for the visual stimulus and response window respectively in the go trials and 16.07 ± 3.15% and 29.76 ± 2.94% the equivalent for the no-go trials. This activity increase over time was significant ($p < 0.001$, repeated measures ANOVA) and there was no significant difference between go and no-go trials at each time point (Figure 4.6D). Interestingly, post hoc analysis revealed this significant change over time only became apparent during the response window at 2.4s after the onset of the visual stimulus.

It was reasoned that, if elevated activity of ACC axons resulted in improved discrimination performance, then axons that exhibited this significantly different response to correct and incorrect trials should also show display increased axonal activity specifically in correct trials regardless of whether the stimulus presented was go or no-go. To test for this possibility, the mean axonal activity for each axon significantly responding during each 0.2s bin was calculated for correct and incorrect completions of both go and no-go trials. The mean axonal response from incorrect trials was then subtracted from that of the correct trials. This resulted in a positive value for axons responding significantly during go trials, consistent with the hypothesis. This was, however, not the case for no-go trials where a negative value indicated a greater amount of axonal activity during incorrect trials, which was significantly different from the positive values observed in the go trials over time ($p < 0.001$, repeated measures ANOVA; Figure 4.6E). Post hoc analysis indicated that the difference between the positive neural activity value during go trials compared to the negative value during no-go trials reached significance at approximately 3.4s after stimulus presentation, during

the response window. Furthermore, mean activity of those axons that discriminated between correct and incorrect trials was greater in correct go trials compared to correct no-go trials (Figure 4.6F). This deviation in neural response between correct go and no-go trials was most apparent during the response window of the task. Overall, this indicated that, on average, increased ACC→V1 axon activity was not associated with improved discrimination performance.

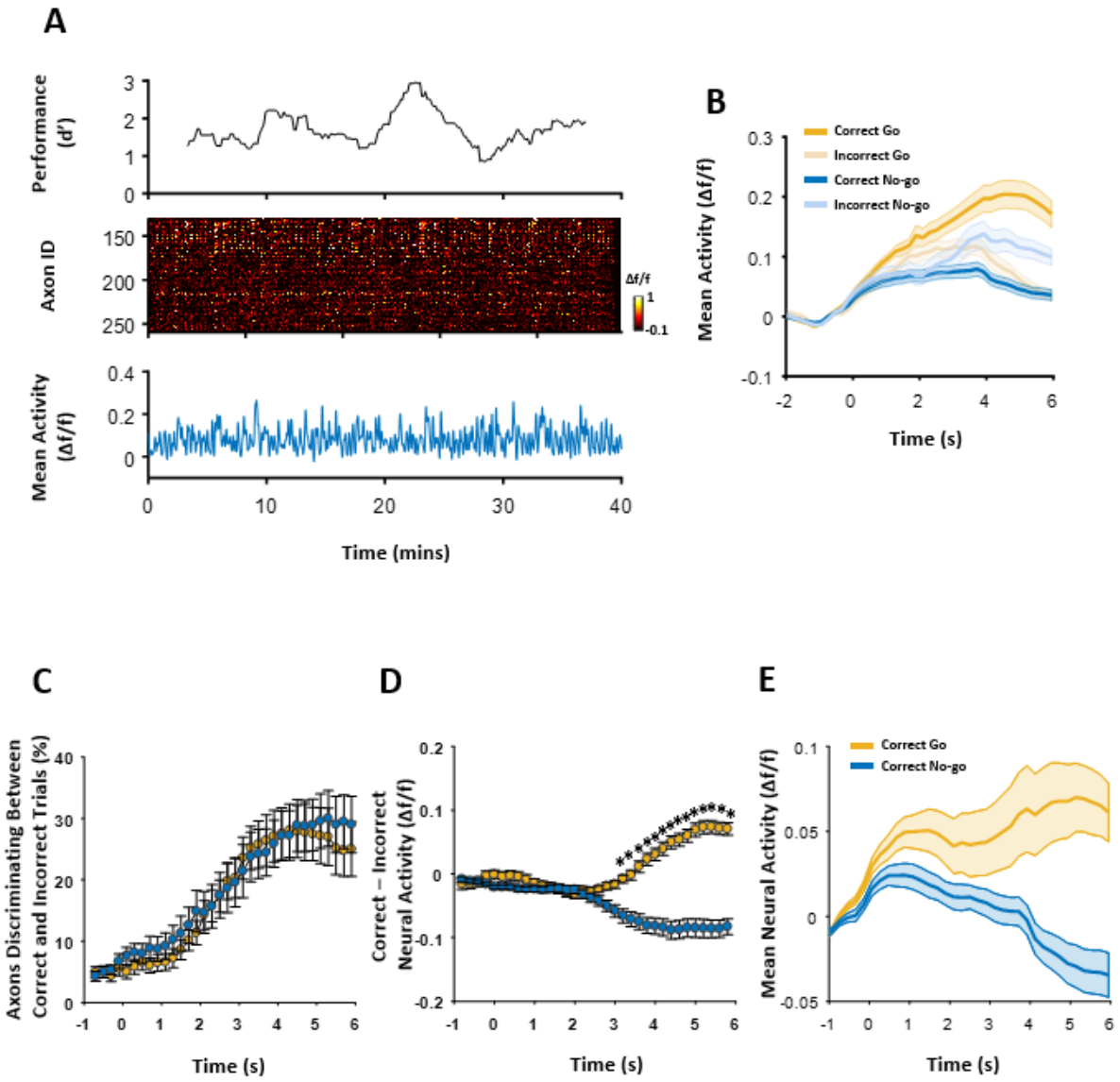

Figure 4.6: Elevated activity in ACC axons is not associated with increased performance in a visual discrimination task

A: Example of performance fluctuation across one session (top), ACC axon activity of all identified axons in the same example session (middle) and the mean activity of all axons shown above. **B:** Mean neural activity of all identified axons in each of the four trial types. **C:** The percentage of ACC axons that respond significantly differently to correct and incorrect trial types binned at 0.2 second intervals across the trial **D:** Subtraction of ACC axon activity during incorrect trials from that during correct trials from axons identified in C **E:** Mean neural activity of axons identified in D in correct go and nogo trials. This experiment involved 16 experimental sessions and 6 mice. The mean number of ACC axons identified per session was 126.44 ± 10.83 and per animal was 337.17 ± 72.33.

4.3.4 Increasing the task difficulty did not alter ACC circuit recruitment

Previous work has suggested that long-range ACC projections are only active when the cognitive demands of the task are relatively high (White et al., 2018). It was therefore reasoned that increased activity in ACC to V1 axons may not have been observed with increased performance because the retinotopically predictable visual discrimination task was too easy.

To increase task difficulty an additional version of the visual discrimination task was developed involving presenting retinotopically unpredictable stimuli. It has been shown that if a stimulus appears in an unpredictable location then performance in visual tasks will decrease (Mangun and Hillyard, 1990), a sign of increased difficulty. ACC has also been shown to be more active in tasks where the location at which the visual stimulus appears is unpredictable (Hahn *et al.,* 2007).

To make the stimulus location retinotopically unpredictable, stimuli were programmed to appear in a pseudorandom fashion to either the contralateral or ipsilateral hemisphere (Figure 4.7A/B). The following study included six mice, nine experimental sessions and 1176 identified axons. It took mice on average 14-15 days to attain high levels of performance after reaching the testing stage of the task, longer than 7-8 days for the retinotopically predictable task. Mean performance levels reached a maximum of 1.82 ± 0.10 at day 16, lower than the 2.47 ± 0.21 for the retinotopically predictable task (Figure 4.7C). The slower learning rate coupled with the lower peak performance showed that the retinotopically unpredictable task was more difficult for the mice. There was no significant difference in performance in response to whether the stimulus was presented to the contralateral or ipsilateral side of the hemisphere processing the visual information.

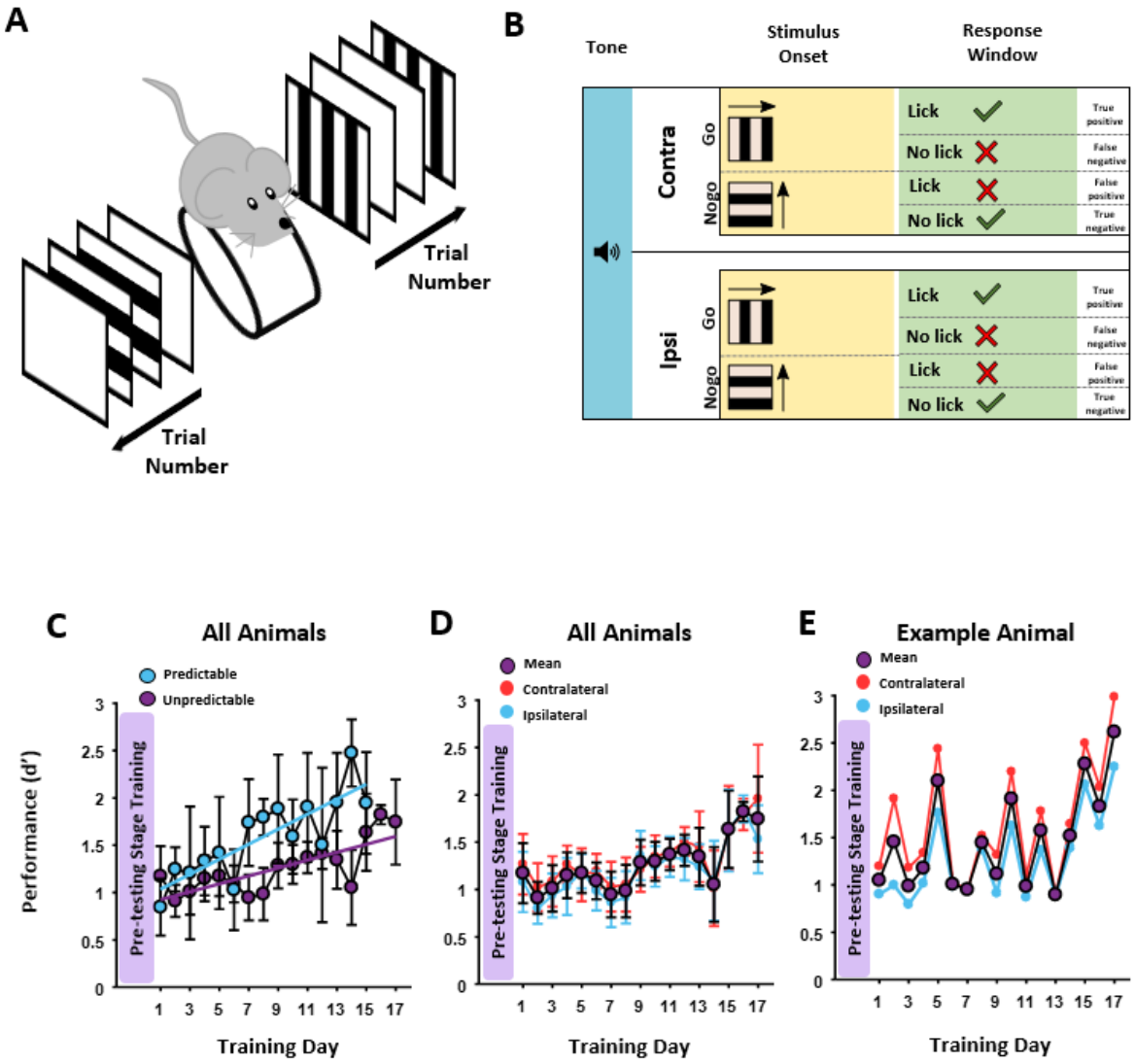

Figure 4.7: Animals can learn a more difficult, retinotopically unpredictable variant of the visual discrimination task

A: Diagram of the retinotopically unpredictable visual discrimination task **B:** Schematic of the task structure. Go or no-go stimuli could be presented to either the contralateral or ipsilateral eye of the imaged hemisphere. **C:** A comparison of performance in the predictable compared to the unpredictable version of the task. **D:** Mean performance of all mice **E:** Example of the performance of an individual mouse.

Using this retinotopically unpredictable variant of the visual discrimination task, it was possible to examine whether axons were recruited in the same phases previously seen in the retinotopically predictable version. I found that subsets of ACC axons responded during the visual stimulus onset and response window phases of the task when the stimulus was presented to either the contralateral or ipsilateral hemisphere. Throughout each trial type the response to the go stimulus was greater than that to the no-go stimulus. In particular, significantly more axons responded to the go stimulus in all phases of the task when the stimulus was presented to the contralateral eye (full trial: $p < 0.01$; visual stimulus onset: $p < 0.001$; response window: $p < 0.001$; one-way ANOVA; Figure 4.8A). Using this task, I asked whether ACC to V1 axon activity was specific to the hemisphere currently processing the task relevant sensory stimuli. A similar trend was observed in the responses of axons to stimuli presented to the ipsilateral side, but this difference was less pronounced and only significant during the response window phase ($p < 0.001$, one-way ANOVA; Figure 4.8b). To investigate whether the same axons were responsive regardless of where the stimulus was presented, the responses of axons during correct go trials were compared. A significantly higher percentage of axons responded regardless of whether the stimulus was presented to the contralateral or ipsilateral eye, especially during the response window phase of the task ($p < 0.05$, one-way ANOVA; Figure 4.8c).

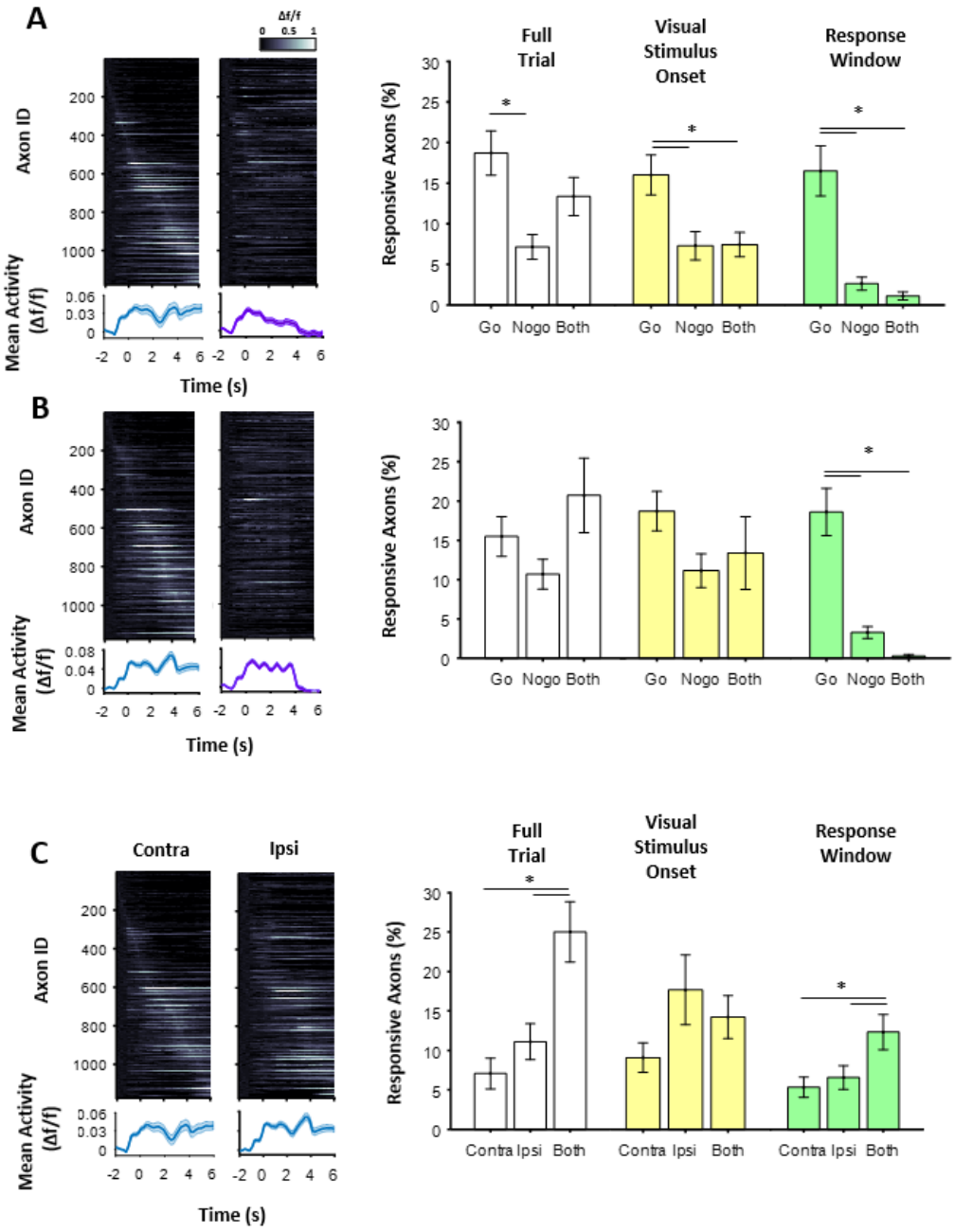

Figure 4.8: Axons respond preferentially to the go stimulus regardless of where the stimulus is, and this response is from the same population of axons

A: Heat plots showing the activity of all identified ACC axons in go and no-go trials sorted by go trials (top left) when the visual stimulus was presented to the ipsilateral eye; the percentage of axons that respond specifically to the go stimulus, the no-go stimulus or those that responded to both stimuli during the full trial, the visual stimulus onset and the response window **B:** As in A but ACC activity was in response to the visual stimulus presented to the ipsilateral eye **C:** As above but comparing go trials from contralateral and ipsilateral visual stimulus presentations.

Next, I examined whether increased ACC axonal activity was associated with improved performance during this more difficult retinotopically unpredictable task. The same analysis performed for the retinotopically predictable task was repeated independently for stimuli presented to either the contralateral or ipsilateral eye. In both instances a change was observed over the course of trials in the percentage of axons with activity that significantly differed between correct and incorrect trials (contra: $p < 0.05$; ipsi: $p < 0.005$, repeated measures ANOVA; Figure 4.9A/D). Furthermore, the percentage of discriminating axons was not significantly different between contralateral and ipsilateral trials in either the go or no-go trial types. The responses of these discriminating axons were examined as before by subtracting the neural response during incorrect trials from correct ones. This resulted in a similar pattern to that observed during the retinotopically predictable task where there was increased neural activity in go trials when completed correctly compared to no-go trials where more neural activity was apparent during incorrect trials. This was observed for both the contralateral and ipsilateral sides and was significant in both cases (contra: $p < 0.01$; ipsi: $p < 0.005$; repeated measures ANOVA; Figure 4.9B/E). Mean neural responses of these axons show increased activity during the response window for correct go trials and decreased activity for correct no-go trials (Figure 7C/F).

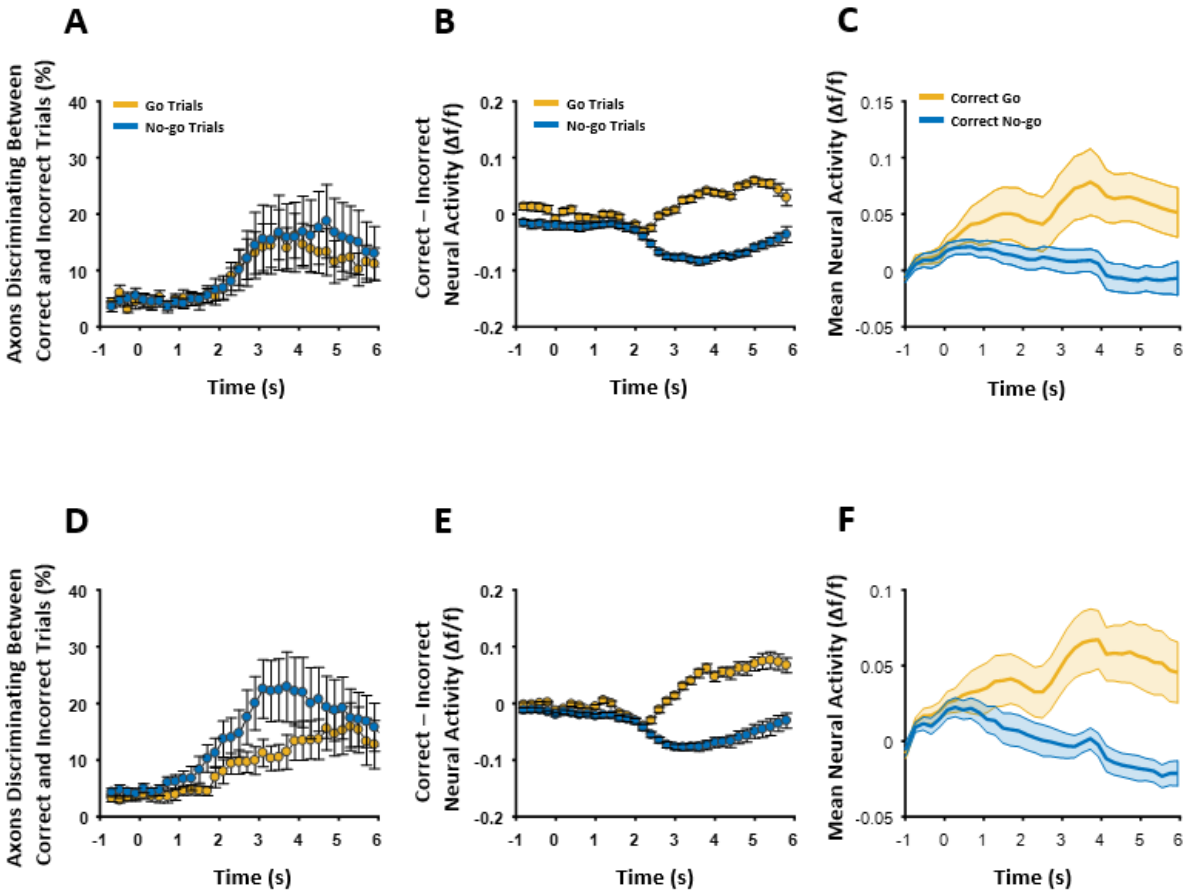

Figure 4.9: The more difficult retinotopically unpredictable version of the visual discrimination task did not recruit ACC axons for improved performance

A/D: The percentage of ACC axons that respond significantly differently to correct and incorrect trial types binned at 0.2 second intervals across the trial in contralateral trials (A) and ipsilateral trials (D) **B/E:** Subtraction of ACC axon activity during incorrect trials from that during correct trials from axons identified in A/D in contralateral trials (B) and ipsilateral trials (E) **E:** Mean neural activity of axons identified in A/D in correct go and no-go trials in contralateral trials (C) and ipsilateral trials (F). This experiment involved 9 experimental sessions and 6 mice. The mean number of ACC axons identified per session was 131.67 ± 13.71 and per animal was 197.50 ± 46.13.

As increasing the difficulty of the task by making the stimulus location unpredictable did not elicit visual responses from ACC axons which discriminated between correct and incorrect trials, the task was then altered to make the perception of the stimulus more difficult. To achieve this, the contrast of the visual stimulus was reduced. It has been shown that reducing the contrast of the visual stimulus in visually-guided tasks will in turn reduce performance if the reduction approaches the minimum detectable contrast (Histed *et al.,* 2012). Using a contrast such as this would allow the mice room for improvement in performance once the rules of the task have been learnt, something that may require this putative attentional signal carried by ACC axons.

Stimulus contrast was altered for the retinotopically unpredictable version of the task (Figure 4.10A). This study involved four mice, six experimental sessions and 676 identified axons. To establish a contrast level at which mice were prone to error but still able to detect the stimulus and perform the task above chance level, a series of visual stimuli with incrementally decreased contrasts were presented in a pseudorandom fashion. As expected, mice performed at chance level when presented with a blank. Dropping the contrast level to 10% resulted in a d' of 0.85 ± 0.26 (Figure 4.10B), indicating that animals still tended towards the correct response but were more prone to error and thus leaving room for improvement, something that the proposed ACC attentional signal may influence. Stimuli of 10% contrast were then intermingled with those of 50% to investigate whether ACC axon levels were elevated when the mice performed the task at the more difficult contrast. Mice were consistently less able to perform the task well at 10% compared to 50% contrast (Figure 4.10C), confirming increased task difficulty. As no significant difference was found in the previous analysis between contralateral and ipsilateral presentation of the stimuli, these groups were pooled and neural activity from incorrect trials was subtracted from correct trials. Again, there was a significant difference between go and no-go trials ($p < 0.005$, repeated

measures ANOVA) which indicated that endogenously elevated ACC→V1 bouton activity was not associated with enhanced task performance.

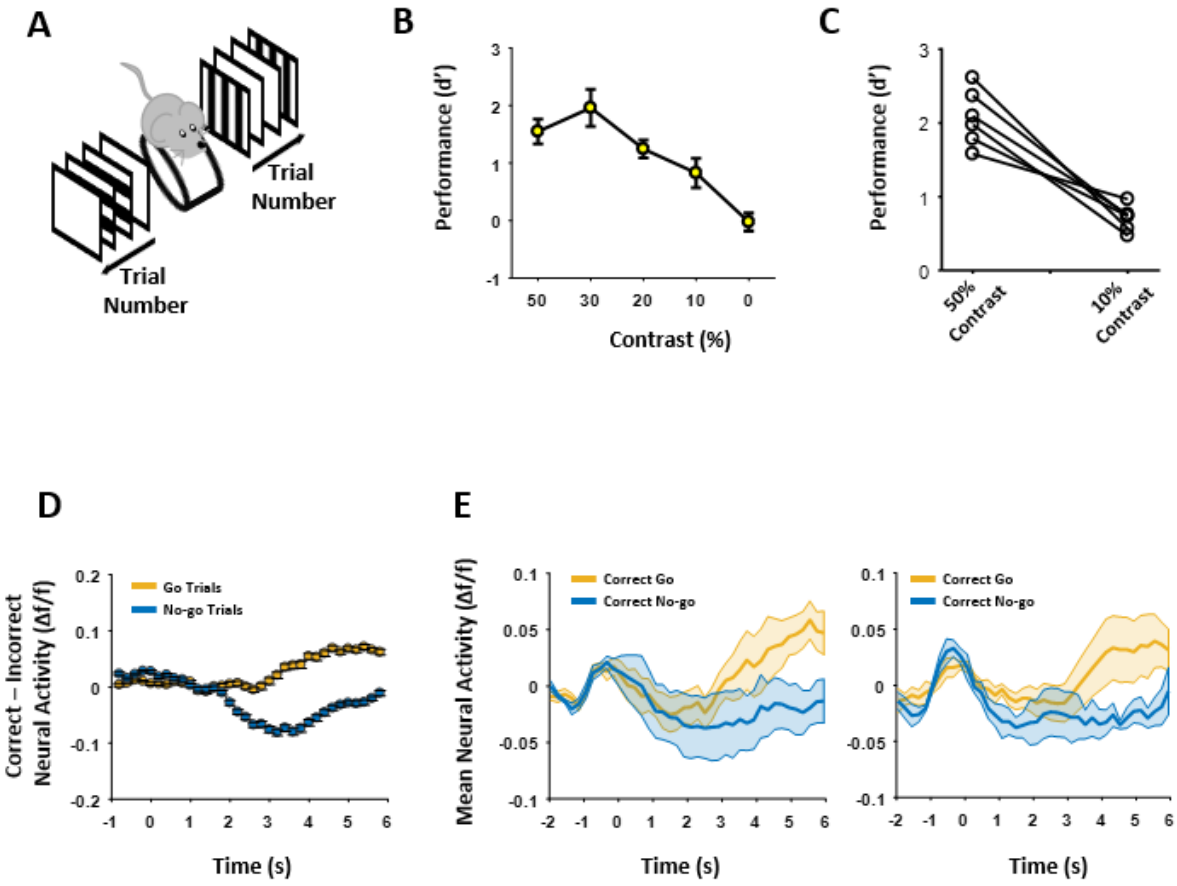

Figure 4.10: The retinotopically unpredictable task with lower contrast variant of the task does not recruit ACC axons

A: Schematic of behaviour **B:** Behavioural performance for each level of contrast tested **C:** behavioural performance for 50% (easy) and 10% (difficult) contrast levels **D:** Subtraction of ACC axon activity during incorrect trials from that during correct trials from axons that respond significantly differently during correct and incorrect trials in high contrast trials (left) and low contrast trials (right) **E:** Mean neural activity of the same population of axons in D. This experiment involved 9 experimental sessions and 6 mice. The mean number of ACC axons identified per session was 131.67 ± 13.71 and per animal was 197.50 ± 46.13.

4.3.5 Detection task and multi-colour labelling

The ACC projection to V1 is thought to drive a phenomenon comparable to surround suppression (Zhang *et al.*, 2014) as well as being retinotopic (Leinweber *et al.*, 2017). This would suggest it has spatially specific properties, something that is well documented in mouse V1 neurons (Niell and Stryker, 2008). If this were the case then it would be plausible that, during the visual discrimination task, effects of ACC on performance could have been overlooked by showing a large stimulus and recording from multiple areas in V1 that were not specifically mapped to respond to the area of visual space in which the stimulus was shown. To investigate this, the size of the stimulus was reduced and a detection task was implemented. To ensure that the retinotopically relevant area of V1 was being imaged, a multi-colour labelling strategy was used where ACC axons were transfected with the green indicator GCaMP6s and layer 2/3 V1 neurons with the red indicator jrGECO1a. Through this it was possible to identify the receptive field for the layer 2/3 somas in the cortical area being recorded using the previously described retinotopic protocol (Figure 4.11A), present the stimulus within this area of visual space and then use multi-plane two-photon imaging to also record from ACC axons directly dorsal to them in layer I of V1 (see general methods).

The detection task, like the previous discrimination task, was based on a go/no-go structure. Stage one and two followed the same method. The visual stimulus presented in this case was a 90˚ stationary grating of 30˚x30˚ and appeared for 1.5s within the receptive field of the layer 2/3 V1 cortical neurons being imaged (Figure 4.11B). No-go trials were introduced during the testing stage and consisted of a blank. There was no air puff, white noise or time-out if the no-go trial was completed incorrectly (Figure 4.11C). Mice were able to maintain high levels of performance across days (Figure 4.11D).

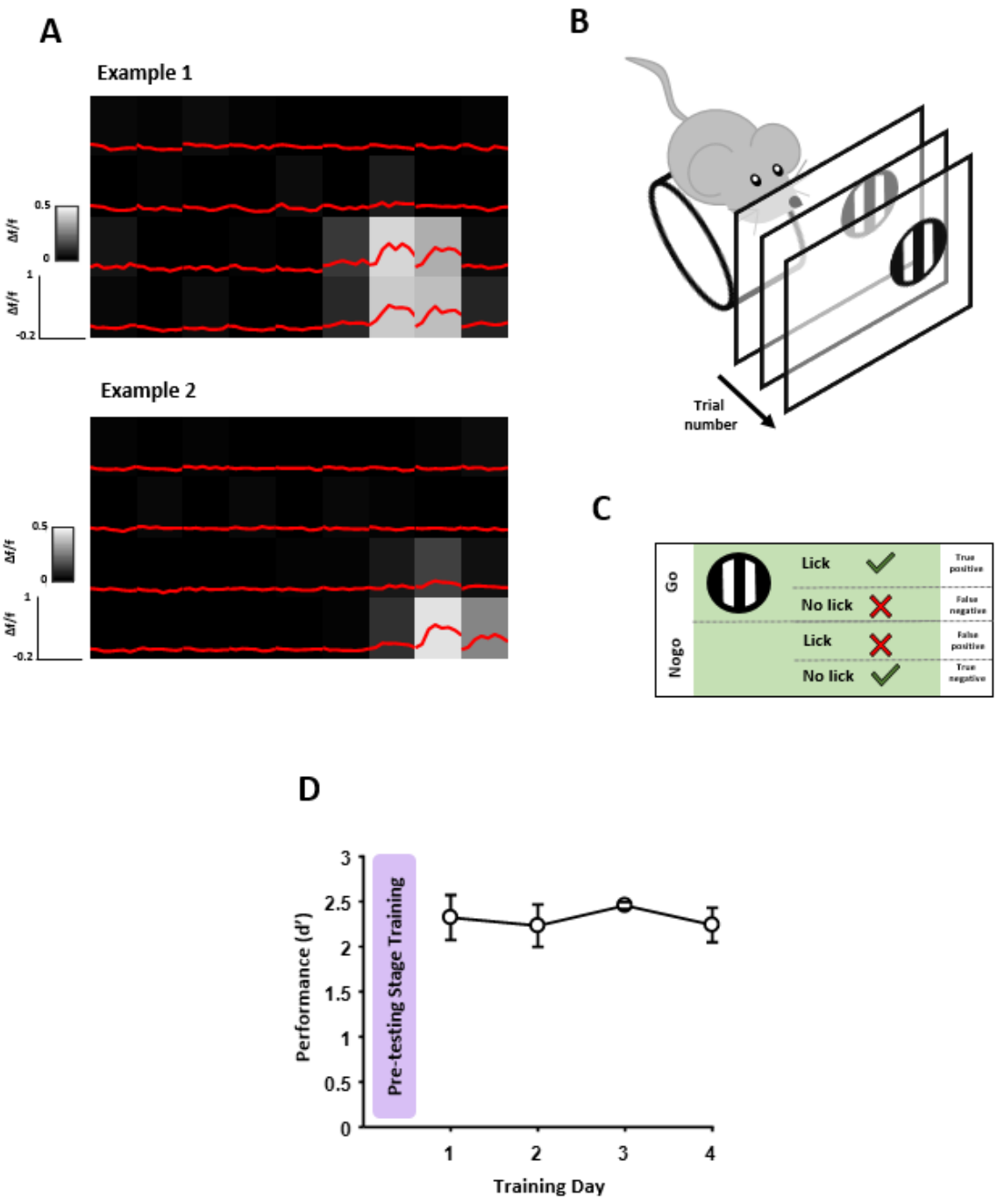

Figure 4.11: Mice are able to learn a visual detection task

A: Responses of layer II V1 somas used to place the visual stimulus within their receptive field Diagram of the detection task **B:** Diagram of the detection task **C:** Schematic of the detection task **D:** Mean performance during the detection task.

Initially I investigated whether either soma or axon activity was elevated when mice were performing the task correctly when the stimulus was presented inside the receptive field of the layer 2/3 V1 somas in the imaging area (Figure 4.12A). This study involved four mice, four experimental sessions, 1370 identified axons and 333 identified somas. Mean neural activity for all detected somas and axons was calculated for each trial type except incorrect go as errors were very rare in go trials. Peak neural activity of both somas and axons was most elevated for go correct trials, and least for correct no-go trials. The peak for incorrect no-go trials was higher for ACC axons than for correct no-go trials (Figure 4.12B). Reaction times of the mice were approximately 0.38 ± 0.026s. To establish whether neural activity was elevated in correct trials of a subset of axons, those showing significantly elevated responses were identified. To do this, the responses of axons to the stimulus and blank were examined by calculating the percentage of neurons that significantly responded if the trial was completed correctly. This was achieved by dividing the trials into 0.2s bins and comparing the activity within each bin to a baseline level 0.5s prior to the start of the trial. The variable quiescent period preceding each trial ensured the mice could not predict the timing of the onset of the visual stimulus. Activity was aligned to the onset of the stimulus, which occurred at 0s, and it was found that there was a significant increase in activity over time in the go trials of both the somas ($p < 0.001$, repeated measures ANOVA; Figure 4.12D) and axons ($p < 0.001$, repeated measures ANOVA; Figure 4.12E). This was not observed in the blank no-go trials. Post-hoc analysis was used to compare each binned go and no-go timepoint. The response of the somas to the stimulus was significantly different than their response to the blank from 0.1s onwards (Figure 4.12F). The response of the axons during the trial was significantly different to the blank from 0.3s onwards. The response of the somas and axons to the stimulus were then compared. Post hoc analysis indicated the responses were significantly different at 0.1s ($p < 0.01$; Figure 4.12F) and 0.3s ($p < 0.005$; Figure 4.12F).

The activity of the somas appeared to increase directly in response to the appearance of the visual stimulus, but the responses of the axons were delayed by approximately 0.3s, aligning more with the reaction time of the mice. This suggested that the response of ACC axons occurred at the time of or even just before the lick response rather than the appearance of the visual stimulus itself, as well as only occurring in correct trials with the motor response of licking. To examine this in more detail, the activity of the somas and axons was aligned to the rewarded lick. Significantly different responses between somas and axons were found at -0.1s, 0.1s and 0.3s ($p < 0.05$, $p < 0.05$, $p < 0.05$ respectively). It was interesting to note that ACC axons responded later in the trial compared to V1 somas, but that this response began slightly before the animal licked the spout to obtain a reward (Figure 4.12G).

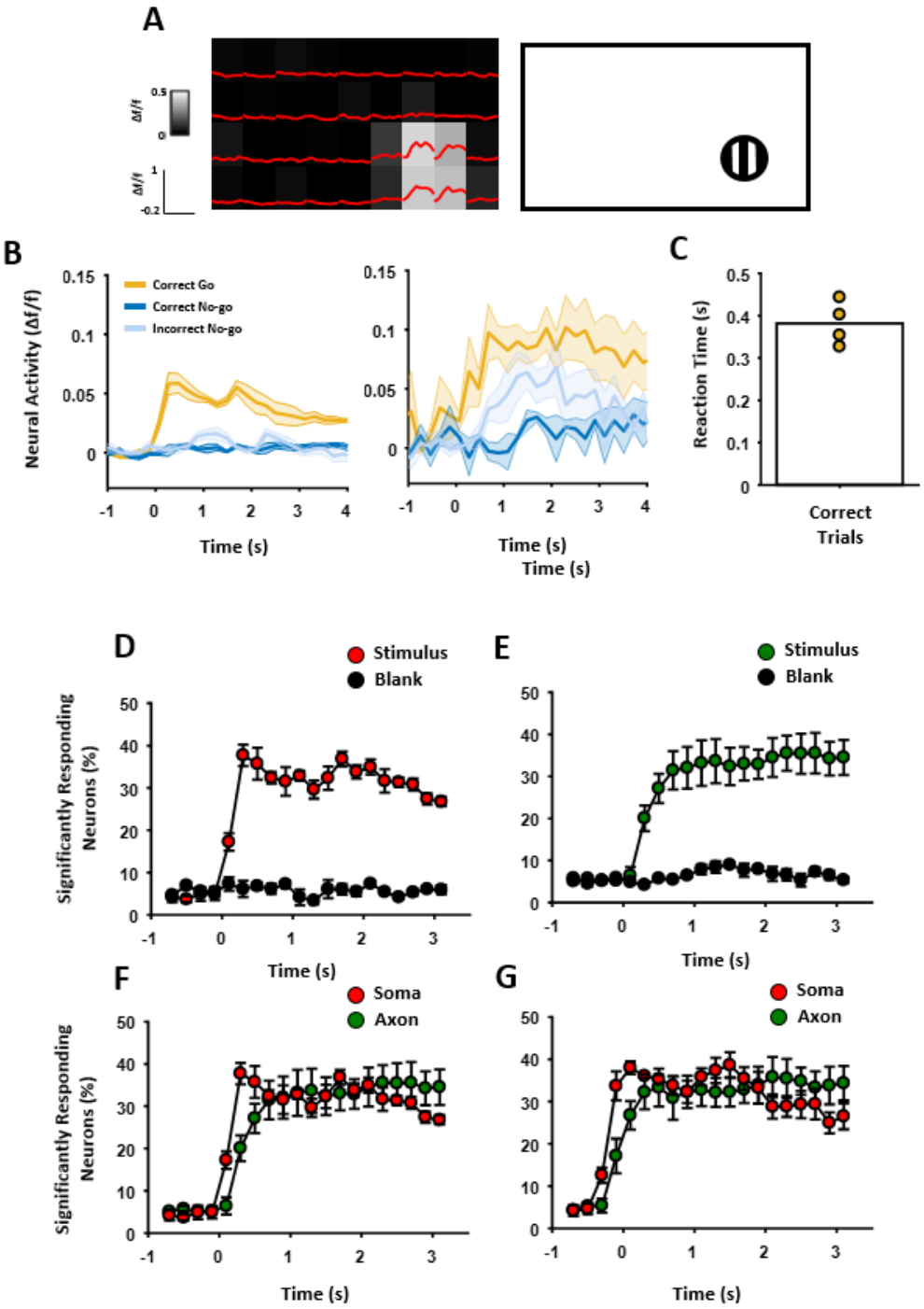

Figure 4.12: V1 soma and ACC axon response when stimulus is presented inside the receptive field

A: Example response profile of a V1 soma to 36 different locations and diagram of the visual stimulus being placed within this receptive field. **B:** Mean activity trace including all identified V1 somas (left) and ACC axons (right) divided by trial type. **C:** Mean reaction times. **D/E:** The percentage of V1 Somas (D) and ACC axons (E) showing significantly increased activity in comparison to a baseline during 0.2 s length bins throughout the trial, aligned to stimulus onset at 0s **F/G:** The activity of layer II V1 somas compared to ACC axons where trials were extracted aligned to the onset of the visual stimulus (F) or the rewarded lick (G). The number of experimental sessions, mice and detected axons and somas are summarised in Table 6.

Exp Type	Exp No	Mouse No	Mean ROI
Inside RF	4	4	342.50 ± 43.25
Inside RF	4	4	83.25 ±9.26
Outside RF	4	4	393.75 ± 50.70
Outside RF	4	4	134.75 ± 50.04

Table 4: The number of experimental sessions and mice used in the detection task

'Exp Type' refers to the experiment type of whether the visual stimulus was shown inside or outside of the receptive field of the V1 region being recorded from. 'Exp No' refers to the number of experimental sessions for each of the experiment types. 'Mouse No' refers to the number of mice used in each of the experimental types and Mean ROI is the mean number of ACC axons (highlighted green) and V1 somas (highlighted red) across sessions. In this case it is the same for both sessions and mice as each mouse only had one imaged region.

This analysis was repeated for somas located in a different retinotopic location of V1 that did not respond to the area of visual space in which the stimulus was presented (Figure 4.13A). This study involved four mice, four experimental sessions, 1575 identified axons and 539 identified somas. The mean activity of all identified ACC axons again showed that the highest peak in activity was during correct go trials, and the lowest in correct no-go trials. There was also elevated activity in ACC axons during incorrect no-go trials. Unexpectedly, V1 somas also exhibited elevated neural activity in correct go trials even though the visual stimulus was not presented inside their receptive field (Figure 4.13B). Reaction time was 0.43 ± 0.085s (Figure 4.13C). Next, V1 somas and ACC axons that significantly responded during correct go or no-go trials were identified as before. Again, there was a significant increase in activity over the course of the trial for both the somas ($p < 0.05$, repeated measures ANOVA; Figure 4.13D) and the ACC axons ($p < 0.005$, repeated measures ANOVA; Figure 4.13E). Again, this was not observed for the blank. This indicated the lack of general elevated activity during correct trials was apparent regardless of whether the stimulus was presented within or outside the receptive field that matched the imaged retinotopic location. Post hoc analysis showed significantly increased activity in ACC axons from 0.3s onwards in trials aligned to the visual stimulus onset (Figure 4.13E), something that was comparable to that observed when the stimulus was presented within the receptive field. The soma response was, however, not comparable, showing significantly elevated activity at 0.3s instead of 0.1s. The percentage of ACC axons or V1 somas significantly responding throughout the trial was not significantly different at any time point, regardless of whether trials were aligned to the visual stimulus onset (Figure 4.13F) or the rewarded lick (Figure 4.13G).

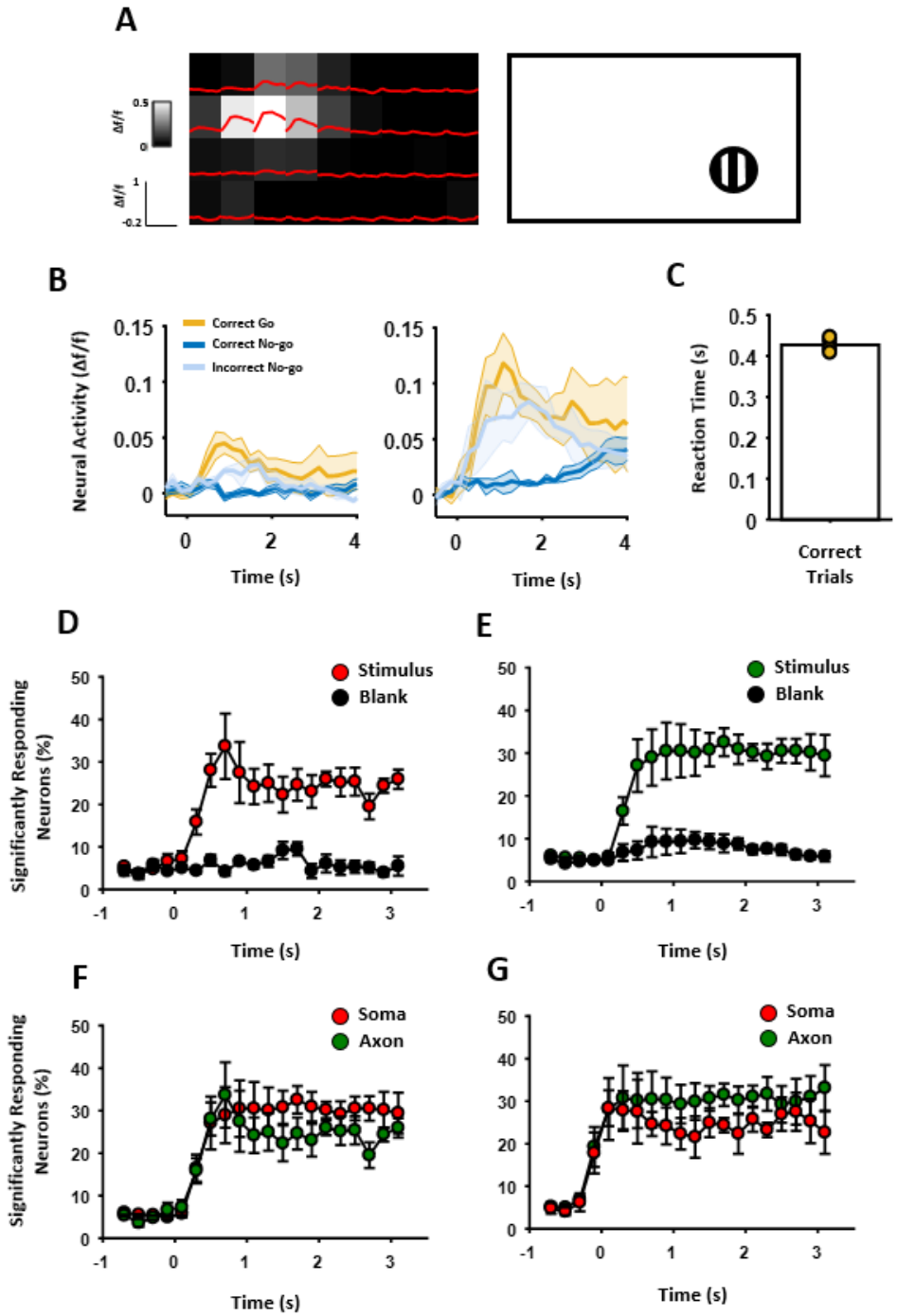

Figure 4.13: V1 soma and ACC axon response when stimulus is presented outside the receptive field

A: Example response profile of a V1 soma to 36 different locations and diagram of the visual stimulus being placed outside this receptive field. **B:** Mean activity trace including all identified V1 somas (left) and ACC axons (right) divided by trial type. **C:** Mean reaction times. **D/E:** The percentage of V1 Somas (D) and ACC axons (E) showing significantly increased activity in comparison to a baseline during 0.2 s length bins throughout the trial, aligned to stimulus onset at 0s **F/G:** The activity of layer II V1 somas compared to ACC axons where trials were extracted aligned to the onset of the visual stimulus (F) or the rewarded lick (G). The number of experimental sessions, mice and detected axons and somas are summarised in Table 6.

4.3.6 Association of ACC activity and lick activity

Each of the previous studies in this chapter have indicated an association between ACC axon activity in layer 1 V1 and the lick response. Firstly, a significantly higher percentage of ACC axons exhibited significantly elevated activity in correct go trials where licking the spout was required, compared to correct no-go trials where it was not. Furthermore, in all variants of the go/no-go visual discrimination task tested, axons that had significantly differing activity levels in correct and incorrect trials also exhibited elevated activity during incorrect no-go trials as well as correct go trials. The common element between these was the animal licking the spout. Additionally, during the detection task, ACC activity was not significantly elevated at the time of stimulus onset, but became so at 0.3s, a delay in time similar to that of reaction time. Motor activity is known to increase neural activity in many regions of the brain (Niell and Stryker, 2010; Keller *et al.,* 2012; Bennett *et al.,* 2013; Saleem *et al.*, 2013; Erisken *et al.*, 2014). Previous studies have shown an integration of motor information into sensory cortices by looking at the activity of V1 neurons (Pakan *et al.*, 2016). I therefore asked whether the observed ACC activity was primarily as a result of licking behaviour.

To explore this, the activity of ACC axons was examined during stage one of the behavioural task where no visual stimuli had been presented. ACC activity was compared to lick frequency using correlational analysis and a permutation test. To achieve this a correlation coefficient was calculated between the ACC activity trace and lick frequency data for the entire session matched over time. The neural activity trace was then shifted 99 times circularly in time to calculate coefficients of unmatched time epochs. If the correlation coefficient of the time-matched traces was in the top fifth percentile of all values then the axon was deemed to be significantly correlated with lick frequency. It was found that 30.54 ± 0.81% of ACC axons were significantly correlated.

Next, this was tested for each the retinotopically predictable, retinotopically unpredictable and detection tasks It was found that the activity of 31.88 ± 1.91%, 34.43 ± 4.34% and 27.67 ± 2.85% of axons were significantly associated with lick frequency (Figure 4.15A/B/C) in each of the three tasks respectively.

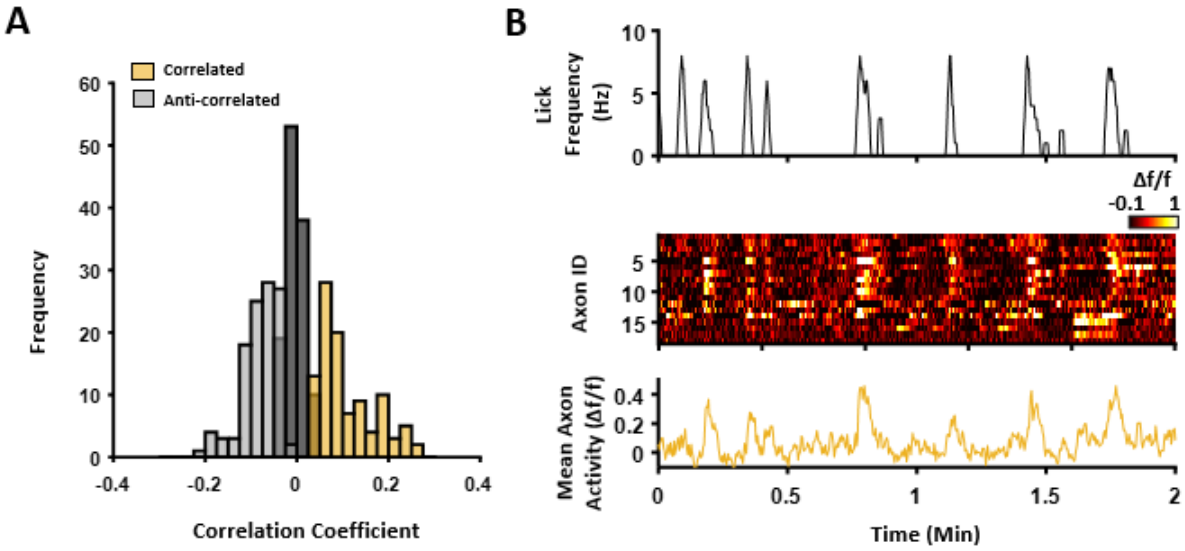

Figure 4.14: ACC activity is linked to lick response before any learning has occurred

A: Correlation coefficients for ACC axon activity and lick frequency. Axons found to be significantly positively correlated with lick frequency are shown in yellow. **B:** Example lick frequency trace (right top); this was aligned to neural activity of each axon significantly correlated with lick frequency (right middle) and average axon activity (right bottom). This experiment consisted of five mice and five experimental sessions. There were a mean of 67.20 ± 6.44 axons per experimental session.

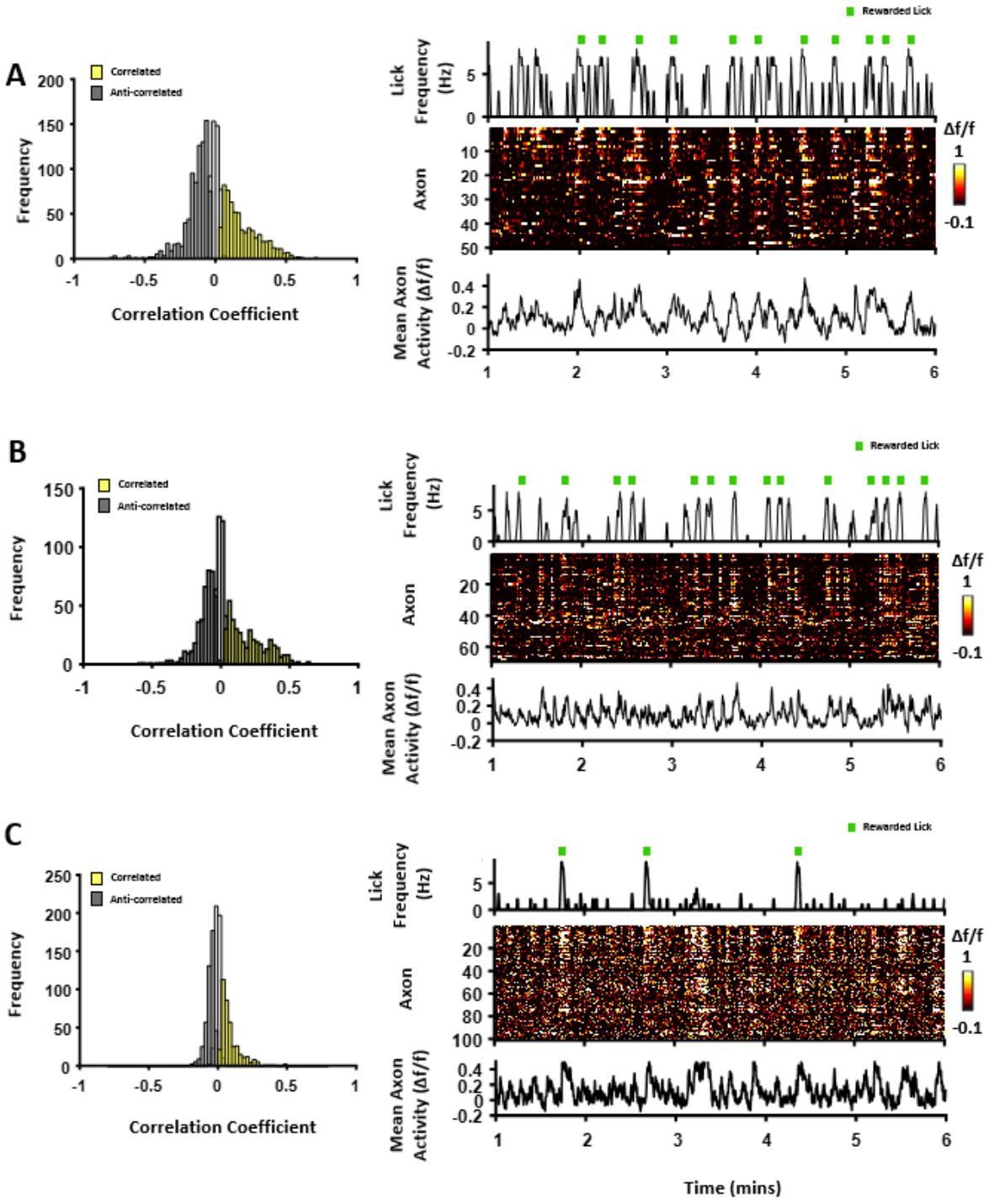

Figure 4.15: Correlation of ACC axon neural activity and lick frequency

A: For the retinotopically predictable discrimination task, lick frequency was compared with ACC axon activity. Axons that were found to be significantly positively correlated with lick frequency using a permutation test are shown in yellow (left). Example lick frequency trace (right top) where green lines indicated rewarded lick timing; this was aligned to neural activity of each axon significantly correlated with lick frequency (right middle) and average axon activity (right bottom) **B:** As in A but for the retinotopically unpredictable discrimination task **C:** As in B but for the visual detection task.

ACC axon activity exhibited during the detection task began slightly before the onset of the licking behaviour suggesting a preparatory response. To investigate this, a cross correlation was run for axons in both the discrimination and detection tasks to identify any lag time of lick activity compared to neural activity. The neural traces were then shifted in time by their lag time and run through the permutation test described previously. Axons where lick activity was significantly associated with neural activity were then taken forward and their lag times examined. It was found that in each of the behavioural tasks the peak lag was -0.49 ± 0.069s, -0.32 ± 0.089s and -0.36 ± 0.059s for the retinotopically predictable discrimination task, the retinotopically unpredictable discrimination task and the detection task respectively (Figure 4.16A/B/C). This indicated that neural activity was occurring in each case before licking activity in axons that were significantly associated with lick. Furthermore, somas where the stimulus was shown within the receptive field in the detection task were examined in the same way and exhibited a peak lag of 0.18 ± 0.095s suggesting that the axons might be exhibiting a preparatory response.

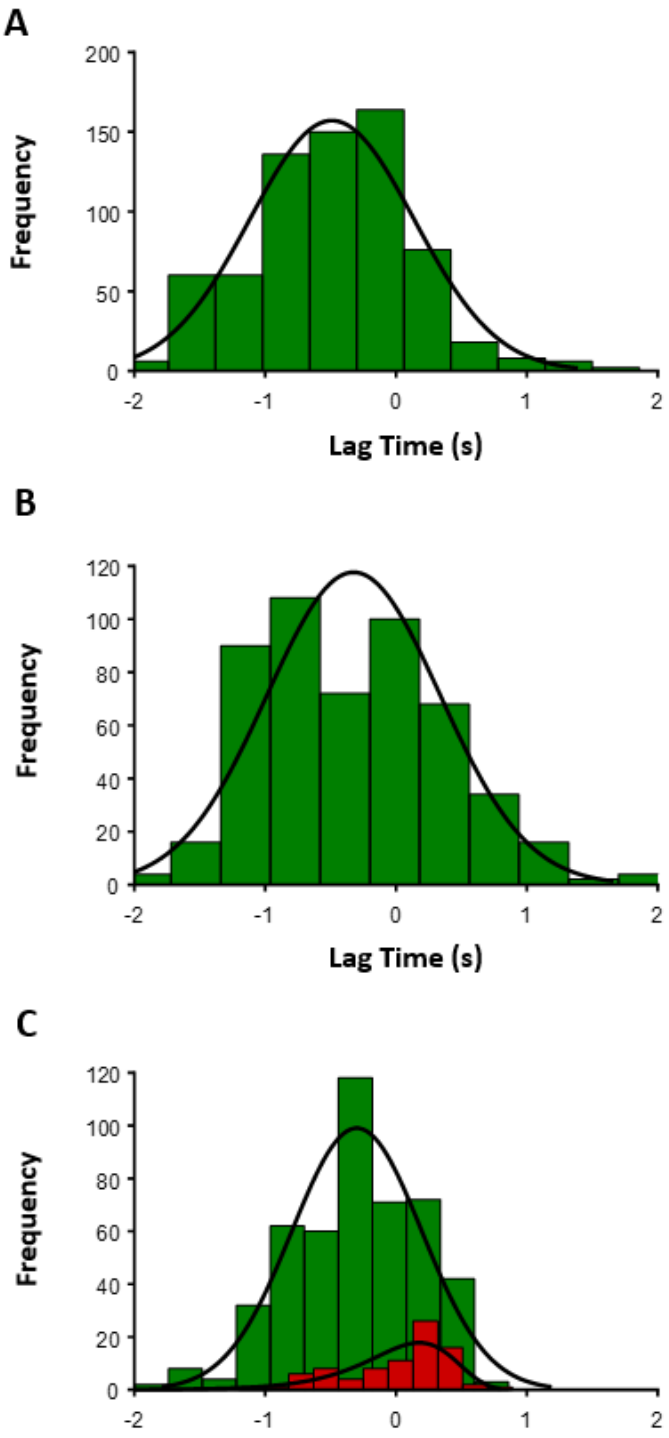

Figure 4.16: Cross Correlation of ACC axon neural activity and lick activity

Frequency of lag times after running a cross correlation analysis between lick frequency and ACC axon activity. **A:** Axons in the retinotopically predictable discrimination task **B:** Axons in the retinotopically unpredictable visual discrimination task **C:** Axons in the visual detection task. Green bars represent ACC axons and red bars represent V1 somas.

After establishing an association between ACC activity and the lick response, it was asked whether ACC axons are associated with locomotion, a motor-related behaviour that was irrelevant to the successful completion of the task. To do this, mice were allowed to run or remain stationary at their own discretion and the resulting ACC axonal activity was compared to run speed using the correlational and permutational analysis described previously. It was found that the activity of 22.48 ± 6.05% axons were significantly associated with locomotion.

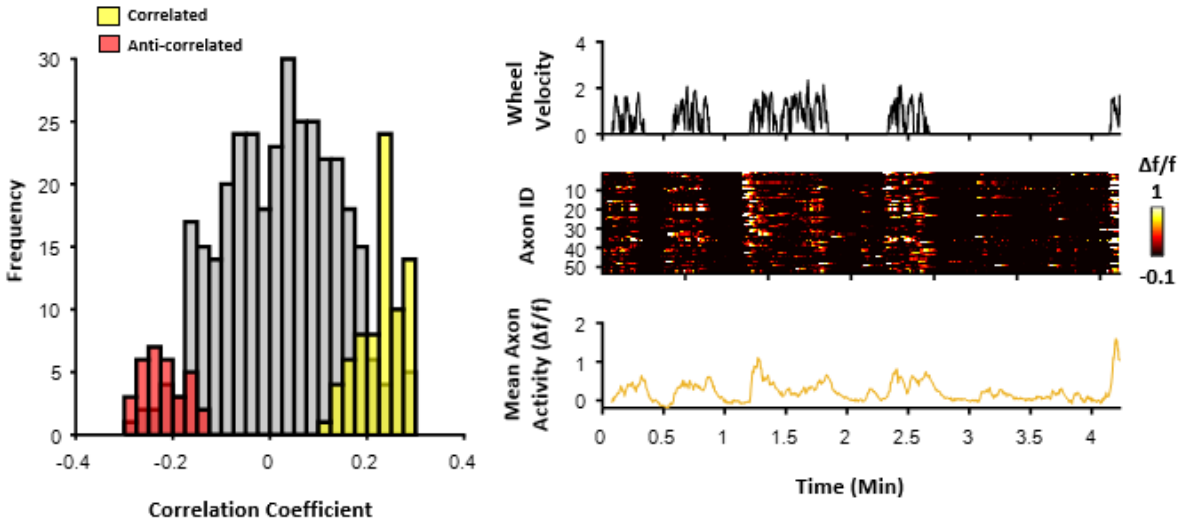

Figure 4.17: ACC activity is linked to locomotion

A: Correlation coefficients for ACC axon activity and locomotion. Axons found to be significantly positively correlated with locomotion are shown in yellow. **B:** Example locomotion trace (right top); this was aligned to neural activity of each axon significantly correlated with locomotion (right middle) and average axon activity (right bottom). This experiment consisted of

4.3.7 ACC activity is associated with reward processing

Elevated activity in ACC has been demonstrated to be aligned with motor responses in human studies involving selective visual attention, especially under conditions of increased response competition (Carter *et al.*, 1998). This chapter has indicated that the activity of a subset of ACC axons that terminate in layer 1 V1 in mice are also associated with the motor response to the task – that of licking. ACC has, however, also been associated with reward processing (Dehkordi *et al.*, 2015; Liu *et al.*, 2016), something that would accompany licks in go trials during each behavioural task presented. It was asked whether this ACC activity associated with licking the spout was independent of gaining a reward. To do this, each rewarded and each quiescent lick was identified, and the equivalent ACC neural activity compared for each axon individually for each behavioural task. It was found that, in all tasks, there were subsets of axons that had significantly higher responses to rewarded licks compared to unrewarded licks (Figure 4.18B/C/D). These subsets were then compared to each other. It was found that a significantly higher percentage of ACC axons responded to the rewarded lick ($p < 0.001$, $p < 0.01$, $p < 0.05$ for the retinotopically predictable discrimination, the retinotopically unpredictable discrimination and the detection task respectively). This suggested an involvement in reward processing.

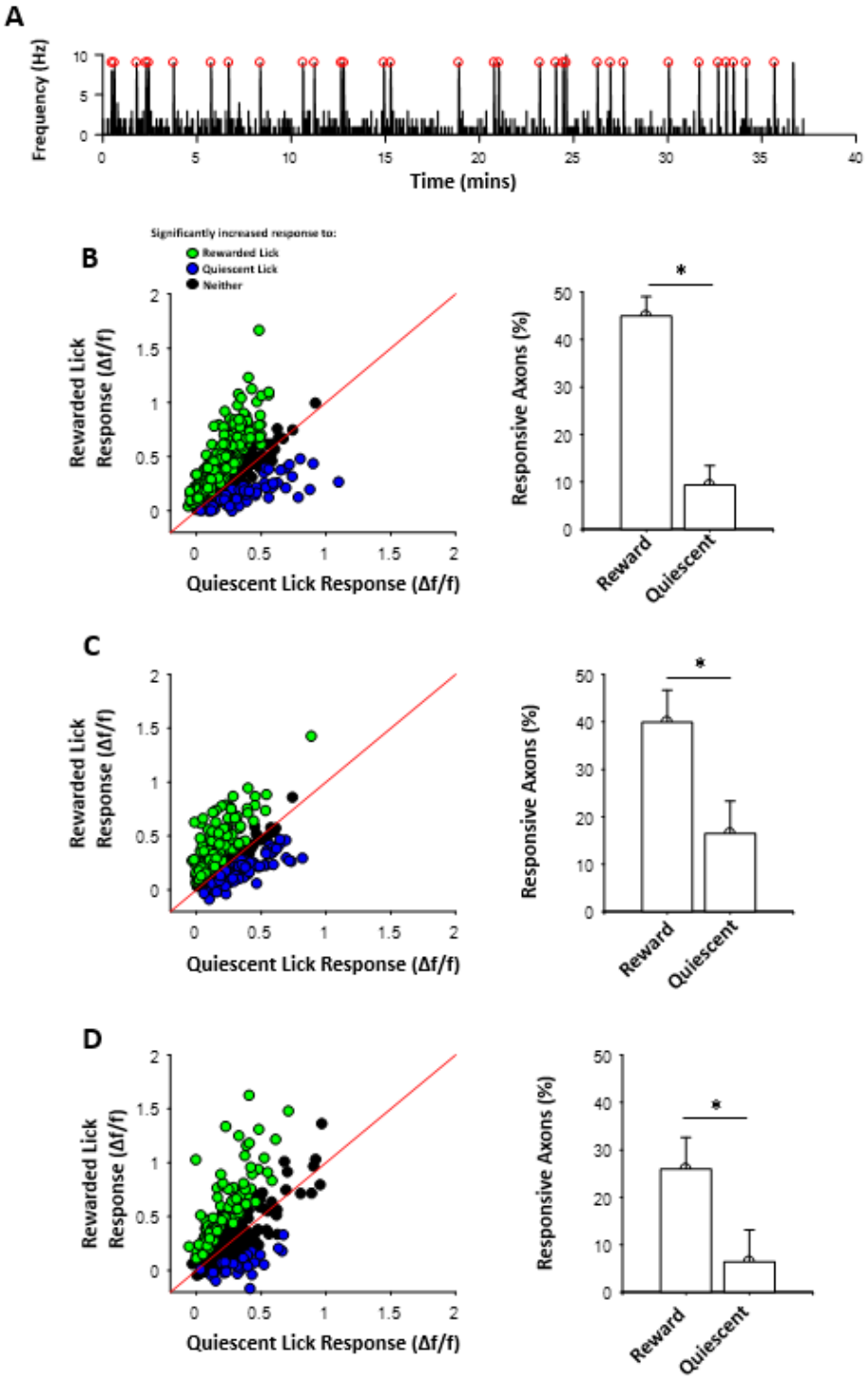

Figure 4.18: ACC axon neural activity is associated with reward

A: Example lick trace where rewarded licks are indicated by a red circle **B:** Comparison of ACC axon response to rewarded lick compared to quiescent lick in the retinotopically predictable task. Each dot represents one axon. Axons responding significantly more to rewarded licks compared to quiescent licks and vice versa are shown in green and blue respectively (left) and this is quantified (right) **C:** As in B but for the retinotopically unpredictable visual discrimination task **D:** As in B but for the visual detection task. The mean number of axons per experimental session is outlined in Table 4.1

Exp Type	Mouse number	Exp Number	Axons per Mouse	Axons per Exp
Retinotopically Predictable	6	16	89.50 ± 7.50	35.8 ± 9.59
Retinotopically Unpredictable	6	9	68.67 ± 18.32	41.2 ± 12.96
Detection	4	4	97.25 ± 19.51	97.25 ± 19.51

Table 4.1: The mean number of axons per mouse and per experiment identified as significantly responding to lick

4.4 Summary of Findings

1. Significantly more axons were active during correct go trials compared to incorrect go trials.
2. For axons that had significantly different levels of activity in correct trials compared to incorrect trials, this activity was higher in correct compared to incorrect go trials, but lower in correct compared to incorrect no-go trials, and this difference was significant.
3. Making the appearance of the visual stimulus unpredictable and thus increasing the difficulty of the task did not result in generally elevated ACC activity during correct trials.
4. Reducing the contrast to make the perception of the visual stimulus more difficult did not result in generally elevated ACC activity during correct trials.
5. Reducing stimulus size and precisely retinotopically matching the stimulus location to the imaged area of V1 did not result in elevated ACC activity either.
6. ACC axonal activity appears be associated with the lick response.
7. Activity of a subset of ACC axons is associated with reward.

5 General Discussion

5.1 Summary of Studies

The aim of these studies was to investigate the properties of the top-down projection from ACC to V1. To do this, two main questions were asked. The first was whether ACC axons in V1 showed any functional organisation where spatial preferences of axons matched those of V1 somas in the same area of V1. I found that RFCs of ACC axons carried signals about stimuli appearing across a larger area of visual space than V1 somas in the same location responded to, and that ACC axon RFCs were offset horizontally compared to V1 somas. This was different to the retinotopic organisation properties of the LM projection to V1, one that has been previously shown to exhibit functional organisation in V1.

The second question was whether an elevation of activity in ACC axons resulted in improved performance in a visually-guided discrimination task. I found that an improvement in performance in this task was not associated with an endogenous general increase in ACC activity. In fact, ACC axon activity appeared to be closely aligned with the behavioural response of licking, and possibly modulated further by obtaining a reward during this time.

5.2 Functional Organisation of anterior cingulate cortex and lateral medial cortex axons terminating in primary visual cortex

5.2.1 ACC axons lack retinotopic organisation but over-represent the horizontal plane relative to V1 somas in the same retinotopic location in V1

It was found that a subset of ACC axons responded to specific areas in visual space, but that the proportion was significantly less than V1 somas. The RFCs of these ACC axons appeared to be spread widely across the visual area in which

stimuli were presented indicating that this top-down projection from ACC conveyed information about a wider range of visual space than the V1 somas located in the same area of V1.

The RFC offset values of ACC axon RFCs compared to the RFC mean of somas in the same retinotopic location in V1 over-represented the horizontal place. This suggested that ACC axons converging on V1 prefer visual space to the left and right of visual space the V1 somas that they are likely making synapses with prefer. This functional organisation of ACC axons was not as expected. It has been shown that this projection is spatially specific (Zhang *et al.*, 2014; Fiser *et al.*, 2016), and that it is involved in selective visual attention (Zhang *et al.*, 2014). In order to be able to modulate V1 responses in a spatial specific way to elicit activity observed in attentional states, it seems logical that the retinotopic arrangement of ACC axons would match closely to those of V1 pyramidal neurons. The current study does not show this, instead ACC axons appear to transmit signals driven by stimuli appearing across the extent of visual space that was tested. One explanation is that this is because the mouse is passively viewing stimuli. It is possible that this expected functional organisation of ACC axons is not seen in this experiment because it does not require the mice to direct visual attention to a specific area of visual space, and that this organisation may either be observable or develop during tasks requiring spatial visual attention.

5.2.2 LM axons show retinotopic organisation and over-represent the area of visual space binocular to V1 somas in the same retinotopic location in

RFCs of LM axons were similarly scattered in azimuth compared to V1 somas, but significantly more so in elevation. This indicated that LM axons matched RFC

scatter properties of the V1 somas in the same area of V1 in azimuth, but conveyed information about a wider visual area in elevation. RFC offset values of LM axons compared to those of V1 somas in the same retinotopic location in V1 over-represented the region of visual space in the binocular direction. There was also a slight bias to higher regions in elevation. This differed from Marques *et al.,* (2018) who showed that, on average, V1 somas and LM axons responded to the same area of visual space. My findings may be as a result of imaging V1 somas directly to calculate their retinotopic preferences rather than estimating them, resulting in consistently being able to measure the difference in RFC at a higher resolution. This binocular bias was observed regardless of whether imaging took place in monocular or binocular V1. Mice that were reared in the dark and thus had no visual experience until after two months of age did not show this over-representation. This offset, coupled with the development of motion perception requiring visual experience to develop (Mitchell, Kennie and Kung, 2009; Bos, Gainer and Feller, 2016) suggests that LM conveys information about objects moving through visual space from the binocular to the monocular receptive field, and that the organisation needed for this to happen requires visual experience to develop.

The LM projection to V1 may be important in predicting the movement of objects. One form of motion processing that this would facilitate would be the movement of stimuli that occurs in the environment as a result of the movement of the mouse itself. Marques *et al.,* (2018) argue that the LM projection to V1 could be involved in motion perception and that it may be specialised for processing movement of stimuli during locomotion. It is possible that LM projections to V1 encode spatial predictions back to V1 (Marques *et al.*, 2018), and the offset in the binocular direction observed in the current study would support this for processing objects

moving in the nasal to temporal direction, something that occurs to stationary objects during locomotion. Figure 5.1 indicates a circuitry that could be behind this. A stimulus in a particular location in visual space would elicit a response in the retinotopically matched area of V1, which is reciprocally connected to LM (Wang and Burkhalter, 2007) and transmits visual information to LM (Glickfeld *et al.*, 2013) which is reflected in the response profiles of the pyramidal neurons located in LM (Andermann *et al.,* 2010). This would result in the activity of LM neurons being directly driven by this visual stimulus. If the stimulus were to then move through visual space in the monocular direction, something that would be predictable due to self-motion, then LM axons can send prediction signals of where the stimulus is likely to be. This would result in LM axons at the imaging area being driven by stimuli that appear earlier in the path of motion of the object, i.e. towards the binocular field of view.

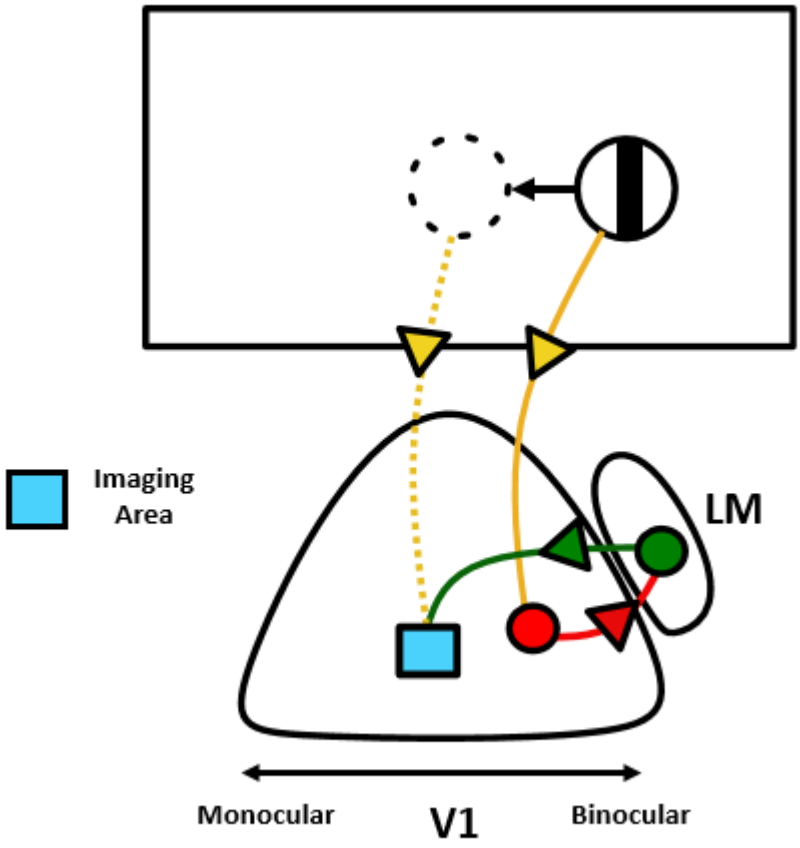

Figure 5.1: A schematic of the theoretical network involved in the prediction of object movement by LM

A stimulus grating is shown with its path of motion indicated by an arrow and dotted outline. Yellow lines indicated the path of the light which would stimulate the bottom-up pathway described in the general introduction and stimulate retinotopically relevant V1 somas (red). This signal would then be transmitted on to neurons in LM (green) before being transmitted back to somas in V1 in a retinotopically relevant position to where the stimulus is likely to move to. Imaging in this area would be one explanation for the LM RFC offset observed.

Another explanation would be processing of the movement of objects, such as that of incoming aerial predators. Mouse behaviour can be driven by the threat of predation and consists of two main responses – freezing or fleeing (De Franceschi *et al.*, 2016). Studies have shown that when mice are presented with a looming stimulus above them that increases in size thus simulating an incoming aerial predator, mice respond quickly by fleeing (Yilmaz and Meister, 2013; De Franceschi *et al.*, 2016). The offset of LM RFCs from those of V1 somas in the binocular direction coupled with a significantly increased scatter in elevation could allow mice to track the movement of a visual stimulus approaching from in front and above them, predict its movement and subsequently make a fast response to evade predation.

Further experimental work will be needed to determine if the LM projection to V1 is involved in either processing stationary stimuli that appear to move as the mouse runs, or with detecting approaching moving objects, such as predators. The former explanation would involve a form of encoding spatial predictions and can be manipulated to produce errors in visual processing which may be reflected in the activity of the projection from LM to V1. One experimental design would be to allow a mouse to navigate a virtual corridor where the movement of the visual environment is matched to the movement of the mouse while imaging from LM axons and V1 somas simultaneously, something that has been shown to work effectively (Poort *et al.*, 2015; Fiser *et al.*, 2016). If LM axons in V1 were delivering predictive information about stimuli during motion of the mouse, then it can be hypothesised that these axons would be active prior to V1 neurons in the same area of visual space. Use of virtual reality would then allow the visual environment to be reversed so that visual stimuli move in the opposite direction to what is expected during movement. If LM axons predict movement in the binocular to monocular direction then it could be hypothesised that

this delay would not be seen. To explore the predatory theory further, the fleeing behaviour of the mouse when faced with an incoming stimulus could be taken advantage of. The first step would be to image in the same region as before and again look for a response of LM axons prior to that of V1 neurons, as well as examine whether animals run in response to the stimulus. LM axons could then be inhibited, possibly using optogenetics, as was done with ACC axons (Zhang et al., 2014), to see whether the animal was less likely to flee, or the reaction time before fleeing was increased.

5.3 The involvement of anterior cingulate cortex axons terminating in primary visual cortex in visually guided tasks

This study was undertaken to ask whether endogenous elevation of the ACC projection to V1 was associated with an increase in performance in a visual discrimination task. Previous experimental work carried out by Zhang *et al.* (2014) suggested a role for ACC axons in selective visual attention. An attentional response is believed to modulate V1 neurons by increasing their response to relevant stimuli and decreasing it to irrelevant stimuli. Zhang *et al.* (2014) demonstrated that optogenetically stimulating ACC axons in layer 1 V1 led to an increase in V1 neuron firing rate to stimuli of the preferred orientation. As well as this, varying the stimulation distance from the V1 neuron in which the response was being recorded from resulted in a surround-suppression-like effect. Both of these are hallmarks of visual attention. They argue that ACC axons are able to modulate both excitatory and inhibitory axonal behaviour through synapsing with pyramidal cells and interneurons involved in this network. A further effect of optogenetically stimulating ACC was improved performance in a visual discrimination task, suggesting these attentional properties of ACC axons are involved. This study, however, did not show whether mice are able to recruit this projection under natural conditions.

To explore whether this ACC to V1 projection was recruited in the same way under natural conditions, mice completed a go/no-go visual discrimination task whilst GCaMP6s-transfected ACC axons were recorded from in V1. I hypothesised that ACC activity would be elevated when the task was being completely correctly, regardless of the trial type. The results are discussed below.

5.3.1 There are more active ACC axons during correct go trials than in correct no-go trials

If the ACC to V1 projection carries an attentional signal and generally elevated ACC activity is associated with improved performance on a discrimination task then it could be hypothesised that (a) ACC activity would be greater during trials when the mice have learned the relevance of each stimuli and (b) ACC activity during correct trials would be comparable, regardless of the trial type. I found that significantly more ACC axons responded during the go trial when the mice performed well on the task compared to when the go trial was first encountered and thus the stimulus had not yet been associated with a reward. On the other hand, ACC activity during the no-go trial was comparable. As well as this, significantly more ACC axons had significantly elevated activity in correct go trials compared to correct no-go trials. This suggested that performing the task correctly was not associated with an endogenous blanket elevation in ACC axon activity during correct trials that would have been comparable to the optogenetic activation of ACC. It has previously been shown that V1 neuronal responses to stimuli directly associated with a reward are increased compared to those not associated, and that this association sharpens the tuning of the neurons to their preferred stimulus (Schoups *et al.*, 2001; Goltstein *et al.*, 2013). This preferential response to a stimulus with a learned association with a reward is likely to be influenced by top-down processing and so it would not be unreasonable to consider

that the ACC, a projection that emanates from a structure involved in reward processing, may be modulating this.

5.3.2 ACC axons that discriminate between correct and incorrect trials show elevated activity during correct go and incorrect no-go trials

Even though significantly more ACC axons exhibited elevated activity during correct completions of go trials compared to correct no-go trials, this did not rule out that their activity was greater compared to incorrect trials. Therefore, it was hypothesised that, if a blanket elevation of ACC axons resulted in improved performance on the visual discrimination task, then ACC axon activity would be elevated in correct trials, regardless of trial type. To test this, a group of ACC axons with significantly differing activity during correct and incorrect trials were identified, and their activity during incorrect trials was subtracted from that during correct trials. Activity of these axons was elevated in correct compared to incorrect iterations of go trials, which was in line with the hypothesis. Unexpectedly, however, the opposite was true for no-go trials. This suggested that, not only was there no blanket elevation in ACC activity when the task was being performed correctly, but also that ACC axons were responsive to something occurring during the incorrect no-go trial. As most activity was observed to occur during the response window, this could have been as a result of the motor response of licking the spout, a response to the air puff or even the detection of an unexpected outcome to the trial.

Furthermore, if ACC axons were involved in visual attention, it would be expected that the timing of their response would align with the presentation of the visual stimulus. Fiser *et al*. (2016) demonstrated that ACC axons in mice exhibited predictive responses to visual stimuli once they had learned their spatial location by navigating a

virtual corridor. In my task the appearance of the visual stimulus was predictable once the auditory cue was sounded, but axons with differing activity in correct and incorrect trials did not show significant changes until 2.4s after the presentation of the visual stimulus, during the response window. This suggested that this population of ACC axons were not involved in the initial perception of the visual stimulus, but instead recruited during the part of the task requiring a behavioural response.

5.3.3 General elevated activity is not observed when the visual discrimination task is more difficult

On the other hand, it has been shown that an ACC projection to claustrum is only active when the cognitive demands of the task are high enough (Carter *et al.*, 2018). Optogenetic activation of ACC by Zhang *et al*. (2014) may have induced a modulation that is only required in more natural conditions when a task is sufficiently difficult, which may not have been the case when using a retinotopically predictable task with 100% stimulus contrast and thus did not recruit the visual attentional properties of this ACC to V1 projection. To increase task difficulty initially, the task was adapted to a retinotopically unpredictable one. In this task structure, mice were unable to Mice were able to learn this task and reach high levels of performance after approximately 14-15 training sessions. This was longer than the time taken on the retinotopically predictable task, and the mice never reached the same peak performance, confirming the increased task difficulty.

Using this method, it was possible to ask whether ACC axon responses were spatially specific, as well as whether there was an elevation of activity across correctly completed trials. Similar to the retinotopically predictable task, more ACC axons showed a significant elevation in activity during go trials compared to no-go trials,

although this was less pronounced when the stimulus appeared on the ipsilateral side to imaging. As a greater amount of activity was observed in the go trials, these were then used to explore whether ACC axons exhibited spatially specific responses. Significantly more ACC axons significantly responded during go trials regardless of whether the stimulus was presented on the contralateral or ipsilateral side of the imaged hemisphere during the trial and especially during the response window. Furthermore, even with this more difficult task, axons which responded significantly differently to correct and incorrect trials also exhibited significantly more activity in correct go and incorrect no-go trials compared to incorrect go and correct no-go trials respectively. These data suggest a number of things. Firstly, the ACC projection does not appear to be spatially specific, something that would be necessary for spatial attentional modulation. Furthermore, even with the increased difficulty, there was no blanket elevation of ACC activity during correct trials. This was examined further by increasing the difficulty of perceiving the visual stimulus by reducing the visual stimulus contrast. Mice were still just able to perform the task but committed more errors. Even after this, ACC activity was significantly elevated in incorrect no-go compared to correct no-go trials, particularly during the response window of the task. This provided further evidence that the endogenous activity of the ACC to V1 projection was unlikely to contribute to improved performance in a visual discrimination task by indiscriminate elevation in activity.

5.3.4 Changing the task and stimulus properties did not result in an attentional signal

There was a possibility that ACC axons were spatially specific and that they exhibit elevated activity levels when performing well in visually guided tasks but the large nature of the stimuli in the discrimination task reduced this effect. Modulation of attention is also believed to involve surround suppression. This is thought to counteract

irrelevant stimuli that appear within or close to the location of the attended stimulus that could elicit a response that would ultimately degrade that to the attended stimulus. Zhang *et al*. (2014) showed that the ACC to V1 projection is spatially specific and that it exhibits activity comparable to surround suppression. Therefore, the attentional response might have been missed by presenting a large stimulus in the same location in both go and no-go trials, as well as not presenting the stimulus in a location of visual space precisely matched to the retinotopically relevant area of V1. To address these points, a detection task with a smaller stimulus where both ACC axons and L2/3 pyramidal somas were recorded from simultaneously was used.

In this task, both V1 somas and ACC axons responded significantly more to the stimulus presentation than to the blank in correct trials, again suggesting that there is not a blanket elevation in ACC activity when performing correctly compared to incorrectly in a visually guided attention task. Interestingly, upon appearance of the stimulus, significantly more V1 somas responded in comparison to ACC axons, but the proportion became comparable 0.4s later, in between the onset of the visual stimulus and the reaction time. This suggested that the ACC axons are driven by the motor response associated with the reward rather than being involved in the initial perception and guiding of selective visual attention to the stimulus, and that the signal may be preparatory. This would be in line with studies that have suggested ACC is involved in the response element of visually guided tasks

5.3.5 ACC axon activity is associated with the lick behavioural response

Each of the previous findings strongly suggest that high performance in a visually guided discrimination task is not associated with a complementary endogenous blanket elevation in ACC activity. It was found that in the discrimination task that there were

significantly more ACC axons active during correct go trials compared to correct no-go trials, that ACC axons responded more to correct go trials compared to incorrect go trials and that ACC axons responded more to incorrect no-go trials than correct no-go trials. In the detection task it was found that ACC axon activity was delayed until after the stimulus, suggesting it is not directly involved in the perception of the visual stimulus. In fact, it aligned more closely with the behavioural response indicating an involvement with the motor response rather than the perception of the visual stimulus itself. Taken together these data suggest that the principal factor driving activity of ACC axons in V1 was licking behaviour. Analysis of the precise relationship of ACC axon activity to licking behaviour indicated that a fraction of axons were significantly correlated. Furthermore, this activity appeared to occur just before the lick behaviour which suggested a preparatory signal. Previous studies in humans have suggested that ACC plays a role in visually guided tasks that require selective attention, and that its activity is elevated specifically during the response element of the task (Pardo *et al.*, 1990; Carter *et al.*, 1998). Taken together, this suggests that ACC is involved in the visual discrimination task, but not the direct perception of the stimulus. Instead, it plays a role in directing the behavioural response to that stimulus. This would also explain why its activity did not appear to depend on the location in which the stimulus was presented (Pardo *et al.*, 1990; Carter *et al.*, 1998; MacDonald *et al.*, 2005).

5.3.6 ACC axon activity is influenced by reward

By comparing the responses of ACC axons to either a rewarded or unrewarded lick, it was found that a fraction of axons had a significantly higher response to one of the two. Furthermore, significantly more axons preferred licks that were rewarded. This suggested that ACC activity was not simply associated with just the lick response, but instead that rewarded licks and non-rewarded licks were processed differently. One such system would be the integration of visual and motor information for the successful

timing of the reward. It has been shown that, over the course of associating a visual stimulus with a reward, a substantial proportion of V1 neurons begin to predict the timing of the reward (Shuler and Bear, 2006), and activity within V1 is coupled to lick responses when animals must make this motor response based on a visual stimulus (Namboodiri *et al.*, 2015). Reward timing is thought to be influenced by top-down processing and rely on cholinergic inputs projecting from the basal forebrain (Chubykin *et al.*, 2013). ACC receives a substantial input of this kind (Zaborszky *et al.*, 2015). Its activity is linked to licking, reflecting the changes observed in V1, but also to the outcome of the lick, suggesting that it is able to integrate information about the visual stimulus and the outcome of the response in order to aid the mouse in making the correct response during a visually guided task. Further study will need to be carried out to explore the possible role of this ACC to V1 projection in reward timing.

5.3.7 Further study into the role of the ACC to V1 projection in visually guided tasks

It could be argued that visual discrimination tasks do not fully test attentional responses as there are no distractors to ignore presented at the same time as either stimulus. Optogenetic stimulation of ACC axons by Zhang *et al.,* (2014) during a visual discrimination task could have led to an artificially induced improvement in performance due to the addition of an attention signal that is not required or attainable under endogenous conditions. It may, therefore, be interesting to further explore a possible role for ACC axons projecting to V1 in attention. One way of doing this would be to introduce distractors into the behaviour. Stimuli would appear in two or more locations, one of which was previously cued. The mouse would then have to pay attention to the stimulus that appears in the cued location and respond accordingly, regardless of the type of stimuli which appear in the other locations. Another approach would be to explore using other tasks believed to engage attention. It has been shown that mice

are able to perform the 5-choice serial reaction time task (5-CSRTT) where animals must respond to unpredictable visual stimuli presented in one of five locations. This task is thought to measure both attention and motor impulsivity (Higgins and Silenieks, 2017). With the advancement of two-photon imaging in freely moving mice (Helmchen, Denk and Kerr, 2013; Ozbay *et al.*, 2018), this type of experiment may not even need to be adapted to head-fixed animals. Using these types of task would not only allow further exploration of attention, but have also been adapted from tasks used with humans (Higgins and Silenieks, 2017). Deficits in attention have been linked to neuropsychiatric conditions such as schizophrenia. Understanding the mechanisms that underlie attention could ultimately help in understanding the pathology of these conditions, and so it is important to design experiments that they are as relevant as possible across species.

On the other hand, it would be interesting to probe the role of ACC axons in the behavioural responses further. A major question here is whether ACC axon activity would be elevated depending on the type of motor behavioural response, especially if that response is not directly linked with a reward. One way to explore this would be to image ACC axons while mice undertake a visually guided task requiring a different behavioural response. An example would be where mice are taught to turn a steering wheel to make two alternative choices similar to that in Burgess *et al.* (2017). This task would involve two motor behaviours, the first being the turning of the wheel in response to an identified visual stimulus. The second would be licking a spout to acquire a reward if this is done correctly. This would result in a task encompassing ACC activity in response to perceiving a visual stimulus, a motor behavioural response that is not licking and is not directly associated with a reward, and the motor response of licking that is associated with a reward that each occur at temporally defined times. Furthermore, it would be interesting to inhibit the activity of ACC axons using

optogenetics once any behaviour task has been learned to explore whether it is alleviated.

5.3.8 Methodological drawbacks of the techniques used

There are a number of methodological drawbacks of the techniques used throughout this thesis that must be understood alongside considering the work presented here. Firstly, although the use of calcium indicators is a powerful technique that allows hundreds of neurons to be imaged down to the level of a single bouton or dendrite, it has several disadvantages against other techniques, for example electrophysiology. One of these is that fluorescence fluctuations are simply a proxy of neuronal activity. This, coupled with the slow decay of the signal, means that the use of this technique does not directly measure neuronal activity, and if the study requires action potential to be identified then this can only be done by modelling methods including deconvolution. It also means that it may not be possible to see subtle and quick changes in neuronal firing patterns that can be observed with electrophysiology. It is important, therefore, that experiments are designed with this in mind. On top of this, light is scattered through the tissue using this technique meaning it can only be used at fairly superficial depths (Girven and Sparta, 2017), this is however being circumnavigated using wavelengths of light less subject to scatter (Dana *et al.*, 2016) and by using microprisms (Andermann *et al.*, 2013). On the other hand, even with the advent of multi-region electrophysiological recordings using polymer electrode assays (Chung *et al.*, 2019), two-photon calcium imaging of calcium indicators has the ability to record from much larger populations of neurons simultaneously (Jercog *et al.,* 2016), something of great importance in understanding how the brain works as an entire network in the years to come.

Another drawback of these methods is the use of mice to understand the visual system. The mouse visual system is less complex than that of humans and so using it as a model in very controlled settings could be viewed as reductionist. On the other hand, it is possible to record neuronal activity down to the resolution of single axons using mice, something that s not currently possible using scanning techniques with humans. It is also possible to get a much higher throughput of data. Furthermore, there are a huge number of sophisticated tools available for experimental studies such as genetic modification, injection of viruses and the use of optogenetics to manipulate specific cell types and circuits (Huberman and Niell, 2011; Ellenbroek and Youn, 2016).

It is important to keep in mind both the huge advantages and criticisms of using two-photon imaging in freely moving mice to study networks in the brain in order to design robust experiments and interpret the results with integrity.

5.3.9 Concluding remarks

Overall, the data presented here indicates that the ACC projection to V1 is involved in visually guided tasks but is associated more with the motor response of licking than the perception of the visual stimulus. The additional modulation by reward suggests that this association depends upon the outcome of trials and may therefore be important for behaviours such as reward timing.

6 References

Andermann, M. L. *et al.* (2013) ‘Chronic Cellular Imaging of Entire Cortical Columns in Awake Mice Using Microprisms’, *Neuron*, 80(4), pp. 900–913.

Andermann, M. L., Kerlin, A. M. and Reid, R. C. (2010) ‘Chronic cellular imaging of mouse visual cortex during operant behavior and passive viewing.’, *Frontiers in cellular neuroscience*, 4, p. 3.

de Araujo, I. E. T. *et al.* (2003) ‘Human cortical responses to water in the mouth, and the effects of thirst.’, *Journal of neurophysiology*. American Physiological Society, 90(3), pp. 1865–76.

Baden, T. *et al.* (2016) ‘The functional diversity of retinal ganglion cells in the mouse’, *Nature*. Nature Publishing Group, 529(7586), pp. 345–350.

Barch, D. M. *et al.* (2012) ‘The clinical translation of a measure of gain control: the contrast-contrast effect task.’, *Schizophrenia bulletin*. Oxford University Press, 38(1), pp. 135–43.

Baumeister, A. A. and Francis, J. L. (2002) ‘Historical development of the dopamine hypothesis of schizophrenia.’, *Journal of the history of the neurosciences*, 11(3), pp. 265–77.

Beauchamp, M. S. *et al.* (2001) ‘A Parametric fMRI Study of Overt and Covert Shifts of Visuospatial Attention’, *NeuroImage*. Academic Press, 14(2), pp. 310–321.

Bennett, C., Arroyo, S. and Hestrin, S. (2013) ‘Subthreshold mechanisms underlying state-dependent modulation of visual responses.’, *Neuron*. Elsevier, 80(2), pp. 350–7.

Bisley, J. W. and Goldberg, M. E. (2010) ‘Attention, Intention, and Priority in the Parietal Lobe’, *Annual Review of Neuroscience*.

Blakemore, C. and Tobin, E. (1972) ‘Lateral inhibition between orientation detectors in

the cat's visual cortex', *Experimental Brain Research*. Springer-Verlag, 15(4), pp. 439–440.

Bos, R., Gainer, C. and Feller, M. B. (2016) 'Role for Visual Experience in the Development of Direction-Selective Circuits.', *Current biology : CB*. NIH Public Access, 26(10), pp. 1367–75.

Braff, D. L. (1993) 'Information processing and attention dysfunctions in schizophrenia.', *Schizophrenia bulletin*, 19(2), pp. 233–59.

Brefczynski, J. A. and DeYoe, E. A. (1999) 'A physiological correlate of the "spotlight" of visual attention', *Nature Neuroscience*. Nature Publishing Group, 2(4), pp. 370–374.

Broersen, L. . and Uylings, H. B. . (1999) 'Visual attention task performance in Wistar and Lister Hooded rats: response inhibition deficits after medial prefrontal cortex lesions', *Neuroscience*. Pergamon, 94(1), pp. 47–57.

Broussard, G. J. *et al.* (2018) 'In vivo measurement of afferent activity with axon-specific calcium imaging', *Nature Neuroscience*. Nature Publishing Group, 21(9), pp. 1272–1280.

Brown, H. *et al.* (2013) 'Active inference, sensory attenuation and illusions', *Cognitive Processing*. Springer Berlin Heidelberg, 14(4), pp. 411–427.

Butler, P. D., Silverstein, S. M. and Dakin, S. C. (2008) 'Visual Perception and Its Impairment in Schizophrenia', *Biological Psychiatry*. Elsevier, 64(1), pp. 40–47.

Cang, J. *et al.* (2005) 'Ephrin-As Guide the Formation of Functional Maps in the Visual Cortex', *Neuron*. Cell Press, 48(4), pp. 577–589.

Carter, A. M. *et al.* (2018) 'Anterior Cingulate Cortex Input to the Claustrum Is Required for Top-Down Action Control', *Cell Reports*.

Carter, C. S. *et al.* (1998) 'Anterior Cingulate Cortex, Error Detection, and the Online

Monitoring of Performance', *Science*. American Association for the Advancement of Science, 280(5364), pp. 747–749.

Carter, J. D. *et al.* (2010) 'Attention deficits in schizophrenia--preliminary evidence of dissociable transient and sustained deficits.', *Schizophrenia research*. NIH Public Access, 122(1–3), pp. 104–12.

Chen, J. L. *et al.* (2013) 'Imaging neuronal populations in behaving rodents: paradigms for studying neural circuits underlying behavior in the mammalian cortex.', *The Journal of neuroscience : the official journal of the Society for Neuroscience*, 33(45), pp. 17631–40.

Chen, T.-W. *et al.* (2013) 'Ultrasensitive fluorescent proteins for imaging neuronal activity.', *Nature*. Nature Publishing Group, a division of Macmillan Publishers Limited. All Rights Reserved., 499(7458), pp. 295–300.

Chen, Y. *et al.* (2008) 'Task difficulty modulates the activity of specific neuronal populations in primary visual cortex', *Nature Neuroscience*. Nature Publishing Group, 11(8), pp. 974–982.

Chubykin, A. A. *et al.* (2013) 'A cholinergic mechanism for reward timing within primary visual cortex.', *Neuron*. NIH Public Access, 77(4), pp. 723–35.

Chung, J. E. *et al.* (2019) 'High-Density, Long-Lasting, and Multi-region Electrophysiological Recordings Using Polymer Electrode Arrays', *Neuron*. Cell Press, 101(1), pp. 21-31.e5.

Clark, A. (2013) 'Whatever next? Predictive brains, situated agents, and the future of cognitive science', *Behavioral and Brain Sciences*, 36(03), pp. 181–204.

Cocker, P. J. *et al.* (2016) 'Activation of dopamine D4 receptors within the anterior cingulate cortex enhances the erroneous expectation of reward on a rat slot machine task.', *Neuropharmacology*, 105, pp. 186–95.

Coleman, M. J. *et al.* (2009) 'Schizophrenia Patients Show Deficits in Shifts of Attention to Different Levels of Global-Local Stimuli: Evidence for Magnocellular Dysfunction', *Schizophrenia Bulletin*. Narnia, 35(6), pp. 1108–1116.

Corbetta, M. *et al.* (1991) 'Selective and Divided Attention during Visual Discriminations of Shape, Color, and Speed: Functional Anatomy by Positron Emission Tomography', *The Journal of Neuroscience*, 1(9), pp. 2393–2402.

Corbetta, M. and Shulman, G. L. (2002) 'Control of goal-directed and stimulus-driven attention in the brain', *Nature Reviews Neuroscience*. Nature Publishing Group, 3(3), pp. 201–215.

Coyle, J. T. (2012) 'NMDA receptor and schizophrenia: a brief history.', *Schizophrenia bulletin*. Oxford University Press, 38(5), pp. 920–6.

Dakin, S., Carlin, P. and Hemsley, D. (2005) 'Weak suppression of visual context in chronic schizophrenia.', *Current biology : CB*. Elsevier, 15(20), pp. R822-4.

Daliri, M. R., Kozyrev, V. and Treue, S. (2016) 'Attention enhances stimulus representations in macaque visual cortex without affecting their signal-to-noise level', *Scientific Reports*.

Dana, H. *et al.* (2016) 'Sensitive red protein calcium indicators for imaging neural activity', *eLife*, 5.

De Franceschi, G. *et al.* (2016) 'Vision Guides Selection of Freeze or Flight Defense Strategies in Mice', *Current Biology*. Cell Press, 26(16), pp. 2150–2154.

Dehaene, S. *et al.* (2003) 'Conscious and subliminal conflicts in normal subjects and patients with schizophrenia: The role of the anterior cingulate', *Proceedings of the National Academy of Sciences of the United States of America*. National Academy of Sciences, 100(23), p. 13722.

Dehkordi, O. *et al.* (2015) 'Neuroanatomical circuitry mediating the sensory impact of

nicotine in the central nervous system.', *Journal of neuroscience research*, 93(2), pp. 230–43.

Desimone, R. and Duncan, J. (1995) 'NEURAL MECHANISMS OF SELECTIVE VISUAL ATTENTION', *Annu. Rev. Neurosci*, 18, pp. 193–222.

Dipoppa, M. *et al.* (2018) 'Vision and Locomotion Shape the Interactions between Neuron Types in Mouse Visual Cortex.', *Neuron*. Elsevier, 98(3), pp. 602-615.e8.

Dräger, U. C. (1975) 'Receptive fields of single cells and topography in mouse visual cortex', *Journal of Comparative Neurology*. John Wiley & Sons, Ltd, 160(3), pp. 269–289.

Dum, R. P. and Strick, P. L. (1991) 'The origin of corticospinal projections from the premotor areas in the frontal lobe.', *The Journal of neuroscience : the official journal of the Society for Neuroscience*. Society for Neuroscience, 11(3), pp. 667–89.

Ellenbroek, B. and Youn, J. (2016) 'Rodent models in neuroscience research: Is it a rat race?', *DMM Disease Models and Mechanisms*. Company of Biologists Ltd, 9(10), pp. 1079–1087.

Erisken, S. *et al.* (2014) 'Effects of locomotion extend throughout the mouse early visual system.', *Current biology : CB*. Elsevier, 24(24), pp. 2899–907.

Feldheim, D. A. and O'Leary, D. D. M. (2010) 'Visual map development: bidirectional signaling, bifunctional guidance molecules, and competition.', *Cold Spring Harbor perspectives in biology*. Cold Spring Harbor Laboratory Press, 2(11), p. a001768.

Filinger, C. *et al.* (2018) 'Efferents of anterior cingulate areas 24a and 24b and midcingulate areas 24a' and 24b' in the mouse.', *Brain Structure and Function*. 223(4), p1747-1778

Fioravanti, M. *et al.* (2005) 'A meta-analysis of cognitive deficits in adults with a diagnosis of schizophrenia', *Neuropsychology Review*.

Fiser, A. *et al.* (2016) ‘Experience-dependent spatial expectations in mouse visual cortex’, *Nature Neuroscience*.

Friston, K. (2005) ‘A theory of cortical responses.’, *Philosophical transactions of the Royal Society of London. Series B, Biological sciences*. The Royal Society, 360(1456), pp. 815–36.

Friston, K. J. (1998) ‘The disconnection hypothesis’, *Schizophrenia Research*. Elsevier, 30(2), pp. 115–125.

Garrett, M. E. *et al.* (2014) ‘Topography and areal organization of mouse visual cortex.’, *The Journal of neuroscience : the official journal of the Society for Neuroscience*, 34(37), pp. 12587–600.

Geisler, S. *et al.* (2007) ‘Glutamatergic afferents of the ventral tegmental area in the rat.’, *The Journal of neuroscience : the official journal of the Society for Neuroscience*. Society for Neuroscience, 27(21), pp. 5730–43.

Girven, K. S. and Sparta, D. R. (2017) ‘Probing Deep Brain Circuitry: New Advances in in Vivo Calcium Measurement Strategies.’, *ACS chemical neuroscience*, 8(2), pp. 243–251.

Glickfeld, L. L. *et al.* (2013) ‘Cortico-cortical projections in mouse visual cortex are functionally target specific’, *Nature Neuroscience*. Nature Publishing Group, 16(2), pp. 219–226.

Goard, M. J. *et al.* (2016) ‘Distinct roles of visual, parietal, and frontal motor cortices in memory-guided sensorimotor decisions’, *eLife*. eLife Sciences Publications Limited, 5, pp. 471–477.

Goldstein, E. B. (1981) ‘The Ecology of J. J. Gibson’s Perception’, *Leonardo*, 14(3), p. 191.

Goltstein, P. M. *et al.* (2013) ‘In vivo two-photon Ca2+ imaging reveals selective reward

effects on stimulus-specific assemblies in mouse visual cortex.', *The Journal of neuroscience : the official journal of the Society for Neuroscience*. Society for Neuroscience, 33(28), pp. 11540–55.

Goltstein, P. M., Meijer, G. T. and Pennartz, C. M. (2018) 'Conditioning sharpens the spatial representation of rewarded stimuli in mouse primary visual cortex', *eLife*, 7.

Goodale, M. A. and Milner, A. D. (1992) 'Separate visual pathways for perception and action', *Trends in Neurosciences*. Elsevier Current Trends, 15(1), pp. 20–25.

Green, M. F. *et al.* (1999) 'Backward masking in unmedicated schizophrenic patients in psychotic remission: possible reflection of aberrant cortical oscillation.', *The American journal of psychiatry*, 156(9), pp. 1367–73.

Gregoriou, G. G. *et al.* (2014) 'Lesions of prefrontal cortex reduce attentional modulation of neuronal responses and synchrony in V4', *Nature Neuroscience*. Nature Publishing Group, 17(7), pp. 1003–1011.

Hahn, B., Ross, T. J. and Stein, E. A. (2007) 'Cingulate Activation Increases Dynamically with Response Speed under Stimulus Unpredictability', *Cerebral Cortex*. Narnia, 17(7), pp. 1664–1671.

Harris, K. D. and Shepherd, G. M. G. (2015) 'The neocortical circuit: Themes and variations', *Nature Neuroscience*. Nature Publishing Group, pp. 170–181.

Helmchen, F., Denk, W. and Kerr, J. N. D. (2013) 'Miniaturization of two-photon microscopy for imaging in freely moving animals.', *Cold Spring Harbor protocols*. Cold Spring Harbor Laboratory Press, 2013(10), pp. 904–13.

Higgins, G. A. and Silenieks, L. B. (2017) 'Rodent Test of Attention and Impulsivity: The 5-Choice Serial Reaction Time Task', in *Current Protocols in Pharmacology*. Hoboken, NJ, USA: John Wiley & Sons, Inc., pp. 5.49.1-5.49.34.

Histed, M. H., Carvalho, L. A. and Maunsell, J. H. R. (2012) 'Psychophysical

measurement of contrast sensitivity in the behaving mouse', *Journal of Neurophysiology*. American Physiological Society Bethesda, MD, 107(3), pp. 758–765.

Hoonakker, M., Doignon-Camus, N. and Bonnefond, A. (2017) 'Sustaining attention to simple visual tasks: a central deficit in schizophrenia? A systematic review', *Annals of the New York Academy of Sciences*. John Wiley & Sons, Ltd (10.1111), 1408(1), pp. 32–45.

Hubel, D. H. and Wiesel, T. N. (1968) 'Receptive fields and functional architecture of monkey striate cortex', *The Journal of Physiology*. John Wiley & Sons, Ltd (10.1111), 195(1), pp. 215–243.

HUBEL, D. H. and WIESEL, T. N. (1959) 'Receptive fields of single neurones in the cat's striate cortex.', *The Journal of physiology*. Wiley-Blackwell, 148(3), pp. 574–91.

HUBEL, D. H. and WIESEL, T. N. (1962) 'Receptive fields, binocular interaction and functional architecture in the cat's visual cortex.', *The Journal of physiology*. Wiley-Blackwell, 160(1), pp. 106–54.

Huberman, A. D. and Niell, C. M. (2011) 'What can mice tell us about how vision works?', *Trends in Neurosciences*, pp. 464–473.

Iacaruso, M. F., Gasler, I. T. and Hofer, S. B. (2017) 'Synaptic organization of visual space in primary visual cortex', *Nature*, 547(7664), pp. 449–452.

Isomura, Y. *et al.* (2003) 'Neural coding of "attention for action" and "response selection" in primate anterior cingulate cortex.', *The Journal of neuroscience : the official journal of the Society for Neuroscience*. Society for Neuroscience, 23(22), pp. 8002–12.

Jercog, P., Rogerson, T. and Schnitzer, M. J. (2016) 'Large-Scale Fluorescence Calcium-Imaging Methods for Studies of Long-Term Memory in Behaving Mammals.', *Cold Spring Harbor perspectives in biology*. Cold Spring Harbor Laboratory Press, 8(5),

p. a021824.

Jiang, X. *et al.* (2015) ‘Principles of connectivity among morphologically defined cell types in adult neocortex’, *Science*. American Association for the Advancement of Science, 350(6264), p. aac9462.

Juavinett, A. L. *et al.* (2016) ‘Automated identification of mouse visual areas with intrinsic signal imaging’, *Nature Protocols*. Nature Research, 12(1), pp. 32–43.

Jurjut, O. *et al.* (2017) ‘Learning Enhances Sensory Processing in Mouse V1 before Improving Behavior’, *Journal of Neuroscience*. Society for Neuroscience, 37(27), pp. 6460–6474.

Kalatsky, Valery A and Stryker, M. P. (2003) ‘New paradigm for optical imaging: temporally encoded maps of intrinsic signal.’, *Neuron*. Elsevier, 38(4), pp. 529–45.

Kalatsky, Valery A. and Stryker, M. P. (2003) ‘New Paradigm for Optical Imaging: Temporally Encoded Maps of Intrinsic Signal’, *Neuron*. Cell Press, 38(4), pp. 529–545.

Kastner, S. *et al.* (1998) ‘Mechanisms of directed attention in the human extrastriate cortex as revealed by functional MRI.’, *Science (New York, N.Y.)*. American Association for the Advancement of Science, 282(5386), pp. 108–11.

Kastner, S. and Ungerleider, L. (2000) ‘Mechanisms of Visual Attention in the Human Cortex’, *Annual Review of Neuroscience*.

Keller, A. J. *et al.* (2017) ‘Stimulus relevance modulates contrast adaptation in visual cortex’, *eLife*.

Keller, G. B., Bonhoeffer, T. and Hübener, M. (2012) ‘Sensorimotor mismatch signals in primary visual cortex of the behaving mouse.’, *Neuron*. Elsevier, 74(5), pp. 809–15.

Kringelbach, M. L. *et al.* (2003) ‘Activation of the Human Orbitofrontal Cortex to a Liquid Food Stimulus is Correlated with its Subjective Pleasantness’, *Cerebral Cortex*,

13(10), pp. 1064–1071.

Lee, A. M. *et al.* (2014) ‘Identification of a brainstem circuit regulating visual cortical state in parallel with locomotion.’, *Neuron*. Elsevier, 83(2), pp. 455–466.

Leinweber, M. *et al.* (2017) ‘A Sensorimotor Circuit in Mouse Cortex for Visual Flow Predictions’, *Neuron*. Cell Press, 95(6), pp. 1420-1432.e5.

Li, R. *et al.* (2018) ‘Two-Photon Functional Imaging of the Auditory Cortex in Behaving Mice: From Neural Networks to Single Spines’, *Frontiers in Neural Circuits*. Frontiers, 12, p. 33.

Li, W., Piëch, V. and Gilbert, C. D. (2008) ‘Learning to Link Visual Contours’, *Neuron*. Cell Press, 57(3), pp. 442–451.

Liu, C. *et al.* (2016) ‘Neuronal activity and the expression of hypothalamic oxytocin and vasopressin in social versus cocaine conditioning.’, *Behavioural brain research*, 310, pp. 84–92.

MacDonald, A. W. *et al.* (2005) ‘Specificity of Prefrontal Dysfunction and Context Processing Deficits to Schizophrenia in Never-Medicated Patients With First-Episode Psychosis’, *American Journal of Psychiatry*. American Psychiatric Publishing, 162(3), pp. 475–484.

Makino, H. and Komiyama, T. (2015) ‘Learning enhances the relative impact of top-down processing in the visual cortex’, *Nature Neuroscience*. Nature Publishing Group, a division of Macmillan Publishers Limited. All Rights Reserved., 18(8), pp. 1116–1122.

Maldonado, P. E. *et al.* (1997) ‘Orientation selectivity in pinwheel centers in cat striate cortex.’, *Science (New York, N.Y.)*. American Association for the Advancement of Science, 276(5318), pp. 1551–5.

Mangun, G. R. and Hillyard, S. A. (1990) ‘Allocation of visual attention to spatial locations: Tradeoff functions for event-related brain potentials and detection

performance', *Perception & Psychophysics*. Springer-Verlag, 47(6), pp. 532–550.

Marques, T. *et al.* (2018) 'The functional organization of cortical feedback inputs to primary visual cortex', *Nature Neuroscience*. Nature Publishing Group, 21(5), pp. 757–764.

Marshel, J. H. *et al.* (2011) 'Functional Specialization of Seven Mouse Visual Cortical Areas', *Neuron*. MIT Press, Cambridge, MA, 72(6), pp. 1040–1054.

McAdams, C. J. and Maunsell, J. H. (1999) 'Effects of attention on orientation-tuning functions of single neurons in macaque cortical area V4.', *The Journal of neuroscience : the official journal of the Society for Neuroscience*. Society for Neuroscience, 19(1), pp. 431–41.

Métin, C., Godement, P. and Imbert, M. (1988) 'The primary visual cortex in the mouse: receptive field properties and functional organization.', *Experimental brain research*, 69(3), pp. 594–612.

Miller, E. K. and Cohen, J. D. (2001) 'AN INTEGRATIVE THEORY OF PREFRONTAL CORTEX FUNCTION'.

Mishkin, M., Ungerleider, L. G. and Macko, K. A. (1983) 'Object vision and spatial vision: two cortical pathways', *Trends in Neurosciences*. Elsevier Current Trends, 6, pp. 414–417.

Mitchell, D. E., Kennie, J. and Kung, D. (2009) 'Development of Global Motion Perception Requires Early Postnatal Exposure to Patterned Light', *Current Biology*. Cell Press, 19(8), pp. 645–649.

Miyamoto, D. *et al.* (2016) 'Top-down cortical input during NREM sleep consolidates perceptual memory', *Science*.

Mizuno, H., Hirano, T. and Tagawa, Y. (2007) 'Evidence for Activity-Dependent Cortical Wiring: Formation of Interhemispheric Connections in Neonatal Mouse Visual Cortex

Requires Projection Neuron Activity', *Journal of Neuroscience*. Society for Neuroscience, 27(25), pp. 6760–6770.

Moran, J. and Desimone, R. (1985) 'Selective attention gates visual processing in the extrastriate cortex', *Science*, (229), pp. 782–784.

Morecraft, R. J. and van Hoesen, G. W. (1992) 'Cingulate input to the primary and supplementary motor cortices in the rhesus monkey: Evidence for somatotopy in areas 24c and 23c', *The Journal of Comparative Neurology*. John Wiley & Sons, Ltd, 322(4), pp. 471–489.

Morin, L. P. and Studholme, K. M. (2014) 'Retinofugal projections in the mouse.', *The Journal of comparative neurology*. NIH Public Access, 522(16), pp. 3733–53.

Motter, B. C. (1994) 'Neural correlates of attentive selection for color or luminance in extrastriate area V4.', *The Journal of neuroscience : the official journal of the Society for Neuroscience*. Society for Neuroscience, 14(4), pp. 2178–89.

Murakami, T., Matsui, T. and Ohki, K. (2017) 'Functional Segregation and Development of Mouse Higher Visual Areas.', *The Journal of neuroscience : the official journal of the Society for Neuroscience*. Society for Neuroscience, 37(39), pp. 9424–9437.

Namboodiri, V. M. K. *et al.* (2015) 'Visually cued action timing in the primary visual cortex', *Neuron*.

Nathanson, J. L. *et al.* (2009) 'Preferential labeling of inhibitory and excitatory cortical neurons by endogenous tropism of adeno-associated virus and lentivirus vectors.', *Neuroscience*. NIH Public Access, 161(2), pp. 441–50.

Neuchterlein, K. H. *et al.* (1991) '9. Information-processing anomalies in the early course of schizophrenia and bipolar disorder', *Schizophrenia Research*. Elsevier, 5(3), pp. 195–196.

Niell, C. M. and Stryker, M. P. (2008) 'Highly selective receptive fields in mouse visual

cortex.', *The Journal of neuroscience : the official journal of the Society for Neuroscience*. NIH Public Access, 28(30), pp. 7520–36.

Niell, C. M. and Stryker, M. P. (2010) 'Modulation of Visual Responses by Behavioral State in Mouse Visual Cortex', *Neuron*. Cell Press, 65(4), pp. 472–479.

Ohki, K. *et al.* (2005) 'Functional imaging with cellular resolution reveals precise micro-architecture in visual cortex', *Nature*. Nature Publishing Group, 433(7026), pp. 597–603.

Ozbay, B. N. *et al.* (2018) 'Three dimensional two-photon brain imaging in freely moving mice using a miniature fiber coupled microscope with active axial-scanning', *Scientific Reports*. Nature Publishing Group, 8(1), p. 8108.

Pachitariu, M. *et al.* (2017) 'Suite2p: beyond 10,000 neurons with standard two-photon microscopy', *bioRxiv*. Cold Spring Harbor Laboratory, p. 061507.

Pakan, J. M. *et al.* (2016) 'Behavioral-state modulation of inhibition is context-dependent and cell type specific in mouse visual cortex', *eLife*, 5.

Pardo, J. V *et al.* (1990) 'The anterior cingulate cortex mediates processing selection in the Stroop attentional conflict paradigm.', *Proceedings of the National Academy of Sciences of the United States of America*. National Academy of Sciences, 87(1), pp. 256–9.

Pfeffer, C. K. *et al.* (2013) 'Inhibition of inhibition in visual cortex: the logic of connections between molecularly distinct interneurons', *Nature Neuroscience*. Nature Publishing Group, 16(8), pp. 1068–1076.

Polack, P.-O., Friedman, J. and Golshani, P. (2013) 'Cellular mechanisms of brain state–dependent gain modulation in visual cortex', *Nature Neuroscience*. Nature Publishing Group, 16(9), pp. 1331–1339.

Poort, J. *et al.* (2015) 'Learning Enhances Sensory and Multiple Non-sensory

Representations in Primary Visual Cortex', *Neuron*.

Powers, A. R., Mathys, C. and Corlett, P. R. (2017) 'Pavlovian conditioning-induced hallucinations result from overweighting of perceptual priors.', *Science (New York, N.Y.)*. American Association for the Advancement of Science, 357(6351), pp. 596–600.

Priebe, N. J. and McGee, A. W. (2014) 'Mouse vision as a gateway for understanding how experience shapes neural circuits', *Frontiers in Neural Circuits*. Frontiers, 8, p. 123.

Qadir, H. *et al.* (2018) 'Structural Connectivity of the Anterior Cingulate Cortex, Claustrum, and the Anterior Insula of the Mouse.', *Frontiers in Neuroanatomy*. 26 p. 100

Ranson, A. *et al.* (2019) 'Top-Down Suppression of Sensory Cortex in an NMDAR Hypofunction Model of Psychosis', *Schizophrenia Bulletin*.

Rao, R. P. N. and Ballard, D. H. (1999) 'Predictive coding in the visual cortex: a functional interpretation of some extra-classical receptive-field effects', *Nature Neuroscience*. Nature Publishing Group, 2(1), pp. 79–87.

Rauss, K. and Pourtois, G. (2013) 'What is Bottom-Up and What is Top-Down in Predictive Coding?', *Frontiers in psychology*. Frontiers Media SA, 4, p. 276.

Reynolds, J. H., Chelazzi, L. and Desimone, R. (1999) 'Competitive mechanisms subserve attention in macaque areas V2 and V4.', *The Journal of neuroscience : the official journal of the Society for Neuroscience*. Society for Neuroscience, 19(5), pp. 1736–53.

Reynolds, J. H., Pasternak, T. and Desimone, R. (2000) 'Attention increases sensitivity of V4 neurons.', *Neuron*. Elsevier, 26(3), pp. 703–14.

Ringach, D. L. *et al.* (2016) 'Spatial clustering of tuning in mouse primary visual cortex', *Nature Communications*. Nature Publishing Group, 7(1), p. 12270.

Rolls, E. T. and McCabe, C. (2007) ‘Enhanced affective brain representations of chocolate in cravers vs. non-cravers’, *European Journal of Neuroscience*. Blackwell Publishing Ltd, 26(4), pp. 1067–1076.

Rubio-Garrido, P. *et al.* (2009) ‘Thalamic Input to Distal Apical Dendrites in Neocortical Layer 1 Is Massive and Highly Convergent’, *Cerebral Cortex*. Narnia, 19(10), pp. 2380–2395.

Saleem, A. B. *et al.* (2013) ‘Integration of visual motion and locomotion in mouse visual cortex’, *Nature Neuroscience*. Nature Publishing Group, 16(12), pp. 1864–1869.

Schoups, A. *et al.* (2001) ‘Practising orientation identification improves orientation coding in V1 neurons’, *Nature*. Nature Publishing Group, 412(6846), pp. 549–553.

Schweimer, J. and Hauber, W. (2005) ‘Involvement of the rat anterior cingulate cortex in control of instrumental responses guided by reward expectancy.’, *Learning & memory (Cold Spring Harbor, N.Y.)*, 12(3), pp. 334–42.

Sengpiel, F., Sen, A. and Blakemore, C. (1997) ‘Characteristics of surround inhibition in cat area 17.’, *Experimental brain research*, 116(2), pp. 216–28.

Shidara, M. and Richmond, B. J. (2002) ‘Anterior Cingulate: Single Neuronal Signals Related to Degree of Reward Expectancy’, *Science*, 296(5573).

Shima, K. (1998) ‘Role for Cingulate Motor Area Cells in Voluntary Movement Selection Based on Reward’, *Science*. American Association for the Advancement of Science, 282(5392), pp. 1335–1338.

Shuler, M. G. and Bear, M. F. (2006) ‘Reward timing in the primary visual cortex.’, *Science (New York, N.Y.)*. American Association for the Advancement of Science, 311(5767), pp. 1606–9.

Smith, I. T. *et al.* (2017) ‘Stream-dependent development of higher visual cortical areas’, *Nature Neuroscience*. Nature Publishing Group, 20(2), pp. 200–208.

Sohya, K. *et al.* (2007) ‘GABAergic neurons are less selective to stimulus orientation than excitatory neurons in layer II/III of visual cortex, as revealed by in vivo functional Ca2+ imaging in transgenic mice.’, *The Journal of neuroscience : the official journal of the Society for Neuroscience*. Society for Neuroscience, 27(8), pp. 2145–9.

Spitzer, H., Desimone, R. and Moran, J. (1988) ‘Increased attention enhances both behavioral and neuronal performance’, *Science*, 240(4850), pp. 338–340.

Squire, R. F. *et al.* (2013) ‘Prefrontal Contributions to Visual Selective Attention’, *Annual Review of Neuroscience*.

Sundberg, K. A., Mitchell, J. F. and Reynolds, J. H. (2009) ‘Spatial attention modulates center-surround interactions in macaque visual area v4.’, *Neuron*. Elsevier, 61(6), pp. 952–63.

Svoboda, K. and Yasuda, R. (2006) ‘Principles of Two-Photon Excitation Microscopy and Its Applications to Neuroscience’, *Neuron*. Cell Press, 50(6), pp. 823–839.

Teufel, C. *et al.* (2015) ‘Shift toward prior knowledge confers a perceptual advantage in early psychosis and psychosis-prone healthy individuals.’, *Proceedings of the National Academy of Sciences of the United States of America*. National Academy of Sciences, 112(43), pp. 13401–6.

Theeuwes, J. (2010) ‘Top–down and bottom–up control of visual selection’, *Acta Psychologica*. North-Holland, 135(2), pp. 77–99.

Tootell, R. B. *et al.* (1998) ‘The retinotopy of visual spatial attention.’, *Neuron*. Elsevier, 21(6), pp. 1409–22.

Treue, S. and Maunsell, J. (1996) ‘Attentional modulation of visual motion processing in cortical areas MT and MST’, *Nature*, (382), pp. 539–541.

Wang, Q. and Burkhalter, A. (2007) ‘Area map of mouse visual cortex.’, *The Journal of comparative neurology*, 502(3), pp. 339–57.

Wang, Y. *et al.* (2008) ‘Spatial distribution of cingulate cortical cells projecting to the primary motor cortex in the rat’, *Neuroscience Research*. Elsevier, 60(4), pp. 406–411.

Weiss, Y., Simoncelli, E. P. and Adelson, E. H. (2002) ‘Motion illusions as optimal percepts’, *Nature Neuroscience*. Nature Publishing Group, 5(6), pp. 598–604.

Williford, T. and Maunsell, J. H. R. (2006) ‘Effects of Spatial Attention on Contrast Response Functions in Macaque Area V4’, *Journal of Neurophysiology*. American Physiological Society, 96(1), pp. 40–54.

Wong, R. O. L., Meister, M. and Shatz, C. J. (1993) ‘Transient period of correlated bursting activity during development of the mammalian retina’, *Neuron*. Cell Press, 11(5), pp. 923–938.

Wu, D. *et al.* (2017) ‘Persistent Neuronal Activity in Anterior Cingulate Cortex Correlates with Sustained Attention in Rats Regardless of Sensory Modality’, *Scientific Reports*. Nature Publishing Group, 7(1), p. 43101.

Wurtz, R. H. (1968) ‘Visual Cortex Neurons: Response to Stimuli during Rapid Eye Movements’, *Science*. American Association for the Advancement of Science, 162(3858), pp. 1148–1150.

Yan, Y. *et al.* (2014) ‘Perceptual training continuously refines neuronal population codes in primary visual cortex’, *Nature Neuroscience*. Nature Publishing Group, 17(10), pp. 1380–1387.

Yilmaz, M. and Meister, M. (2013) ‘Rapid innate defensive responses of mice to looming visual stimuli’, *Current biology : CB*. NIH Public Access, 23(20), pp. 2011–5.

Zaborszky, L. *et al.* (2015) ‘Neurons in the basal forebrain project to the cortex in a complex topographic organization that reflects corticocortical connectivity patterns: an experimental study based on retrograde tracing and 3D reconstruction.’, *Cerebral cortex (New York, N.Y. : 1991)*. Oxford University Press, 25(1), pp. 118–37.

Zhang, S. *et al.* (2014) ‘Selective attention. Long-range and local circuits for top-down modulation of visual cortex processing.’, *Science (New York, N.Y.)*. American Association for the Advancement of Science, 345(6197), pp. 660–5.

Zhang, S. *et al.* (2016) ‘Organization of long-range inputs and outputs of frontal cortex for top-down control’, *Nature Neuroscience*.

Zhou, H. and Desimone, R. (2011) ‘Feature-Based Attention in the Frontal Eye Field and Area V4 during Visual Search’, *Neuron*.